REPORT DOCUMENTATION PAGE

Form Approved
OMB NO. 0704-0188

1. AGENCY USE ONLY (Leave Blank)	2. REPORT DATE ~~4/3/03~~	3. REPORT TYPE AND DATES COVERED Progress Report: 10/01/01 – 7/31/04

4. TITLE AND SUBTITLE
Developing Effective Strategies and Performance Metrics for Automatic Target Recognition

5. FUNDING NUMBERS
43004-CI

DAAD19-01-1-0728

6. AUTHOR(S)
M. S. Alam (PI), A. A. S. Awwal and K. Iftekharuddin

7. PERFORMING ORGANIZATION NAME(S) AND ADDRESS(ES)
University of South Alabama, 307 N. University Blvd., Mobile, AL 36688
Subcontracters: Wright State University, Dayton, OH, and
University of Memphis, Memphis, TN

8. PERFORMING ORGANIZATION REPORT NUMBER
030105

9. SPONSORING / MONITORING AGENCY NAME(S) AND ADDRESS(ES)
U. S. Army Research Office
P.O. Box 12211
Research Triangle Park, NC 27709-2211

10. SPONSORING / MONITORING AGENCY REPORT NUMBER
43004.1-CI

11. SUPPLEMENTARY NOTES
The views, opinions and/or findings contained in this report are those of the author(s) and should not be construed as an official Department of the Army position, policy or decision, unless so designated by other documentation.

12 a. DISTRIBUTION / AVAILABILITY STATEMENT
Approved for public release; distribution unlimited.

12 b. DISTRIBUTION CODE

13. ABSTRACT (Maximum 200 words)

University of South Alabama segment: In this report, we presented four multiple target tracking algorithms and two data/decision fusion algorithm for efficient target tracking in FLIR imagery. The performance of these algorithms has been evaluated using two approaches - evaluation based on the input scene data complexity, and evaluation based on the correlation output produced by each algorithm. Finally, we investigated target detection in the initial frame of a sequence using two techniques assuming no target information is known *a priori.* (Details included in the report).

University of Memphis segment: We primarily focus on the performance measure characterization for both the dataset and our developed algorithms. We developed a composite metric table with different performance measures that demonstrates the capability of our two specific techniques, such as intensity and correlation algorithms, for detection and tracking. We also developed additional metric such as signal-to-noise ratio and classification for the entire dataset into low, medium and high categories. (Details included in the report).

Wright State University segment: In this report, we explored the search engine design which allows for easy plug in of multiple search methods. Therefore, scenes can be evaluated based upon the performance of different matching algorithms. The key idea of this search method is to take advantage of the "divide and concur" concept. Instead of searching for a pattern in a large image, a smart approach is taken to divide the image space into overlapping pattern of sub-images. Search is then based on upon best match with sub-image. (Details included in the report).

14. SUBJECT TERMS	15. NUMBER OF PAGES
Joint transform correlation, target tracking, image sequence, power spectrum, fringe-adjusted filter, intensity variation function, template matching, data/decision fusion, target detection, performance metrics, data complexity, signal to noise ratio, ground truth data, phase-only filter, neural networks	75 16. PRICE CODE

17. SECURITY CLASSIFICATION OR REPORT	18. SECURITY CLASSIFICATION ON THIS PAGE	19. SECURITY CLASSIFICATION OF ABSTRACT	20. LIMITATION OF ABSTRACT
UNCLASSIFIED	UNCLASSIFIED	UNCLASSIFIED	UL

NSN 7540-01-280-5500

Standard Form 298 (Rev.2-89)
Prescribed by ANSI Std. 239-18
298-102

Developing Effective Strategies and Performance Metrics for Automatic Target Recognition

(ARO Proposal Number: 43004-CI)

Final Report

Submitted to:

Dr. William A. Sander
US Army Research Laboratory, US Army Research Office
Associate Director, Computing & Information Science Division
P.O. Box 1221 RTP, NC 27709-22111

Submitted by:

Dr. Mohammad S. Alam (PI/PD), Professor and Chair
Department of Electrical and Computer Engineering
University of South Alabama, Mobile, AL 36688

September 10, 2004

List of Contents

Developing Effective Strategies and Performance Metrics for Automatic Target Recognition

(Work Done at the University of South Alabama)

Abstract

The final report that summarizes the work performed at University of South Alabama (USA). Four different target tracking algorithms and two data fusion algorithms have been developed for single/multiple target detection and tracking purposes. Each tracking algorithm utilizes various properties of targets and image frames of a given sequence. The data fusion algorithms employ complementary features of two or more of the above mentioned algorithms. Thus, the data fusion technique has been found to yield the best performance.

The performance of the above mentioned algorithms was evaluated using two approaches - evaluation based on the input scene data complexity, and evaluation based on the correlation output produced by each algorithm. We developed two new performance metrics to evaluate the effect of input plane data complexity on the performance of the algorithms. To evaluate the output produced by each of the aforementioned algorithms, we used four performance metrics, such as peak-to-sidelobe ratio, peak-to-correlation energy, peak-to-clutter ratio, and Fisher ratio.

Finally, we investigated the problem of target detection in the initial frame of a video sequence using two techniques, namely feature vectors and multilevel data fusion, assuming that no target information is known *a priori*.

1. Multiple Target Tracking Algorithms

We developed four new multiple target tracking algorithms which are based on fringe-adjusted joint transform correlation (FJTC), intensity variation function (IVF) and template matching (TM) techniques. The performance of these algorithms were tested using 50 real life forward looking infrared (FLIR) image sequences supplied by the Army Missile Command (AMCOM).

1.1 FJTC, IVF and TM (FJTC-IVF-TM) Based Multiple Target Tracking

In this section, we introduce FJTC-IVF-TM based multiple target tracking algorithm which includes frame preprocessing, motion estimation and target tracking. In the initial stage, we utilized the FJTC technique [1]. Using FJTC results, the current frame of the image sequence is recovered after global motion compensation. For the tracking algorithm, IVF and TM techniques have been used. The IVF based target tracking approach primarily utilizes target intensity information associated with the previous frame and the current frame. Initially, a target reference window and a subframe are segmented from consecutive frames. Then the IVF is generated by sliding target window inside the frame or the subframe, which yields maximum peak value for a match between the intensity variations of the known reference target and the unknown candidate target window in the frame or the subframe as shown in Fig.1.

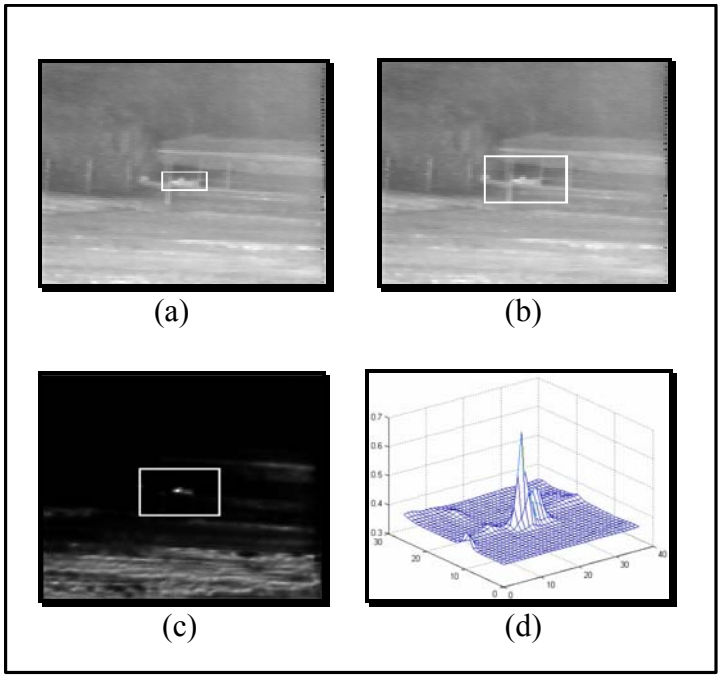

Fig. 1. Intensity variation function based target detection in a sequence (lwir_1913), a) Reference target window segmentation from previous frame, b) Subframe segmentation from the subsequent frame, c) IVF result , d) Highest peak produced in the IVF output plane.

From Fig. 1, it is evident that the candidate target coordinates can be obtained from the maximum peak value. When the candidate target coordinates are less reliable, the TM technique is triggered. It generates the highest peak value based on the similarity between reference target and candidate target by sliding target window inside the subframe [2]. Using the new target coordinates, target model is updated for target detection in the next frame as well as the tracking process. The aforementioned steps are repeated until all frames of the sequence are processed. The target tracking results obtained using the FJTC-IVF-TM algorithm is shown in Appendix A.

1.2 Normalized Crosscorrelation, IVF and TM (CC-IVF-TM) Based Multiple Target Tracking

In this algorithm, we proposed a new frame preprocessing algorithm using regional segmentation and normalized crosscorrelation based template modeling technique. The regional segmentation approach alleviates the effects of several detrimental factors such as smoke motion and effects of background while reducing the computation time. In addition, the template modeling technique enhances processing speed and increases the accuracy of the tracking algorithm.

For estimating the shift distance, template modeling algorithm is used which yields the highest value corresponding to the correlation coefficients between known reference image and unknown input image. The correlation coefficients provide a measure of association of the relationship between two images. It is defined as the ratio of the observed covariance of two standardized variables, divided by the highest possible covariance. When the observed covariance corresponds to the possible covariance value, the correlation operation generates a

value of 1, indicating a perfect match between the two images. In contrast, a correlation value of 0 indicates a random relationship between the two images.

The frame preprocessing is achieved by determining the highest correlation coordinate between the reference image and template image obtained from the subframe. Using the frame preprocessing, the current frame of the image sequence is recovered. For tracking, we used the IVF-TM tracking algorithm explained earlier in Section 1.1. The multiple target tracking results corresponding to the CC-IVF-TM algorithm is depicted in Appendix A.

1.3. Normalized Crosscorrelation, FJTC, and TM (CC-FJTC-TM) Based Multiple Target Tracking

In this tracking algorithm, we used the normalized crosscorrelation based preprocessing technique explained in Subsection 1.2. For tracking purposes, we used the FJTC and template modeling techniques. The FJTC technique has been found to yield excellent correlation discrimination between a known reference and an unknown target in an input scene. After preprocessing and applying the FJTC operation, a shift vector is obtained using the difference between the reference correlation peak and the new correlation peak coordinates as shown in Fig 2. The shift vector is used to calculate new target coordinates.

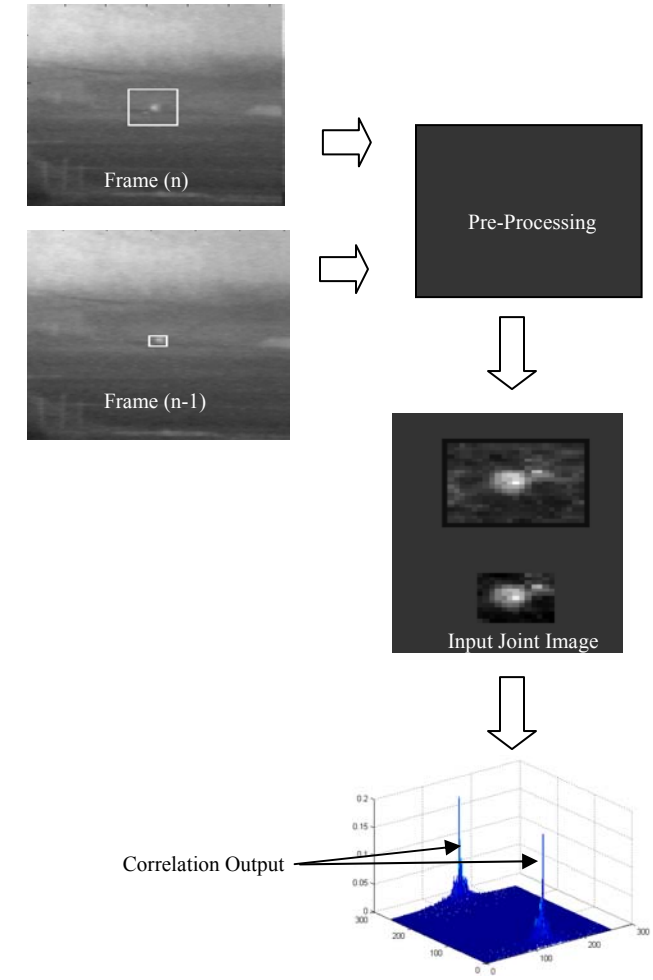

Fig.2 FJTC based target detection algorithm scheme.

When the FJTC algorithm yields poor results due to blending or background clutter problems, template modeling technique is employed as a compensation technique. Thereafter, the target model is updated and is used as a reference for the subsequent frame. This procedure is repeated until all frames of the sequence are processed. The target tracking results corresponding to the CC-FJTC-TM algorithm is included in Appendix A.

1.4 Modified SDF based Invariant FJTC (FJTC-MSDF-FJTC) Target Tracking

This is a vigorous approach for real-time target tracking in FLIR imagery in the presence of various distortions in target features and background properties. The proposed approach utilizes FJTC technique for real-time estimation of target motion and utilizes a concept similar to the synthetic discriminant function (SDF) filter to update the reference target model in order to alleviate the effects of noise, 3D distortions, and hazards generated by bad frames yielding significantly improved overall tracking performance [3].

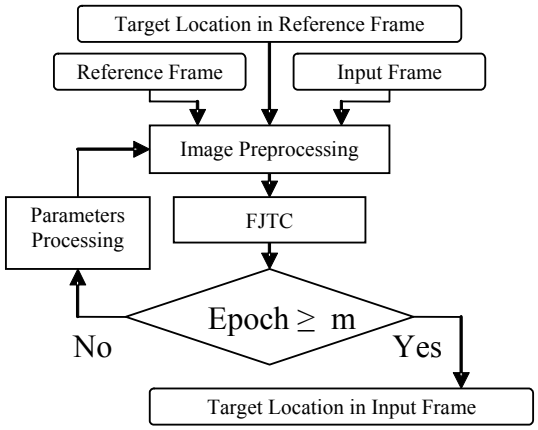

Fig. 3. FJTC Tracking Algorithm

The FJTC technique is used for correlation due to its low sensitivity to scale and rotation variations, small correlation side-lobes, and low zero-order peak. Moreover, FJTC can be easily implemented and is very suitable for real-time applications. Figure 3 shows the block diagram of the proposed FJTC tracking system.

A FLIR image generally smoothes out object edges and corners, and thus leads to a reduction of distinct features. The solution is to apply image preprocessing to both the input and reference images before the application of every FJTC operation. Image preprocessing involves various procedures such as edge enhancement and local intensity normalization. In the proposed FJTC algorithm, image segmentation technique is used to improve target tracking with conventional FJTC. In this method, several steps of motion preprocessing are used to effectively handle complicated scenarios such as multiple independently moving objects, distortions due to skew, rotation as well as other artifacts.

In addition, a filter is used to preserve the information available from the preceding target reference images in order to reduce the effects of noise and hazard associated with bad frames, as

well as other artifacts as shown in Fig. 4. The results corresponding to the modified SDF based invariant FJTC target tracking algorithm are illustrated in Appendix A (Algorithm #4). Finally each tracking algorithm results are summarized in Appendix B.

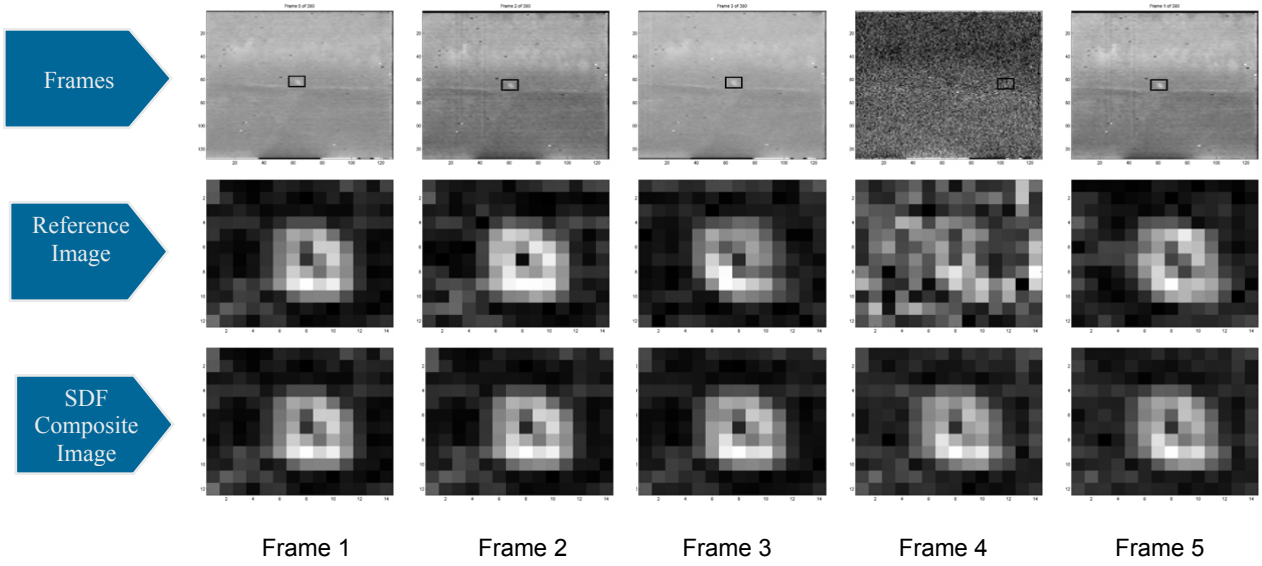

Fig.4 Modified SDF model based reference target update scheme.

2. Data/Decision Fusion

We proposed a novel data/decision fusion algorithm for target tracking in FLIR image sequences. The algorithm allows the fusion of complementary preprocessing and tracking algorithms. We identified three modes that contribute to the failure of the tracking system: (1) the motion failure mode, (2) the tracking failure mode, and (3) the reference image distortion induced failure mode. The strategy in the design of the proposed algorithm is to prevent these failure modes from developing tracking failures. The overall performance of the algorithm is guaranteed to be much better than any of the individual tracking algorithms used in the fusion. One important aspect of the proposed algorithm is its recoverability property i.e., the ability to recover following a failure at a certain frame.

The flowchart shown in Fig. 5 summarizes the basic building blocks of the proposed algorithm. In its initial appearance, the location of the target is determined from the ground truth file. The tracking in the subsequent frames are done automatically without any assistance from the ground truth file.

2.1 Ego-motion Compensation Component

The first component of the proposed algorithm is the ego-motion compensation (EMC). Different and complementary ego-motion compensation algorithms are used to generate initial locations for the target. In the flowchart of Fig. 5, we assume that two EMC algorithms are used and the two initial target locations are referred to as (x_1,y_1) and (x_2, y_2), respectively. For demonstration purposes, we assume that the compensation is achieved by the registration of the

large white box of the previous frame as shown in Fig. 6. We observe that EMC algorithm #1 succeeded in compensating the ego-motion, while algorithm #2 failed. For the subsequent target tracking to be successful, at least one EMC algorithm should succeed in placing the target within the operational limits of the tracking algorithm. The failure of all EMC algorithms will result in unrecoverable tracking error.

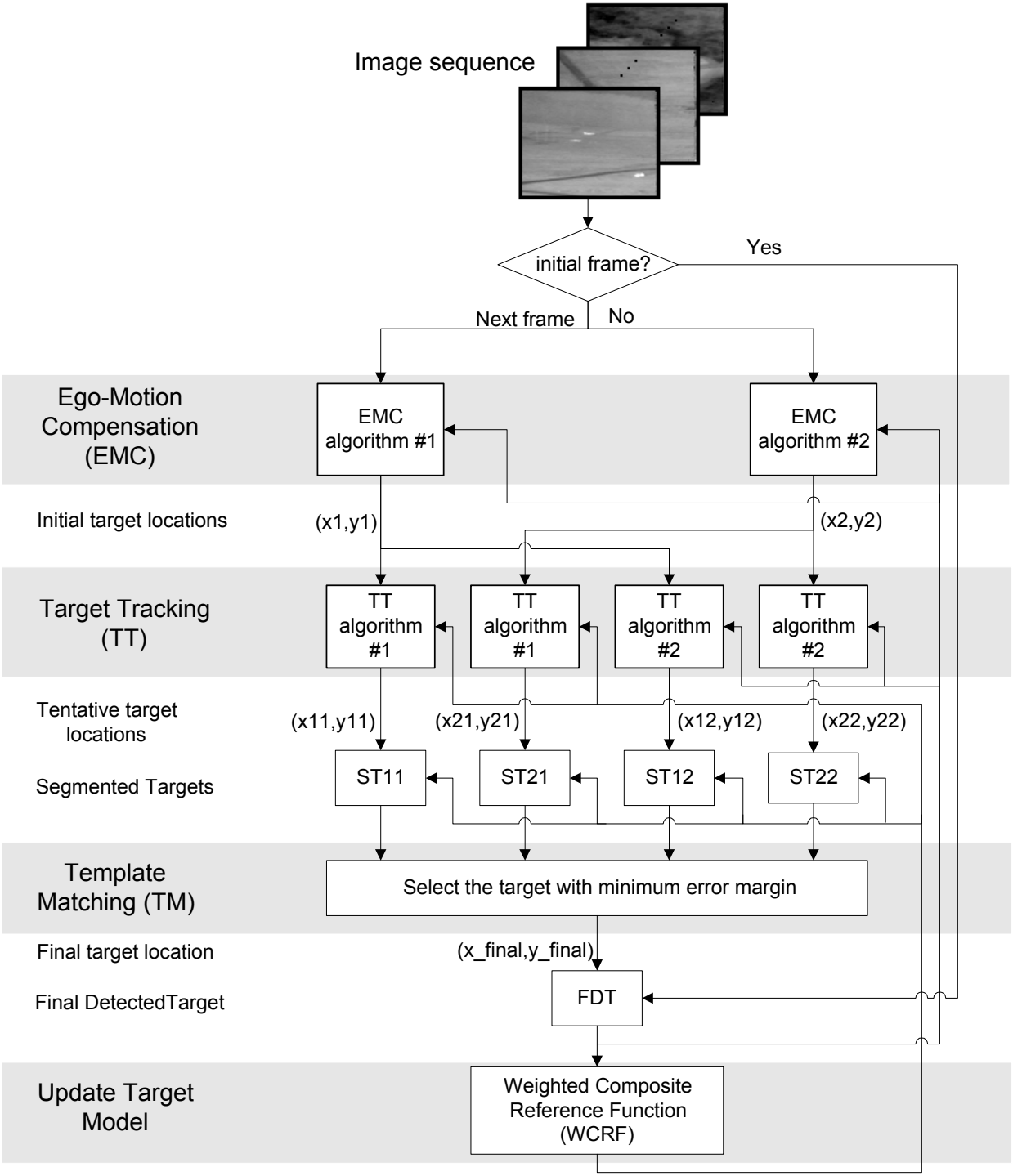

Fig. 5 Flowchart of proposed decision-fusion algorithm for correlation-based target tracking in FLIR imagery.

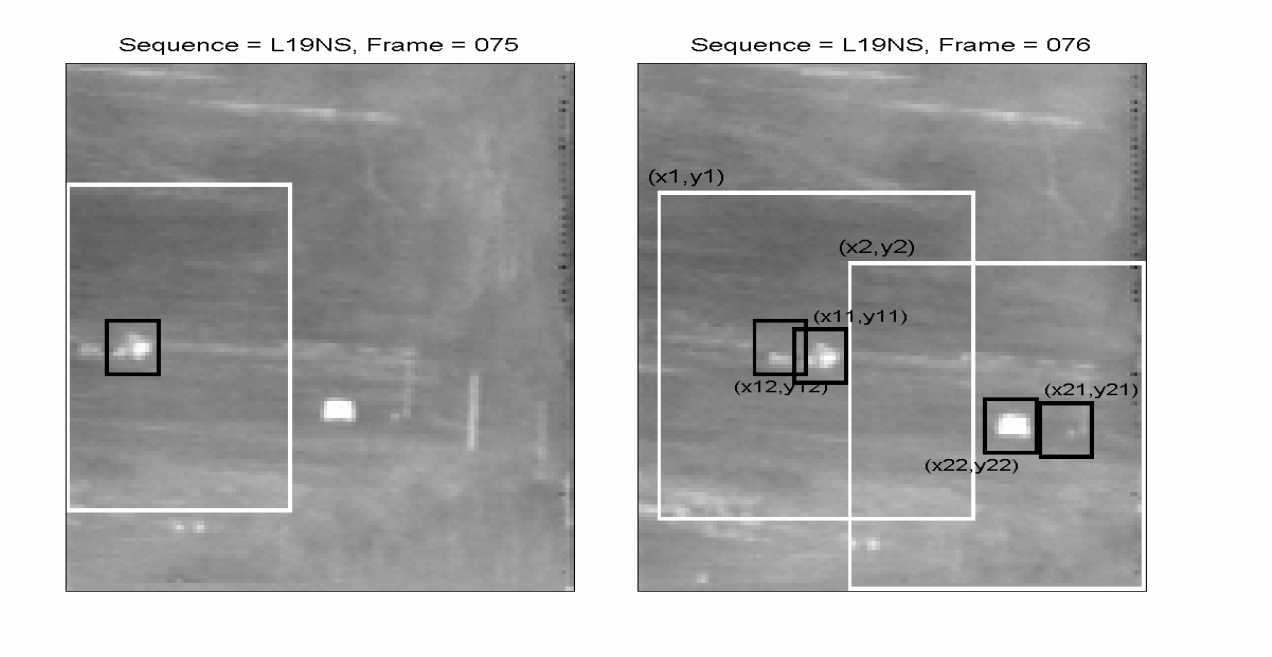

Fig. 6 Example demonstrating the initial target locations generated by the ego-motion compensation algorithms, (x_1,y_1) and (x_2,y_2), and tentative target locations generated by the tracking algorithms, (x_{11},y_{11}), (x_{12}, y_{12}), (x21,y21) and (x_{22},y_{22}).

2.2 Target Tracking Component

The next component of the proposed algorithm is target tracking (TT). In the vicinity of the initial locations generated by EMC algorithms, different TT algorithms are used to pinpoint the target by generating tentative locations. In the flowchart of Fig. 5, we assume that two TT algorithms are used. The number of tentative target locations is the product of the number of EMC algorithms times the number of TT algorithms. Consequently, in the example of Fig. 6, four tentative target locations, referred to as (x_{11},y_{11}), (x_{12}, y_{12}), (x_{21},y_{21}) and (x_{22},y_{22}), are generated. The correct location of the target is (x_{11},y_{11}) and the other locations are false alarms.

2.3 Template Matching Component

This component selects the final target location from the tentative locations determined in the preceding steps. This is achieved by template matching. Segmented targets (ST_{ij}) from the tentative locations are compared with a reference image for the target, called the Weighted Composite Reference Function (WCRF), which is discussed in next subsection. An Error Margin (EM_{ij}) is computed for every ST_{ij}, where EM_{ij} reflects the dissimilarity between ST_{ij} and the reference image WCRF. The ST_{ij} with the lowest EM_{ij} is selected as the Final Detected Target (FDT). In the example of Fig. 6, EM_{11} has the lowest EM. Therefore, (x_{11},y_{11}) is selected as the final target location, and FDT is selected as ST_{11}.

2.4 Update Target Model

The last component of the proposed algorithm is updating the target model. A Weighted Composite Reference Function (WCRF) is used to update the target model. The WCRF is generated by summing the multiplication of FDT images of the target used in the previous

frames with a set of weighted coefficients. By allowing WCRF to preserve its history, we effectively alleviate the distortion of the reference image.

2.5 Data/Decision Fusion Results

The experiments performed on the AMCOM FLIR data set verify the robustness of the proposed data/decision fusion algorithm. By using different and complementary ego-motion compensation and tracking algorithms, we have improved the chances of detecting the target. The template matching step, which selects the best match to the target model from the possible locations, insures the rejection of false alarm related errors. The WCRF method used for updating the target model alleviates the distortion of the reference image, and at the same time, it allows the target model to update its shape, size and orientation from frame to frame. It also enhances the probability of recovering after a failure at a certain frame. The multiple target tracking results obtained using the data/decision fusion algorithm are shown in Appendix C. Summarized fusion results are also shown in Appendix D. In the first experiment we fused CC-IVF-TM and FJTC-MSDF-FJTC tracking algorithms. The fusion algorithms performed better than the individual algorithms used in the fusion. In the second experiment, we obtained better results by fusing four algorithms: the two algorithms used in the first experiment plus two additional algorithms, FJTC-IVF-TM and CC-FJTC-TM.

3. Performance Metrics

FLIR image sequences are very complex in terms of the target signature and background, which makes the tracking very difficult. We observed that the input data complexity directly affects the performance of various tracking algorithms. On the other hand, the performance of the tracking algorithms can be evaluated by analyzing the output results.

3.1 Effect of Data on the Performance of an Algorithm

Input data complexity directly influences the amount of useful information available in the target signature. We developed two new performance metrics to measure the effect of input data on the performance of the target tracking algorithms which include local intensity ratio and local contrast ratio. The local intensity ratio (LIR) corresponds to the intensity variation between the target and the neighboring background in the infrared input image. The local contrast ratio (LCR) corresponds to the contrast variation between the target and the neighboring background in the infrared input image. Fig. 7 shows the data complexity in terms of LIR and LCR for all frames of a test sequence (L1415), which contains a single target of interest. Fig. 8 shows the same parameters for a multi-target image sequence (L1817S1).

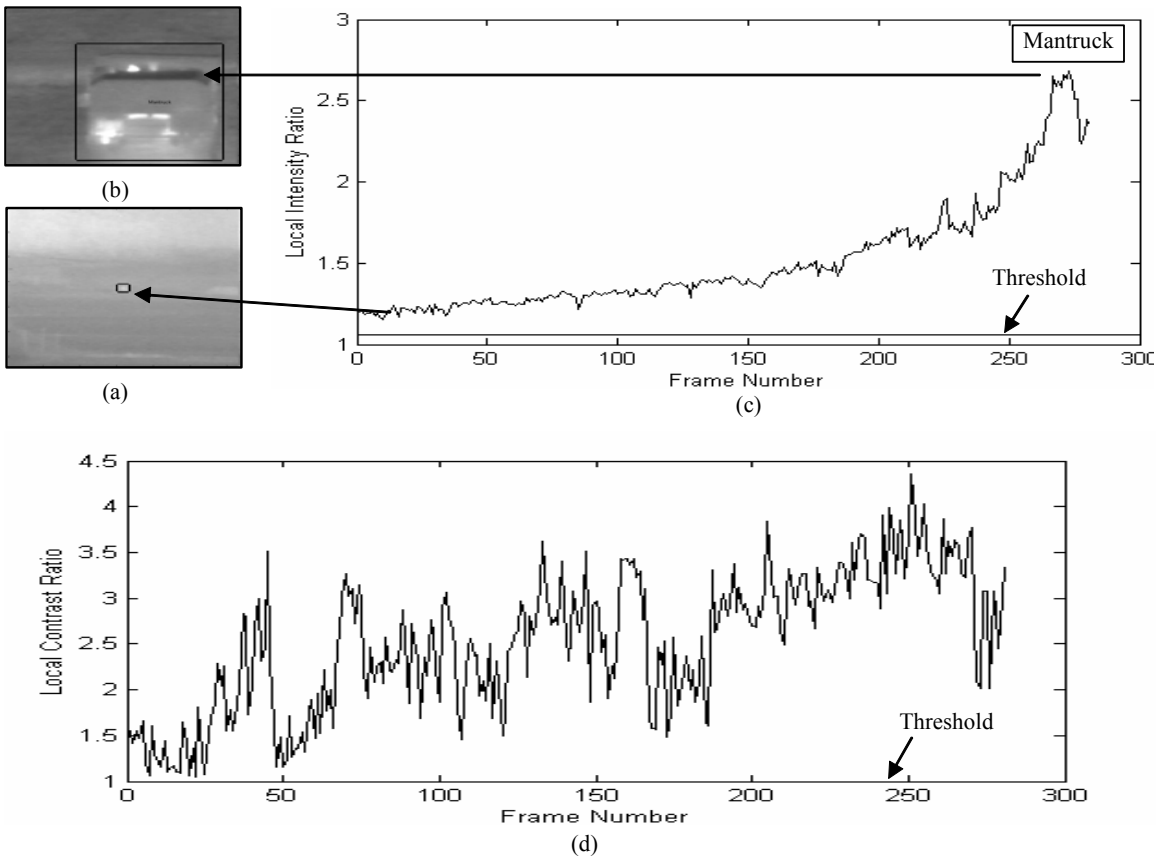

Fig. 7 LIR and LCR results for sequence (L1415), a) first frame, b) last frame, c) LIR result, and d) LCR result with 100 % tracking.

After testing the LIR and LCR metrics with all sequences, we found a threshold value of 1.05 for LIR and 1.0 for LCR. If LIR is above 1.05 and LCR is above 1, it is highly likely that a tracking algorithm will successfully track the target. If LIR is close to 1.05 and LCR is close to 1, a tracking algorithm may or may not detect and track the target. If the LCR is below 1.05 and LCR is below 1, it is highly likely that a tracking algorithm will fail to detect and track the target.

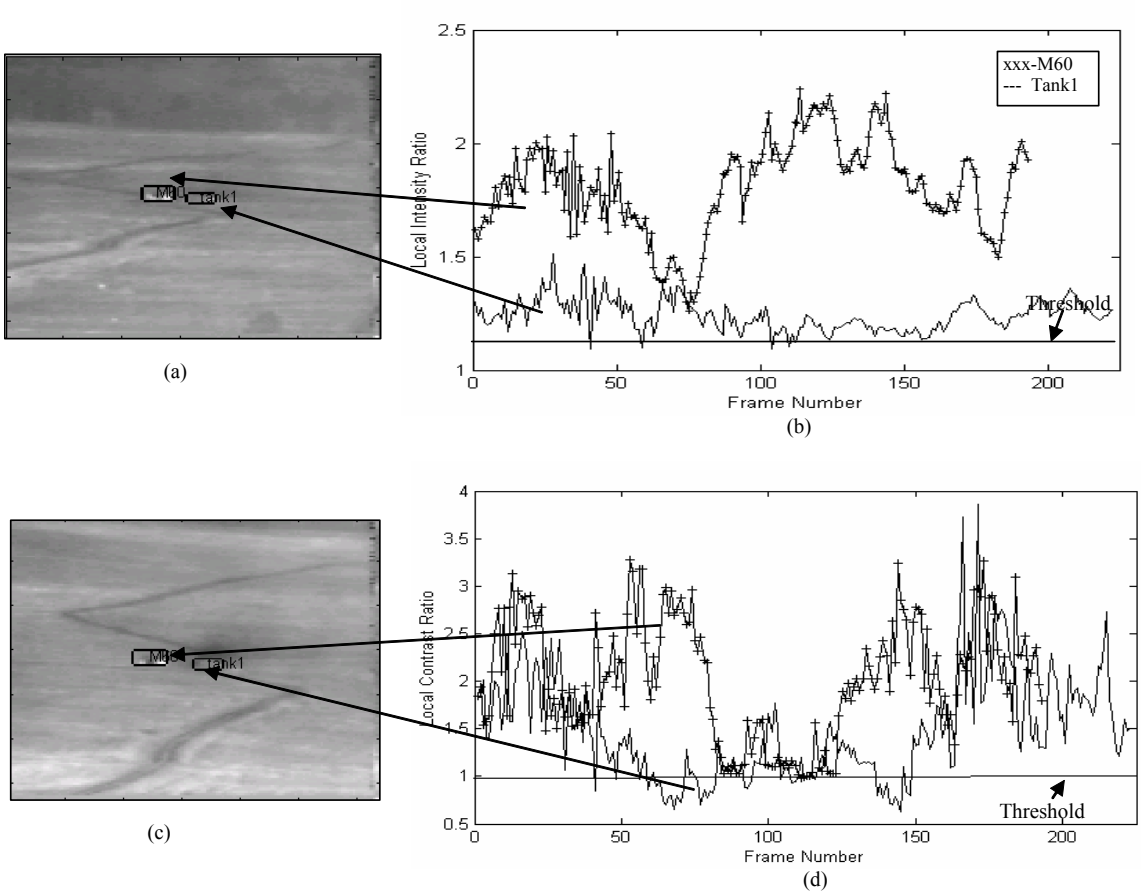

Fig. 8 LIR and LCR results for sequence (L1817S1): a) first frame, b) LIR result, c) frame # 63 , and d) LCR result.

3.2 Metrics for Evaluating Performance of a Tracking Algorithm

The similarity between a target and background, blended target, rotation and scale variations of the target, noise and clutter present in FLIR images pose various challenges in target detection and tracking. We investigated the performance of the tracking algorithms using various performance metrics for real life FLIR image sequences. We choose three metrics to evaluate the tracking algorithms which are peak-to-sidelobe ratio (PSR), peak-to-correlation energy (PCE) and Fisher ratio (FR) [4,5]. These performance metrics are used to estimate the reliability of the tracking algorithm. For illustration purposes, we report herein the performance of the CC-FJTC-TM algorithm using the aforementioned metrics.

The PSR determines the sharpness of the peak by comparing the highest peak intensity with a side-lobe peak intensity. The PCE calculates the ratio between the correlation peak energy and the total energy of the correlation plane. The higher the value of PCE, the sharper the correlation

peak. Fisher ratio is used to measure the performance of an algorithm with respect to the distortions associated with a target. It is utilized to evaluate the performance of an algorithm for distortion invariant target detection. When the FR is close to zero, it indicates that the target in the previous and current frames is same. When FR is higher than zero, it implies that the targets are different or there are significant variations between the target in the previous frame and the current frame. Figures 9, 10 and 11 show the performance results of CC-FJTC-TM for two sequences (L1415 and L1871S1), respectively.

To determine the thresholds for each of these performance metrics, we considered the tracking results for all sequences and determined the threshold for PSR, PCE and FR as 15, 0.002 and 0.5, respectively. For the first sequence (L1415), PSR and PCE are above their threshold and FR is below the threshold for all frames as shown in Figs. 9(a), 9(b) and 9(c), respectively. Therefore, the CC-FJTC-TM algorithm tracks the target in this sequence with 100% accuracy.

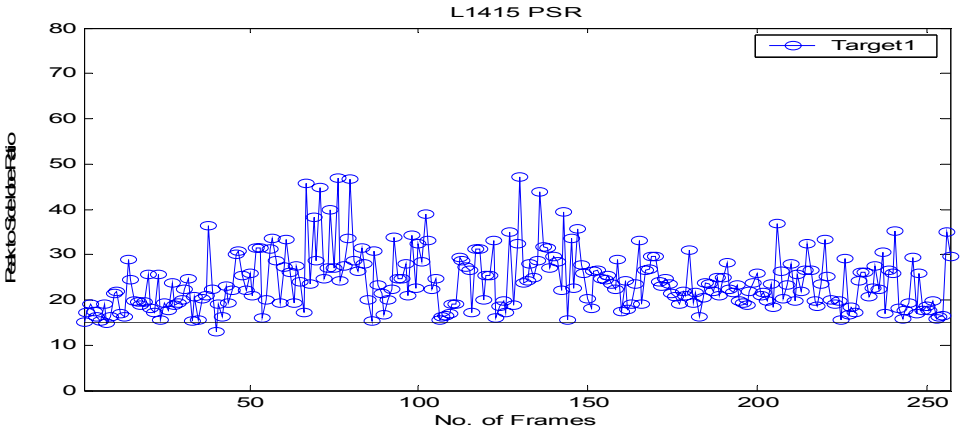

(a)

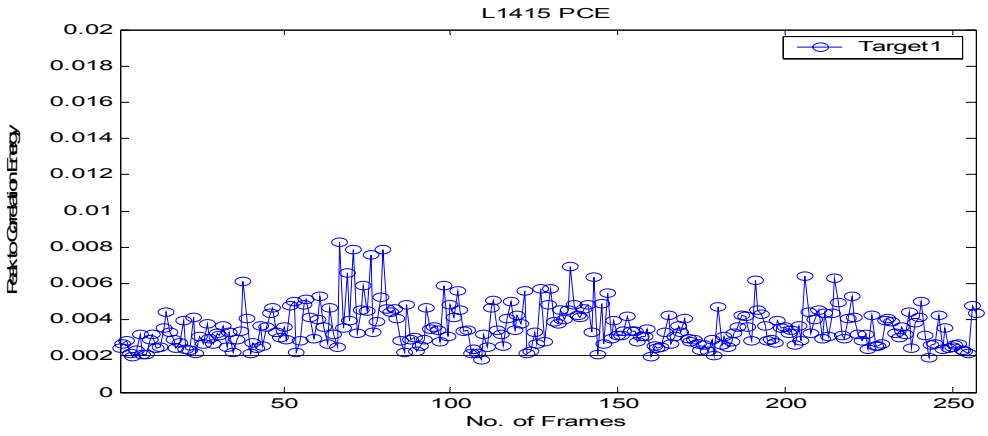

(b)

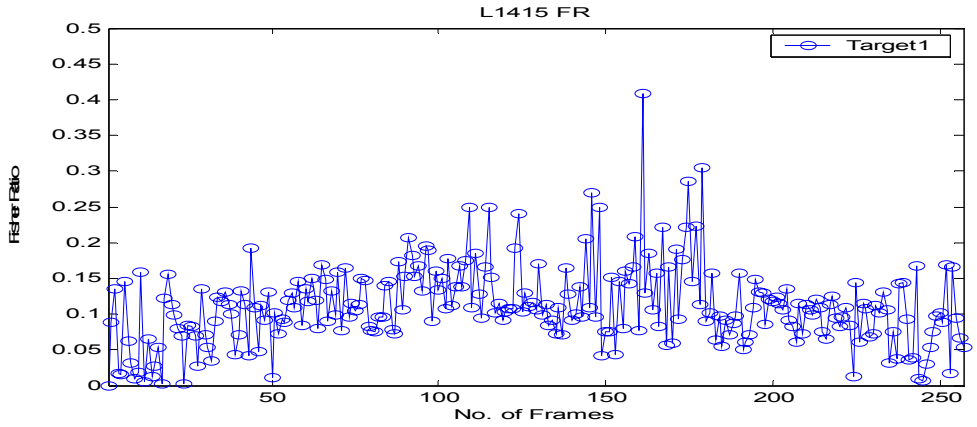

(c)

Fig. 9 (a) PSR for L1415, (b) PCE for L1415 and (c) FR for L1415.

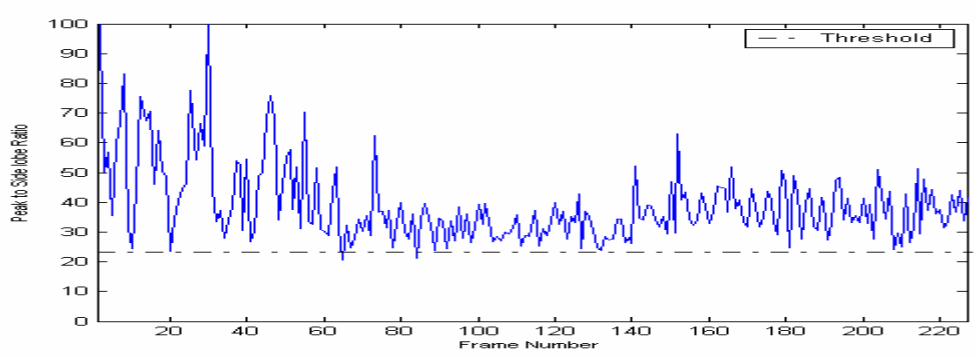

(a)

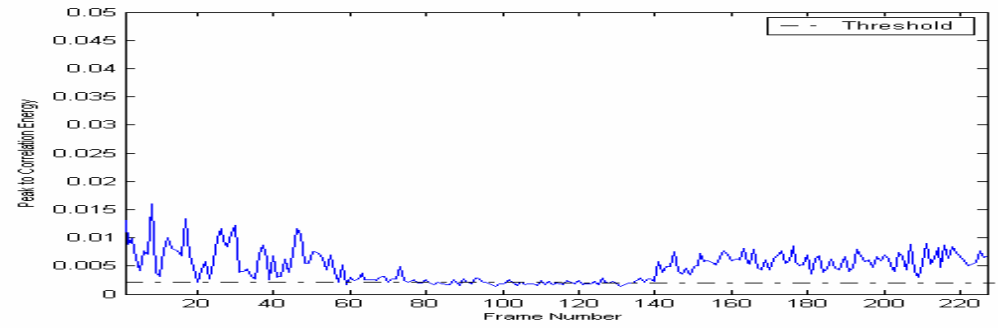

(b)

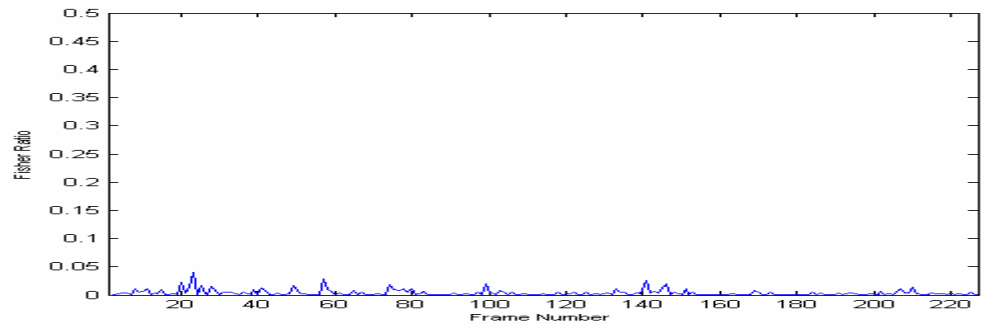

(c)

Fig. 10 (a) PSR results for target-1 in sequence L1817S1, (b) PCE results, and (c) FR results.

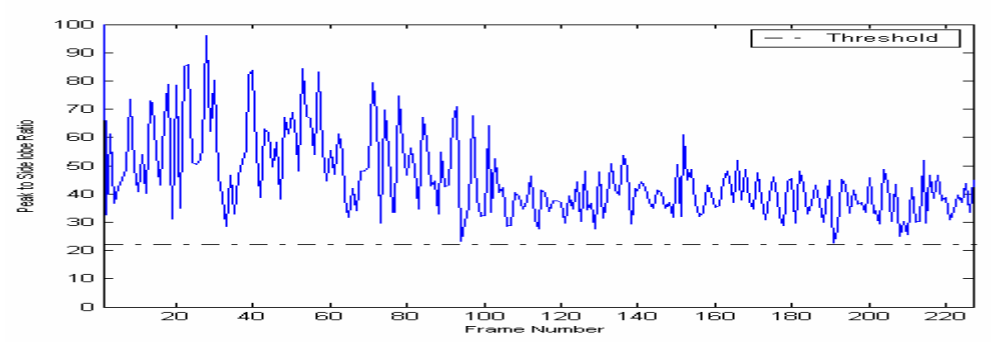

(a)

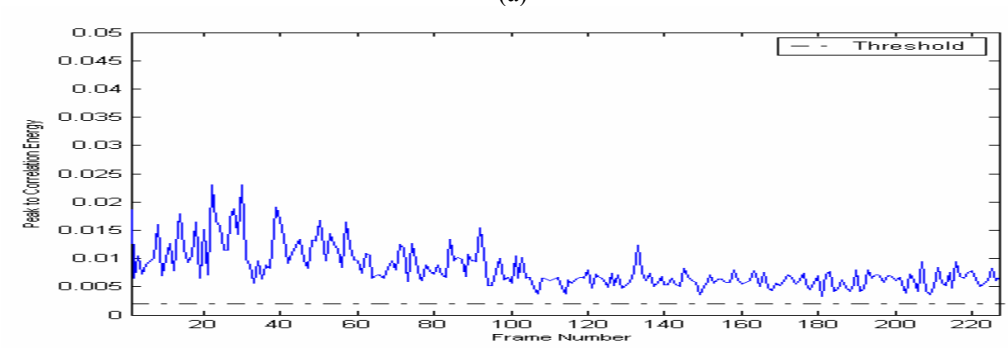

(b)

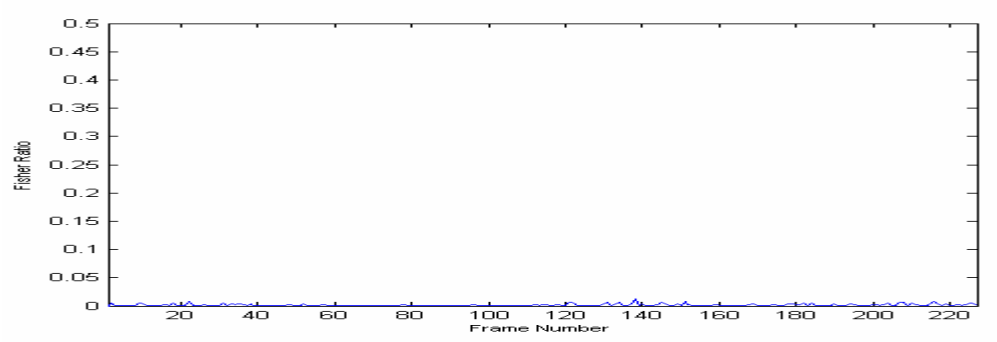

(c)

Fig. 11 (a) PSR results for target-2 in sequence L1817S1, (b) PCE results, and (c) FR results.

The performances metrics for the second sequence (L1817S1) is shown in Figs. 10 and 11. From Fig. 10, it is evident that the PSR and PCE values for Target #1 change dramatically i.e., the values drop lower than the threshold at around frame number 60. This implies that this algorithm fails to track Target #1 at around frame number 60. If we consider Target #2 (Figure 11) in the same sequence, it is evident that the PCE and PSR values are above the threshold and FR is close to 0, implying that the algorithm can detect and track Target #2 with 100% accuracy.

4. Target Detection

We investigated two algorithms for target detection in the initial frame of a sequence using (i) multilevel data fusion technique assuming no *a priori* information is available about the target, and (ii) Law's Texture Energy Measures assuming the number of targets present in the image are

known *a priori*. The developed algorithms utilize target intensity, contrast, as well as other properties to detect brighter hot spots which correspond to possible targets.

4.1 Target Detection Using Multilevel Data Fusion

This technique was originally introduced by Borghys *et al*. [6]. It is based on constructing co-occurrence matrix locally for the entire input image to calculate features such as energy, contrast, maximum probability, entropy, homogeneity and variance. These features are then fused together based on their coefficients obtained through training. However, for some cases, we found that the final output may split a probable single target into two parts if the existing technique is used. This may complicate the target detection process. To eliminate this limitation, an average filtering approach is used for the final output to join the small pieces that appear closer to each other. This enhances the detection accuracy and eliminates false alarms. Thereafter, a threshold operation is applied to reject unwanted regions. Two examples of target detection in the first frame using the above mentioned technique are depicted in Figs. 12 and 13, respectively.

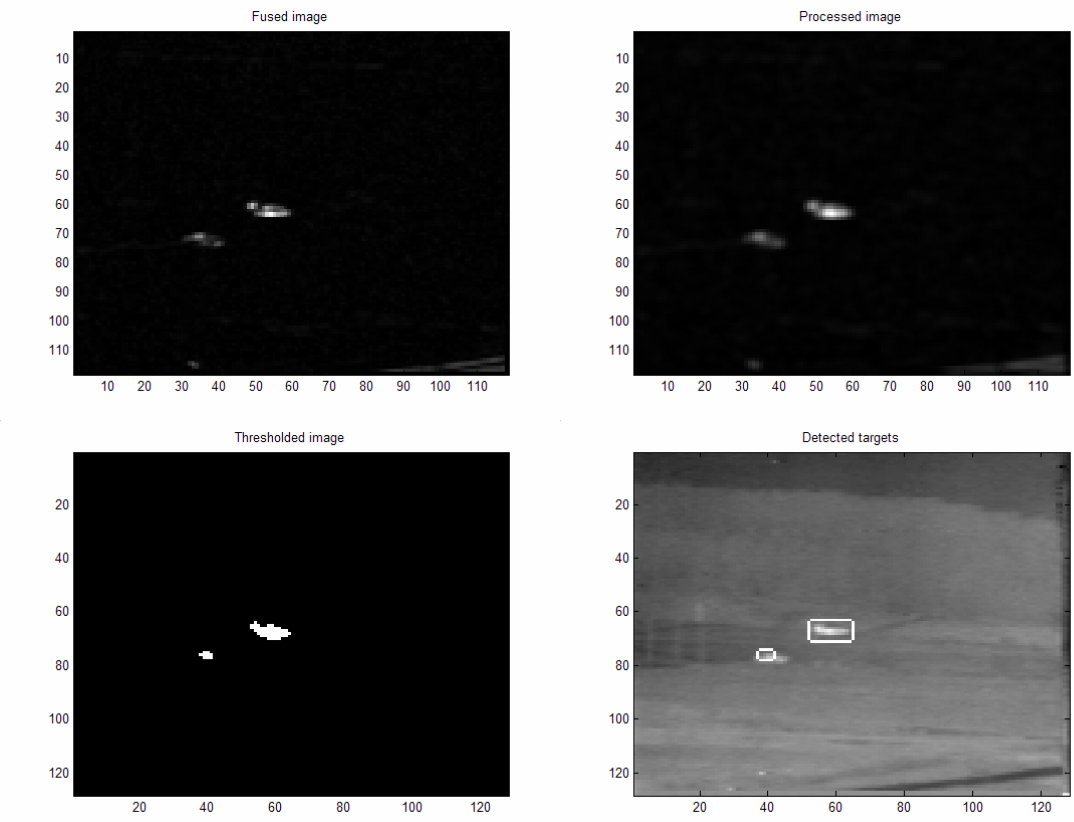

Fig. 12 Target detection using multilevel data fusion in sequence L1608

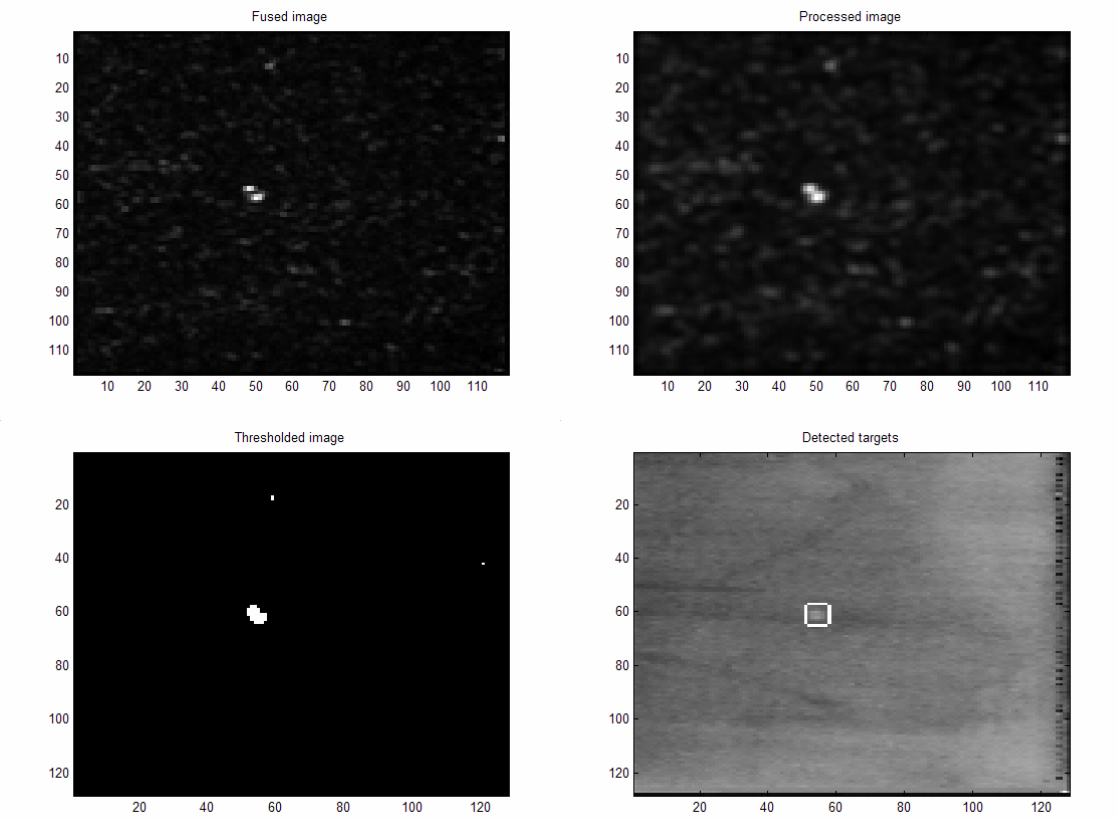

Fig. 13. Target detection using multilevel data fusion in sequence L2312.

This technique shows some promising results but it requires a lot of computation as a co-occurrence matrix needs to be constructed for every sub-region of the image. After further testing, we obtained similar results by applying a combination of a standard deviation filter and an average filter to the input image. This technique requires less computation time and does not need any training when compared to the previous technique. Figures 14 and 15 show the results obtained for the same sequence using our enhanced algorithm.

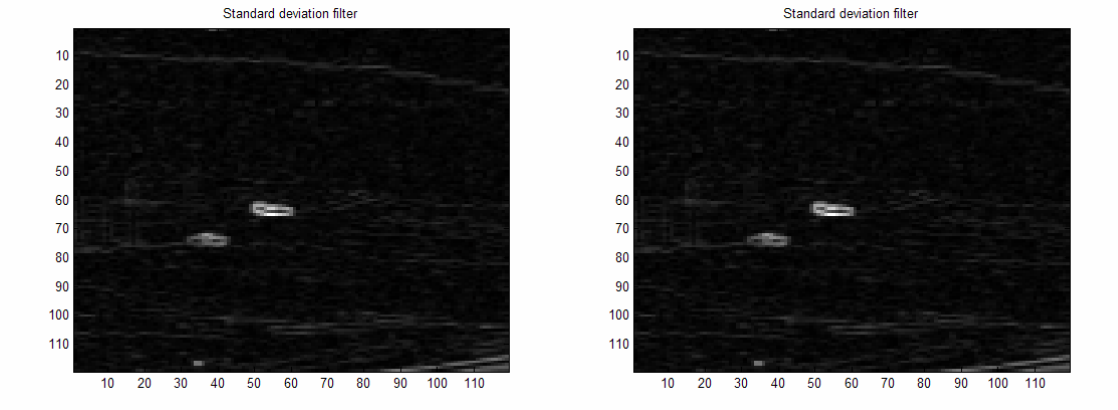

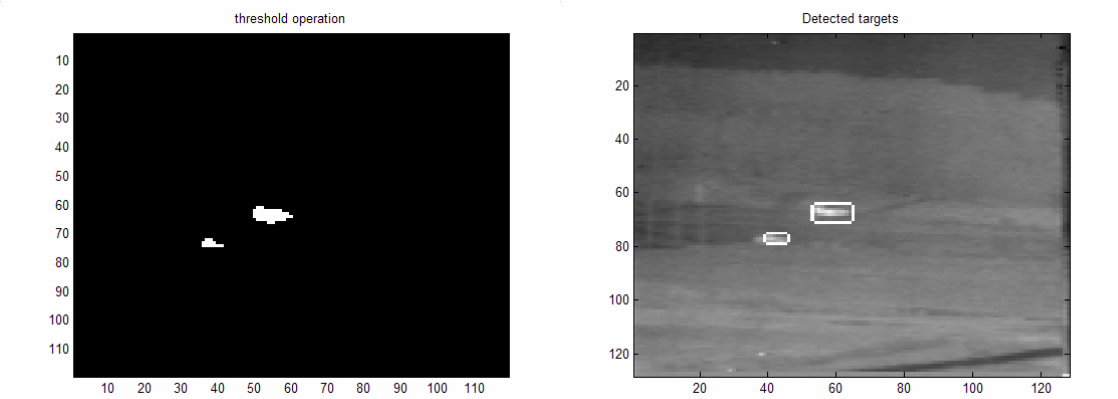

Fig. 14. Target detection using standard deviation and multilevel data fusion in sequence L1608.

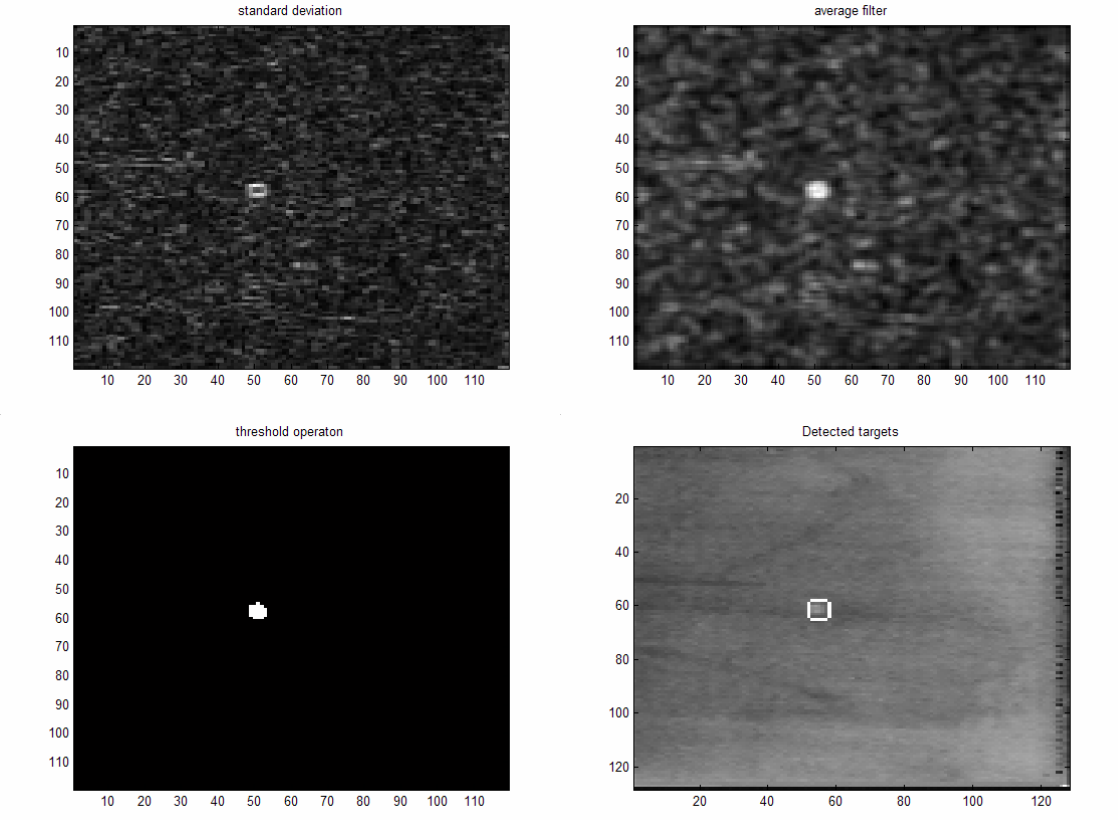

Fig. 15. Target detection using standard deviation and multilevel data fusion in sequence L2312

4.2 Target Detection Using Law's Texture Energy Measures

In this work, to detect targets in the initial frame, morphological operators and Law's texture energy measures [7-10] are used. Before starting any processing on the images, the gray levels of each image are rescaled between 0 to 255. At first, the following steps are followed to find the local maxima:

1) Morphological dilation with a centered horizontal element **H** of width 3 is applied so that small objects become more perceptible.
2) Difference between dilated image and original image yields the edge.
3) Addition of the original image with the image obtained from step 2, generates an enhanced version of the original image.
4) For further enhancement, the image from step 3 is again dilated with the same horizontal element H of width 3.
5) Subtraction of the original image from the image at step 5 yields broad or wide edges.
6) Average filtering of the image at step 5 fills the blank space enclosed by the edge of any object.
7) A threshold is then applied to the image at step 6 to eliminate unwanted smaller regions.
8) After the application of threshold, average filtering is reapplied to connect adjacent parts of an object if there are any.

The threshold value is chosen adaptively depending on the ratio between the maximum intensity of an image and mean intensity of the same image. The resulting images, obtained after each of the above steps, are shown in Figs. 16 through 23, respectively.

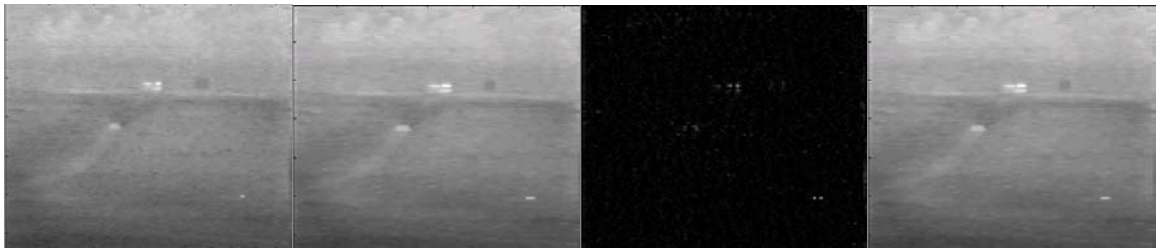

Fig. 16. Original rescaled image. Fig. 17. Output of step 1. Fig. 18 Output of step 2. Fig. 19 Output of step 3.

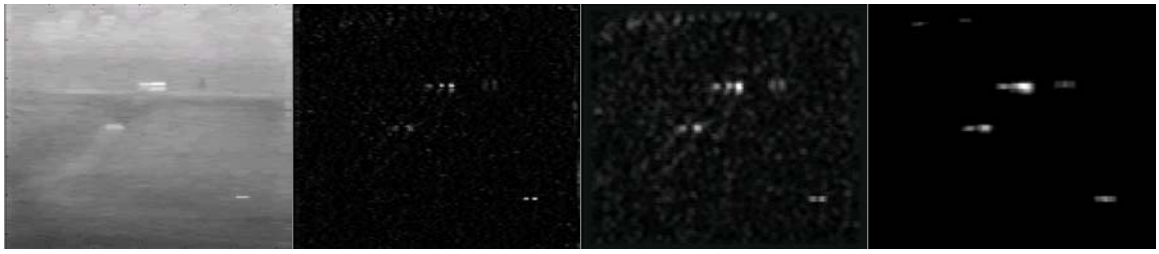

Fig. 20 Output of step 4. Fig. 21 Output of step 5. Fig. 22 Output of step 6. Fig. 23 Output of step 8.

Thereafter, Law's texture energy measures are applied to find the possible targets among the local maxima shown in Fig. 23. The target detection algorithm then searches for any non-zero values in the image resulting from step 8. All adjacent non-zero pixels are considered as a single object. After applying the search operation, the resulting detected regions containing both potential targets and non-target objects are obtained as shown in Fig. 24.

Now the challenge is to discriminate true targets from non-target objects. Texture may be used to distinguish between true targets or target like background in FLIR Imagery. Law's texture energy measures are basically feature extraction schemes based on gradient operators. This

scheme uses 5 masks which are obtained by convolving five 1-dimentional vectors, each representing level, edge, spot, wave and ripple, respectively, as shown below:

- Level L5 = [1 4 6 4 1]
- Edge E5 = [-1 -2 0 2 1]
- Spot S5 = [-1 0 2 0 -1]
- Wave W5= [-1 2 0 -2 1]
- Ripple R5= [1 -4 6 -4 1]

The following 5 masks are then applied to the image to eliminate the false positives from Fig. 24. The five output images of the five masks are shown in Figs. 25 to 29, respectively.

$$(E5')L5 = \begin{bmatrix} -1 & -4 & -6 & -4 & -1 \\ -2 & -8 & -12 & -8 & -2 \\ 0 & 0 & 0 & 0 & 0 \\ 2 & 8 & 12 & 8 & 2 \\ 1 & 4 & 6 & 4 & 1 \end{bmatrix}$$

$$(R5')L5 = \begin{bmatrix} 1 & 4 & 6 & 4 & 1 \\ -4 & -16 & -24 & -16 & -4 \\ 6 & 24 & 36 & 24 & 6 \\ -4 & -16 & -24 & -16 & -4 \\ 1 & 4 & 6 & 4 & 1 \end{bmatrix}$$

$$(S5')E5 = \begin{bmatrix} 1 & 2 & 0 & -2 & -1 \\ 0 & 0 & 0 & 0 & 0 \\ -2 & -4 & 0 & 4 & 2 \\ 0 & 0 & 0 & 0 & 0 \\ 1 & 2 & 0 & -2 & -1 \end{bmatrix}$$

$$(S5')S5 = \begin{bmatrix} 1 & 0 & -2 & 0 & 1 \\ 0 & 0 & 0 & 0 & 0 \\ -2 & 0 & 4 & 0 & -2 \\ 0 & 0 & 0 & 0 & 0 \\ 1 & 0 & -2 & 0 & 1 \end{bmatrix}$$

$$(R5')R5 = \begin{bmatrix} 1 & -4 & 6 & -4 & 1 \\ -4 & 16 & -24 & 16 & -4 \\ 6 & -24 & 36 & -24 & 6 \\ -4 & 16 & -24 & 16 & -4 \\ 1 & -4 & 6 & -4 & 1 \end{bmatrix}.$$

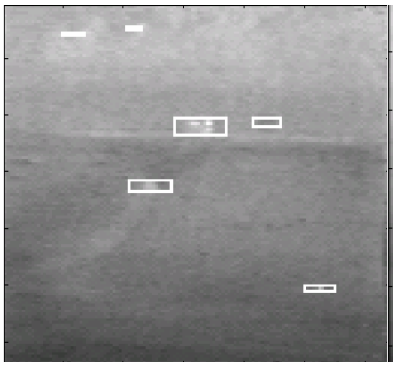

Fig. 24 Candidate targets' positions

Fig. 25 Output of mask (E5′)L5

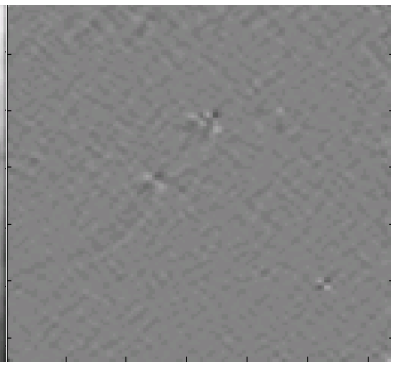

Fig. 26 Output of mask (R5′)L5

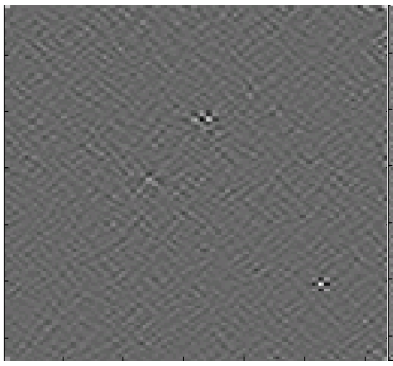

Fig. 27 Output of mask (S5′)E5

Fig. 28 Output of mask (S5′)S5

Fig. 29 Output of mask (R5′)R5

After calculating the above features for the detected objects' region, true targets are separated from non-target objects. The final detection result of the true targets, after eliminating the false target like background using Law's Texture Energy Measures, is shown in Fig. 30. It is found that the texture feature values are much higher for potential targets than non-targets. The results of this algorithm for target detection in the frame, where the target appears first, are shown in Appendix E.

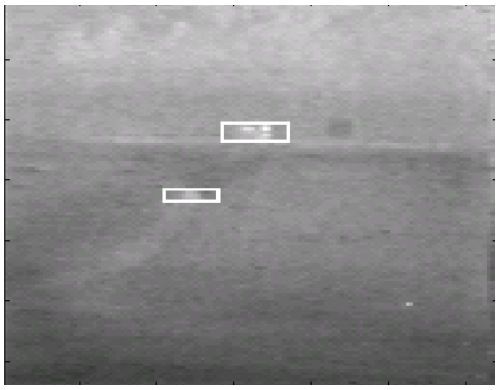

Fig. 30 Detected true targets using Law's Texture Energy Measures.

5. Conclusion

In this report, we presented an overview of the works that was performed during the stated period. The USA segment of the research work lead to the development of four target tracking algorithms and two data/decision fusion algorithms. The performance of these algorithms has been tested using real life FLIR image sequences supplied by AMCOM. The publications resulted from this project are listed in Appendix F.

The main characteristic of the FJTC-IVF-TM algorithm is that it uses target intensity and shape information for detection and tracking. Normalized cross-correlation techniques (CC-IVF-TM and CC-FJTC-TM) further enhances the robustness of the tracking algorithm. The modified SDF based invariant FJTC (FJTC-MSDF-FJTC) target tracking algorithm efficiently utilizes scale, rotation as well as neighborhood information for efficient target tracking. The data/decision fusion algorithm combines two or more of the above algorithms to ensure much better detection and tracking performance.

The impact of input data complexity and correlation output results are analyzed and metrics are developed to quantify the tracking performance for both input data (image sequences) and results generated by the various algorithms. In the above mentioned tracking techniques, we assume that the target is known in the first frame. To detect the target in the first frame without any *a priori* knowledge is a challenging task. In this project, we also investigated two algorithms for detecting target(s) in the initial frame of a FLIR sequence.

Appendix A: Target Detection and Tracking Results Generated by the Algorithms Developed at USA

Algorithm #1: FJTC-IVF-TM algorithm
Algorithm #2: CC-IVF-TM algorithm
Algorithm #3: CC-FJTC-TM algorithm
Algorithm #4: FJTC-MSDF-FJTC algorithm

Seq no.	Sequence name	Total frames	Targets	Tracking Results			
				Alg#1	Alg#2	Alg#3	Alg#4
1	L14_15	281	tar 1 - mantruck	100%	100%	100%	100%
2	L15_20	215	tar 1 - tank	100%	100%	100%	100%
3	L15_NS	320	tar 1 - tank1	100%	6%	100%	100%
			tar 2 - truck1	25%	65%	100%	100%
4	L16_04	400	tar 1 - tank1	100%	0%	100%	100%
5	L16_07	410	tar 1 - tank1	0%	0%	25%	2%
			tar 2 - mantruck	100%	45%	100%	100%
6	L16_08	290	tar 1 - m60	100%	100%	100%	100%
			tar 2 - apc1	100%	100%	100%	100%
			tar 3 - mantruck?	76%	70%	76%	76%
7	L16_18	300	tar 1 - m60	100%	100%	100%	100%
			tar 2 - apc	100%	100%	100%	100%
			tar 3 - truck	100%	100%	100%	100%
8	L17_01	388	tar 1 - bradley	100%	100%	100%	100%
			tar 2 - pickup	100%	100%	100%	100%
9	L17_02	698	tar 1 - mantruck	45%	100%	100%	100%
			tar 2 - pickup	20%	100%	100%	100%
			tar 3 - bradley	20%	2%	50%	67%
			tar 4 - mantruck	0%	0%	100%	1%
			tar 5 - tank	0%	100%	100%	100%
10	L17_20	778	tar 1 - target	0%	100%	100%	0%
			tar 2 - m60	0%	0%	100%	100%
11	L18_03	450	tar 1 - bradley	1%	1%	100%	100%
12	L18_05	779	tar 1 - tank1	100%	50%	100%	100%
			tar 2 - apc1	60%	100%	100%	100%
			tar 3 - m60	0%	0%	1%	2%
			tar 4 - tank1	0%	0%	1%	100%
13	L18_07	260	tar 1 - bradley	10%	7%	100%	100%
14	L18_12	300	tar 1 - tank1	80%	100%	100%	53%
			tar 2 - bradley	100%	100%	100%	100%
			tar 3 - m60	100%	100%	100%	100%
15	L18_13	326	tar 1 - tank1	100%	80%	100%	100%
			tar 2 - m60	100%	100%	100%	100%
			tar 3 - apc	100%	100%	100%	100%
16	L18_15 Seq 1	339	tar 1 - m60	50%	1%	100%	100%
			tar 2 - truck	100%	100%	100%	100%
			tar 3 - bradley	0%	0%	100%	10%

			tar 4 - tank1	0%	0%	100%	100%
17	L18_15 Seq 2	342	tar 1 - tank1	30%	30%	100%	100%
			tar 2 - bradley	50%	0%	100%	4%
			tar 3 - m60	90%	0%	100%	100%
18	L18_16	328	tar 1 - tank1	60%	6%	100%	16%
			tar 2 - m60	50%	80%	100%	1%
19	L18_17 Seq 1	240	tar 1 - tank1	50%	25%	50%	15%
			tar 2 - m60	100%	100%	100%	100%
20	L18_17 Seq 2	266	tar 1 - tank1	50%	25%	50%	43%
			tar 2 - m60	100%	100%	100%	100%
21	L18_18	365	tar 1 - mantruck	20%	50%	50%	37%
			tar 2 - target	10%	100%	100%	100%
			tar 3 - apc1	10%	50%	100%	100%
			tar 4 - m60	10%	0%	10%	10%
			tar 5 - tank1	50%	0%	1%	100%
			tar 6 - testvan	40%	100%	100%	100%
22	L19_01	240	tar 1 - tank1	1%	5%	1%	100%
23	L19_02	270	tar 1 - tank1	0%	1%	1%	100%
24	L19_04	270	tar 1 - tank1	90%	100%	100%	37%
25	L19_06	265	tar 1 - tank1	5%	5%	1%	100%
			tar 2 - apc	5%	5%	1%	0%
			tar 3 - mantruck	100%	100%	100%	100%
			tar 4 - van	100%	100%	100%	100%
26	L19_07	195	tar 1 - mantruck	0%	0%	100%	100%
27	L19_10	130	tar 1 - tank1	100%	100%	100%	100%
			tar 2 - apc	100%	100%	100%	100%
28	L19_11	165	tar 1 - tank1	100%	100%	1%	100%
			tar 2 - apc	100%	100%	100%	100%
29	L19_13	265	tar 1 - tank1	95%	100%	70%	100%
			tar 2 - apc	95%	100%	100%	100%
			tar 3 - m60	100%	100%	100%	100%
			tar 4 - mantruck	95%	100%	100%	100%
30	L19_15	350	tar 1 - tank1	10%	0%	100%	24%
			tar 2 - apc1	95%	96%	100%	3%
			tar 3 - m60	10%	0%	70%	1%
			tar 4 - van	50%	0%	100%	2%
31	L19_18	260	tar 1 - tank1	20%	10%	100%	100%
			tar 2 - m60	100%	100%	100%	100%
32	L19_NS	275	tar 1 - m60	50%	100%	60%	100%
			tar 2 - mantruck	100%	100%	100%	100%
			tar 3 - tank1	90%	2%	100%	25%
33	L20_04	368	tar 1 - apc1	100%	100%	100%	100%
34	L20_08	348	tar 1 - apc1	10%	5%	100%	100%
35	L20_17	308	tar 1 - tank1	3%	2%	100%	100%
36	L20_18	448	tar 1 - tank1	100%	100%	100%	100%
37	L20_20	420	tar 1 - tank1	10%	15%	10%	0%
			tar 2 - target	20%	100%	50%	89%
38	L21_04	760	tar 1 - bradley	0%	28%	100%	36%

			tar 2 - tank1	0%	3%	10%	1%
39	L21_15	738	tar 1 - bradley	10%	3%	5%	1%
40	L21_17	360	tar 1 - apc1	0%	100%	100%	1%
41	L22_06	348	tar 1 - tank1	40%	35%	100%	11%
42	L22-08	380	tar 1 - apc1	0%	0%	100%	1%
43	L22_10	398		100%	100%	100%	100%
44	L22_14	350	tar 1 - m60	5%	0%	100%	13%
			tar 2 - target	0%	0%	100%	100%
45	L23_12	368	tar 1 - apc1	100%	100%	100%	100%
46	M14_06	380	tar 1 - bradley	100%	100%	100%	100%
47	M14_07	400	tar 1 - bradley	100%	100%	100%	100%
48	M14_10	498	tar 1- tank1	100%	100%	90%	100%
			tar 2 - mantruck	80%	98%	40%	79%
49	M14_13	380	tar 1 - mantruck	100%	100%	100%	100%
50	M14_15	528	tar 1 - mantruck	0%	100%	70%	70%
			tar 2 - target	0%	100%	1%	33%

Appendix B: Comparative performance evaluation of the four tracking algorithms developed at USA

Total number of sequences	50			
Total number of multiple targets sequences	28			
Total number of reappearing targets	16			
Total number of targets in all 50 sequences	101			
	Tracking Algorithm Type			
	FJTC-IVF-TM	**CC-IVF-TM**	**CC-FJTC-TM**	**FJTC-MSDF-FJTC**
Total number of successful tracked sequences:	15	18	31	23
Total number of successful tracked targets excluding reappearance:	38	50	75	65
Total percentage of successful tracking excluding reappearance:	55%	58%	82%	72%
Total number of targets' tracking failure due to overlapping :	3	3	3	3
Total number of targets' tracking failure due to camera noise :	7	6	3	3
Total number of targets' tracking failure due to smoke :	24	24	3	20
Total number of targets' tracking failure due to scaling :	0	0	0	1
Total number of targets' tracking failure due to distraction by vicinity object	3	3	3	5
Total number of targets' tracking failure due to other reasons :	26	15	14	4

Appendix C: Target Detection and Tracking Results Generated by the Data/ Decision Fusion Algorithms Developed at USA

Algorithm #5 (DF #1): 2 USA algorithms (CC-IVF-TM and FJTC-MSDF-FJTC)
Algorithm #6 (DF #2): 4 USA algorithms (CC-IVF-TM, FJTC-IVF-TM, CC-FJTC-TM, FJTC-MSDF-FJTC)

Seq no.	Sequence name	Total frames	Targets	Tracking Results (DF #1)	Tracking Results (DF #2)
1	L14_15	281	tar 1 - mantruck	100%	100%
2	L15_20	215	tar 1 - tank	100%	100%
3	L15_NS	320	tar 1 - tank1	100%	100%
			tar 2 - truck1	100%	100%
4	L16_04	400	tar 1 - tank1	100%	100%
5	L16_07	410	tar 1 - tank1	10%	30%
			tar 2 - mantruck	100%	100%
6	L16_08	290	tar 1 - m60	100%	100%
			tar 2 - apc1	100%	100%
			tar 3 - mantruck?	100%	100%
7	L16_18	300	tar 1 - m60	100%	100%
			tar 2 - apc	100%	100%
			tar 3 - truck	100%	100%
8	L17_01	388	tar 1 - bradley	100%	100%
			tar 2 - pickup	100%	100%
9	L17_02	698	tar 1 - mantruck	100%	100%
			tar 2 - pickup	100%	100%
			tar 3 - bradley	18%	41%
			tar 4 - mantruck	0%	55%
			tar 5 - tank	100%	100%
10	L17_20	778	tar 1 - target	100%	100%
			tar 2 - m60	100%	100%
11	L18_03	450	tar 1 - bradley	100%	70%
12	L18_05	779	tar 1 - tank1	100%	100%

			tar 2 - apc1	100%	100%
			tar 3 - m60	100%	100%
			tar 4 - tank1	100%	100%
13	L18_07	260	tar 1 - bradley	100%	100%
14	L18_12	300	tar 1 - tank1	100%	100%
			tar 2 - bradley	100%	100%
			tar 3 - m60	100%	100%
15	L18_13	326	tar 1 - tank1	100%	100%
			tar 2 - m60	100%	100%
			tar 3 - apc	100%	100%
16	L18_15 Seq 1	339	tar 1 - m60	100%	100%
			tar 2 - truck	100%	100%
			tar 3 - bradley	100%	100%
			tar 4 - tank1	35%	35%
17	L18_15 Seq 2	342	tar 1 - tank1	100%	100%
			tar 2 - bradley	35%	100%
			tar 3 - m60	100%	100%
18	L18_16	328	tar 1 - tank1	100%	100%
			tar 2 - m60	100%	100%
19	L18_17 Seq 1	240	tar 1 - tank1	100%	100%
			tar 2 - m60	100%	100%
20	L18_17 Seq 2	266	tar 1 - tank1	100%	100%
			tar 2 - m60	100%	100%
21	L18_18	365	tar 1 - mantruck	50%	100%
			tar 2 - target	100%	100%
			tar 3 - apc1	100%	50%
			tar 4 - m60	10%	25%
			tar 5 - tank1	1%	1%
			tar 6 - testvan	100%	100%
22	L19_01	240	tar 1 - tank1	100%	100%
23	L19_02	270	tar 1 - tank1	100%	100%
24	L19_04	270	tar 1 - tank1	100%	100%

25	L19_06	265	tar 1 - tank1	100%	85%
			tar 2 - apc	100%	100%
			tar 3 - mantruck	100%	100%
			tar 4 - van	100%	100%
26	L19_07	195	tar 1 - mantruck	100%	100%
27	L19_10	130	tar 1 - tank1	100%	100%
			tar 2 - apc	100%	100%
28	L19_11	165	tar 1 - tank1	100%	100%
			tar 2 - apc	100%	100%
29	L19_13	265	tar 1 - tank1	100%	100%
			tar 2 - apc	100%	100%
			tar 3 - m60	100%	100%
			tar 4 - mantruck	100%	100%
30	L19_15	350	tar 1 - tank1	45%	100%
			tar 2 - apc1	100%	100%
			tar 3 - m60	100%	100%
			tar 4 - van	100%	100%
31	L19_18	260	tar 1 - tank1	100%	100%
			tar 2 - m60	0%	0%
32	L19_NS	275	tar 1 - m60	100%	100%
			tar 2 - mantruck	100%	100%
			tar 3 - tank1	3%	100%
33	L20_04	368	tar 1 - apc1	100%	100%
34	L20_08	348	tar 1 - apc1	100%	100%
35	L20_17	308	tar 1 - tank1	100%	100%
36	L20_18	448	tar 1 - tank1	100%	100%
37	L20_20	420	tar 1 - tank1	100%	100%
			tar 2 - target	89%	95%
38	L21_04	760	tar 1 - bradley	100%	100%
			tar 2 - tank1	100%	100%
39	L21_15	738	tar 1 - bradley	100%	100%
40	L21_17	360	tar 1 - apc1	100%	100%

41	L22_06	348	tar 1 - tank1	100%	100%
42	L22-08	380	tar 1 - apc1	100%	100%
43	L22_10	398		100%	100%
44	L22_14	350	tar 1 - m60	18%	100%
			tar 2 - target	100%	100%
45	L23_12	368	tar 1 - apc1	100%	100%
46	M14_06	380	tar 1 - bradley	100%	100%
47	M14_07	400	tar 1 - bradley	100%	100%
48	M14_10	498	tar 1- tank1	100%	100%
			tar 2 - mantruck	100%	100%
49	M14_13	380	tar 1 - mantruck	100%	100%
50	M14_15	528	tar 1 - mantruck	100%	100%
			tar 2 - target	100%	100%

Appendix D: Performance evaluation of data/decision fusion algorithms

Algorithm #5 (DF #1): 2 USA algorithms (CC-IVF-TM and FJTC-MSDF-FJTC)
Algorithm #6 (DF #2): 4 USA algorithms (CC-IVF-TM, FJTC-IVF-TM, CC-FJTC-TM, FJTC-MSDF-FJTC)

Total number of sequences :	50
Total number of multiple targets sequences:	28
Total number of reappearing targets :	16
Total number of targets :	101

	DF # 1	**DF # 2**
Total number of successful tracked sequences:	31	31
Total number of successful tracked targets excluding reappearance:	89	93
Total percentage of successful tracking excluding reappearance:	91%	94%
Total number of targets' tracking failure due to overlapping :	2	2
Total number of targets' tracking failure due to camera noise :	2	2
Total number of targets' tracking failure due to smoke :	2	2
Total number of targets' tracking failure due to scaling :	0	0
Total number of targets' tracking failure due to distraction by vicinity object	2	1
Total number of targets' tracking failure due to other reasons :	4	1

Appendix E: Target Detection at the Frame of First Appearance

Total number of sequences :		50
Total number of multiple targets sequences:		28
Total number of frames where target appears for the first time:		65
Total number of targets :		101
Total number of successful detected targets:		38
Total number of targets which cannot be discriminated:		32
Total number of targets which cannot be detected:		30
Total percentage of successful detection:	38/101=	38%

Seq no.	Seq name	Total frame	Targets' names	Frame number at which target appears for the first time	Detection Results		
					Can detect and discriminate from nontargets	Can detect but fail to discriminate from nontargets	Can not detect
1	L14_15	281	tar 1 - mantruck	1	yes		
2	L15_20	215	tar 1 - tank	1	yes		
3	L15_NS	320	tar 1 - tank1	1		yes	
			tar 2 - truck1	1		yes	
4	L16_04	400	tar 1 - tank1	1			yes
5	L16_07	410	tar 1 - tank1	200			yes
			tar 2 - mantruck	222		yes	
6	L16_08	290	tar 1 - m60	1	yes		
			tar 2 - apc1	1	yes		
			tar 3 - mantruck	190	yes		
7	L16_18	300	tar 1 - m60	1	yes		
			tar 2 - apc	1	yes		
			tar 3 - truck	1	yes		
8	L17_01	388	tar 1 - bradley	1	yes		
			tar 2 - pickup	1	yes		
9	L17_02	698	tar 1 - mantruck	114	yes		
			tar 2 - pickup	134	yes		
			tar 3 - bradley	138			yes
			tar 4 - mantruck	174			yes
			tar 5 - tank	538			yes
10	L17_20	778	tar 1 - target	1	yes		
			tar 2 - m60	44	yes		

11	L18_03	450	tar 1 - bradley	1			yes
12	L18_05	779	tar 1 - tank1	1		yes	
			tar 2 - apc1	1			yes
			tar 3 - m60	441			yes
			tar 4 - tank1	696			yes
13	L18_07	260	tar 1 - bradley	1		yes	
14	L18_12	300	tar 1 - tank1	1		yes	
			tar 2 - bradley	1		yes	
			tar 3 - m60	67	yes		
15	L18_13	326	tar 1 - tank1	1	yes		
			tar 2 - m60	1	yes		
			tar 3 - apc	1	yes		
16	L18_15 Seq 1	339	tar 1 - m60	1		yes	
			tar 2 - truck	11		yes	
			tar 3 - tank1	51			yes
			tar 4 - bradley	51		yes	
17	L18_15 Seq 2	342	tar 1 - m60	1		yes	
			tar 2 - tank1	36			yes
			tar 3 - bradley	42		yes	
18	L18_16	328	tar 1 - tank1	1			yes
			tar 2 - m60	1		yes	
19	L18_17 Seq 1	240	tar 1 - tank1	1	yes		
			tar 2 - m60	1	yes		
20	L18_17 Seq 2	266	tar 1 - tank1	1		yes	
			tar 2 - m60	1	yes		
21	L18_18	365	tar 1 - mantruck	1		yes	
			tar 2 - target	3		yes	
			tar 3 - apc1	22		yes	
			tar 4 - m60	82		yes	
			tar 5 - tank1	152		yes	
			tar 6 - testvan	362	yes		
22	L19_01	240	tar 1 - tank1	1			yes
23	L19_02	270	tar 1 - tank1	1			yes
24	L19_04	270	tar 1 - tank1	1	yes		
25	L19_06	265	tar 1 - apc	1			yes
			tar 2 - tank1	1		yes	
			tar 3 - mantruck	1		yes	
			tar 4 - van	55		yes	

26	L19_07	195	tar 1 - mantruck	120		yes	
27	L19_10	130	tar 1 - tank1	17			yes
			tar 2 - apc	57			yes
28	L19_11	165	tar 1 - tank1	1		yes	
			tar 2 - apc	1		yes	
29	L19_13	265	tar 1 - tank1	1			yes
			tar 2 - apc	1			yes
			tar 3 - m60	178		yes	
			tar 4 - mantruck	232		yes	
30	L19_15	350	tar 1 - tank1	1			yes
			tar 2 - apc1	1	yes		
			tar 3 - m60	1	yes		
			tar 4 - van	1			yes
31	L19_18	260	tar 1 - tank1	27		yes	
			tar 2 - m60	27	yes		
32	L19_NS	275	tar 1 - m60	1	yes		
			tar 2 - mantruck	87	yes		
			tar 3 - tank1	147			yes
33	L20_04	368	tar 1 - apc1	1	yes		
34	L20_08	348	tar 1 - apc1	1			yes
35	L20_17	308	tar 1 - tank1	116		yes	
36	L20_18	448	tar 1 - tank1	1		yes	
37	L20_20	420	tar 1 - tank1	1			yes
			tar 2 - target	150			yes
38	L21_04	760	tar 1 - bradley	1			yes
			tar 2 - tank1	70			yes
39	L21_15	738	tar 1 - bradley	1			yes
40	L21_17	360	tar 1 - apc1	1	yes		
41	L22_06	348	tar 1 - tank1	1			yes
42	L22-08	380	tar 1 - apc1	1	yes		
43	L22_10	398	tar 1 - target	1	yes		
44	L22_14	350	tar 1 - m60	1		yes	
			tar 2 - target	1			yes
45	L23_12	368	tar 1 - apc1	1	yes		
46	M14_06	380	tar 1 - bradley	1		yes	
47	M14_07	400	tar 1 - bradley	1	yes		
48	M14_10	498	tar 1- tank1	1	yes		

			tar 2 - mantruck	1	yes		
49	M14_13	380	tar 1 - mantruck	1	yes		
50	M14_15	528	tar 1 - mantruck	1	yes		
			tar 2 - target	1	yes		

Appendix F: Publications and Theses Generated from This Project

F.1. Refereed Journal Publications

1. A. Dawoud, M. S. Alam, A. Bal and C. Loo, "Decision Fusion Algorithm for Target Tracking in Infrared Imagery," accepted for publication, Journal of Optical Engineering, Vol. 44, 2005.
2. A. Bal and M. S. Alam, "Dynamic Target Tracking Using Fringe-adjusted Joint Transform Correlation and Template Matching," accepted for publication, Journal of Applied Optics, Vol. 43, 2004.
3. H. C. Loo and M. S. Alam, "Invariant Object Tracking Using Fringe-adjusted Joint Transform Correlation," accepted for publication, Journal of Optical Engineering, Vol. 43, 2004.
4. M. S. Alam, M. Haque, J. Khan and H. Kettani, "Target Tracking in Forward Looking Infrared (FLIR) Imagery Using Fringe-adjusted Joint Transform Correlation," Journal of Optical Engineering, Vol. 43, p. 1407-1413, 2004.
5. M. S. Alam, J. Khan and A. Bal, "Hetero-associative multiple target tracking using fringe-adjusted joint transform correlation," Journal of Applied Optics, Vol. 43, p. 358-365, 2004.
6. Five additional journal papers are currently undergoing review.

F.2. Conference Publications (Includes 1 Invited Papers)

1. M. S. Alam and A. Bal, "Automatic Target Tracking Using Global Motion Compensation and Fringe-adjusted Joint Transform Correlator," to appear, Proceedings of the SPIE Conference on Algorithms and Systems for Optical Information Processing (part of 49th Annual Meeting of the International Society for Optical Engineering), Denver, Colorado, August 2004.
2. A. Bal and M. S. Alam, "Feature extraction technique based on Hopfield neural network and joint transform correlation," to appear, Proceedings of the SPIE Conference on Algorithms and Systems for Optical Information Processing (part of 49th Annual Meeting of the International Society for Optical Engineering), Denver, Colorado, August 2004.
3. A. Bal and M. S. Alam, "Automatic Target Tracking in FLIR Image Sequences," to appear, Proceedings of the SPIE Conference on Automatic Target Recognition, Orlando, Florida, April 2004.
4. M. S. Alam, E. Horache and S. F. Goh, "Performance Evaluation for Cluttered Infrared Images Using Fringe-adjusted Joint Transform Correlation," Proceedings of the SPIE Conference on Optical Pattern Recognition, (part of 2004 SPIE Defense/Security Symposium), Vol. 5437, pp. 63-74, Orlando, Florida, 12-16 April, 2004.

5. M. S. Alam, J. Khan and A. Bal, "Fringe-adjusted joint transform correlation based hetero-associative multiple target tracking," to appear, Proceedings of the SPIE Conference on Automatic Target Recognition, Orlando, Florida, April, 2004.
6. H. C. Loo and M. S. Alam, "Fringe-Adjusted Joint Transform Correlation Based Invariant Target Tracking in FLIR Image Sequences (**Invited Paper**)," Proceedings of the SPIE Conference on Optical Pattern Recognition (part of 2003 SPIE Defense/Security Symposium), Vol. 5437, pp. 38-50, Orlando, Florida, 12-16 April, 2004.
7. A. Dawoud, M. S. Alam, A. Bal and C. H. Loo, "Data Fusion Framework for Target Tracking in Airborne Forward Looking Infrared Imagery," to appear, Proceedings of the SPIE Conference on Multisensor Data Fusion, Orlando, Florida, April 2004.
8. M. S. Alam, A. El-saba, E. Horache and S. Regula, "Joint Transform Correlation for Fingerprint Identification (Invited Paper)," to appear, Proceedings of the SPIE Conference on Optical Pattern Recognition, San Jose, California, January 26-29, 2004.
9. M. S. Alam, H. Kettani, M. Haque, J. Khan, A. A. S. Awwal and K. M. Iftekharuddin, "Fringe-adjusted JTC Based Target Detection and Tracking Using Subframes from a Video Sequence," Proceedings of the SPIE Conference on Photonic Devices and Algorithms for Computing V (part of 48th Annual Meeting of the International Society for Optical Engineering), Vol. 5201, p. 85-96, SPIE, San Diego, California, 3-8 August, 2003.
10. M. S. Alam, "Parallel optoelectronic pattern recognition architectures and algorithms (Invited Paper)," Proceedings of the 25th Conference on Opto-electro-techniques and Laser Applications, p. C01-C06, IEEE, Jakarta, Indonesia, October 2-3, 2002.
11. M. S. Alam, "Real Time Pattern Recognition and Tracking (Invited Paper)," Abstracts of the 2002 Annual Meeting of the Optical Society of America, p. 122, OSA, Orlando, September 29 - October 4, 2002.
12. M. S. Alam, "Class-associative pattern recognition using joint transform correlation (Invited Paper)," Proceedings of the SPIE Conference on Photorefractive Fiber and Crystal Devices: Materials, Optical Properties, and Applications VIII (part of 47th Annual Meeting of the International Society for Optical Engineering), p. 79-89, Vol. 4803, Seattle, Washington, 7 - 11 July, 2002.

F.3. Theses Generated from This Project

1. A. Sharma, Thesis Title: Fusion of edge information in image segmentation, University of South Alabama, Graduation date: December 2004.
2. S. M. A. Bhuyian, Thesis Title: Pattern Recognition and Tracking in Forward Looking Infrared Imagery Using Correlation Filters, University of South Alabama, Graduation date: December 2004.
3. N. Radhakrisna, Thesis Title: Performance Metrics for Pattern Recognition Algorithms, University of South Alabama, Graduation Date: August 2004.
4. J. Khan, Thesis Title: Class-associate Fringe-adjusted JTC Based Multiple Target Detection and Tracking, University of South Alabama, Graduation Date: May 2004.

References

1. M. S. Alam and M. A. Karim, “Fringe-adjusted joint transform correlation”, App. Opt., vol. 32, pp. 4344-4350 (1993).
2. K. Briechle and U.D. Hanebeck, “Template matching using fast normalized cross correlation”, Optical Pattern Recognition Procc. of SPIE, vol. 4387 (2001).
3. D. Casasent and W. T. Chang, “Correlation synthetic discriminant functions,” Appl. Opt. vol. 25, pp. 2343-2350 (1986).
4. B. V. K. Vijaya Kumar and L. Hassebrook, "Performance measures for correlation filters", Appl. Opt., vol. 29, pp. 2997-3006 (1990).
5. B. V. K. Vijaya Kumar, D. W. Carlson, and A. Mahalanobis, “Optimal trade-off synthetic discriminant function filters for arbitrary devices,” Opt. Lett., vol. 19, pp. 1556–1558 (1994).
6. D. Borghys, P.Verlinde, C. Perneel and M. Acheroy, “Multi-Level Data Fusion for the Detection of Targets using multi-spectral Image Sequences”SPIE/Optical Engineering's special issue on Sensor Fusion, Opt. Eng., vol 37, pp 477-484(1998).
7. U. Braga-Neto, and J. Goutsias, “Automatic target detection and tracking in forward-looking infrared image sequences using morphological connected operators,” Proceedings of the Conference on Information Sciences and Systems (CISS), Baltimore, Maryland, March 17-19 (1999).
8. A. Soffer, “Image Categorization Using Texture Features,” 4th Int. Conf. on Document Analysis and Recognition, Ulm, Germany, Aug. 1997
9. R. M. Haralick, K. Shanmugam, and I. Dinstein, “ Textural features for image classification,” IEEE Transaction on System, Man and Cybernetic, vol. SMC-3, pp. 610-621 (1973).
10. K. I. Laws, "Texture Energy Measures", in DARPA Image Understanding Workshop, pp. 47-51 (1979).

Developing Effective Strategies and Performance Metrics for Automatic Target Recognition
(Final report on the work performed at the University of Memphis)

Co-PI: Dr. K. M. Iftekharuddin
ECE Department, University of Memphis

Executive Summary

The problems of automatic target detection, tracking, recognition and classification have been active research fields in image processing and Neural Networks (NN). In this report, we explore novel ATR techniques such as object pre-processing, detection, tracking and classification of sequence of Infrared (IR) images provided by the Army Missile Command (AMCOM), Huntsville AL. The target images in the IR database contain various distortions such as translation, scale or rotation (both in-plane and out-of-plane) as well as extensive background clutter and noise. We present image pre-processing, detection and tracking algorithms for both single and multiple objects that segment, detect and track the object(s) based on four different techniques such as i) intensity; ii) correlation time; iii) correlation frequency; and iv) Bayesian. For the first three techniques, we attempt to detect and track the targets automatically without the prior knowledge of the location and size of the object in the reference frame. For our fourth technique (Bayesian), we assume full knowledge of the object using ground truth (GT) data. In addition, we exploit an elegant mathematical approach using Hilbert transform pair of wavelet bases in the determination of exact angle of rotation for targets. We compare the relative performance of Hilbert wavelet, Hilbert transform in determination of in-plane and out- of plane rotation angles. Note that this Hilbert-wavelet analysis is performed as part of our other ongoing research in the relevant areas.

In our proposed detection and tracking algorithms, we preprocess the image sequences to segment the object from the background clutter and noise and extract relevant statistical and intensity object features. We enhance our algorithm to track multiple objects in image frames based on the knowledge of the histogram of the targets. In some example image frames, we obtain detection and tracking of the background instead of the objects due to presence of excessive amount of background clutter. This problem of background detection and tracking is magnified for the first three techniques (such as intensity, correlation time and correlation frequency) wherein the initial selection of the reference frame is quite arbitrary. However, improved detection and tracking performance may be achieved in the Bayesian technique since the knowledge of the target location in the first frame is initially known from the GT data. We obtain extensive comparative performance metrics of our proposed techniques in detecting and tracking the objects. We also devise graphical user interfaces (GUI) to facilitate such comparison of the metrics.

Finally, we take advantage of our detection and tracking algorithms to extract the best possible features of the image to feed to the neural network (NN) for classification. In this work, we use self-organizing map (SOM) and k-nearest neighbor NN techniques to classify the dataset. We use different image statistical features as well as intensity and shape of the object for classification. An edge-tracing method is also investigated which sequentially traces all the connected points in the edge to form the shape of the image. Our classification algorithms successfully clusters the image sequences into pre-defined classes based on the size of the object. Note that the success of any NN classification depends on the availability of representative

references data sets. The AMCOM IR datasets do not contain such pristine reference image of the targets. Thus, the goal of our image classification in this project has been to identify useful classification methods for future investigation.

1. Introduction

The problems of automatic target recognition (ATR) and image classification have been active research fields in image processing and neural networks. The image classification is often limited by the presence of background clutter noise. Further, the image may be subjected to different type of distortions such as scale, translation and rotation. Thus, the researchers of animal and machine vision have researched distortion-invariant ATR and Image Understanding (IU) actively. The present state of the art machine vision systems do not even approach the performance of human vision in IU, which implies that there is still much to be learned from biological vision systems. With this in mind, researchers have chosen biomorphic-engineering approaches such as Neural Networks to solve rather intricate ATR and IU Problems. ATR is the processing and understanding of an image in order to recognize the targets. The long time objective of ATR research is to derive useful approximations or bounds on the performance of ATR systems in distortion-related cases. It is understood that the most accurate estimates of the performance of a particular ATR system are obtained by compiling the results of end-to-end systematic experiments on rich sets of measured data. Unfortunately, the end-to-end experiments are fiscally and computationally expensive. More importantly, the task of measuring or simulating a set of targets over the variety and range of extended operating conditions is beyond current capability. Therefore, almost all the ATR studies involve either simulated or limited scale ground data such as grayscale, synthetic aperture radar (SAR) or infrared images.

ATR functionally relies in some way on its knowledge of how the objects and classes of interest appear. The 'comparison' of this knowledge to the current information on new object determines the results of the recognition process. In order to train and verify the performance of a classifier, it is necessary to have truth data for all image objects used during training and verification. Exogenous information such as fields of view and horizontal, vertical and depression angles can be used to a greater advantage along with the primary data stream. Motion tracking is also an important task in computer vision especially when objects are subjected to certain viewing transformations. Even though the feature space maximizes the similarity of objects in the same class and minimizes the similarity of objects in different classes, the general nature of ATR imagery makes feature based classification a very hard problem. A variety of classification schemes have been implemented and evaluated. Structural constraints reduce the number of independent weights by using a locally connected structure or sharing the same weights on many connections.

2. Detection and Tracking Results

2.1 Intensity-based Algorithm

a) Single object case

We apply our preprocessing and detection algorithm on one L17_20 of the IR public image database [25]. These are the scaled and rotated images from the database. Fig.1 shows some of the results of detection and tracking obtained. Out of 778 images in the database, a total of 750 images are detected and tracked correctly. We have applied our detection and tracking algorithm on other sequences of the database [25] and obtained the similar results.

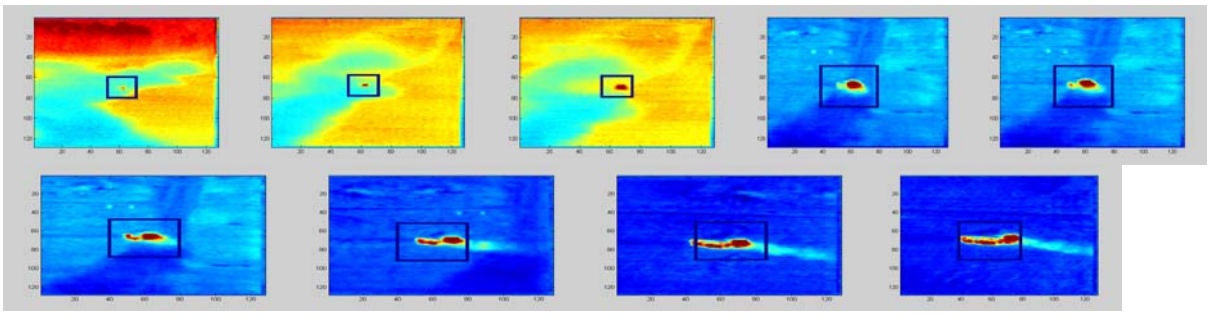

Fig. 1 Detection and tracking of objects at different scales and angles

b) Multiple object case

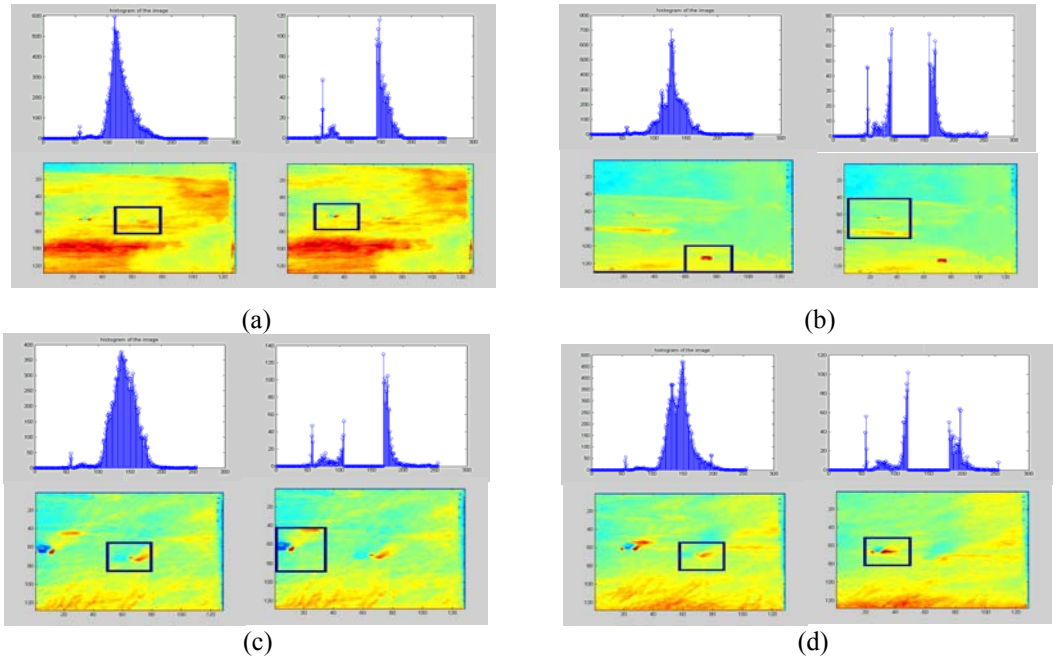

Fig. 2 Detection and Tracking multi- object case

The plots in the Fig. 2 correspond to the detection and tracking of 2 different images in multiple frames. The plots on the top left corner in Fig. 2(a), (b), (c) and (d) show the histogram of the raw image. The peak in the histogram corresponds to the intensities of the most dominant object in the frames. The plots on the lower left in all Figures correspond to the detection and tracking using the raw images with no intensities removed. The plot on the top right corresponds to the histogram of the image with the intensities of the most dominant object removed while the plots on the lower right correspond to the detection and tracking of next dominant object in the frame. We have experimented with algorithm to detect and track the multiple objects on other image sequences in the database and obtained the similar results.

c) Selection of Initial Reference frame (Intensity Algorithm)

The first reference frame is selected from the sequence L17_20 as shown in Fig. 3(a). Note that this selection is quite arbitrary. We only need a reference frame that helps us in

Fig .3 a) Raw Reference frame (L17_20, frame number 350) and b) Pre-processed frame (L17_20, frame number 500)

locating the high intensity region in the sequence for detection and tracking of targets. It is important to note that while our algorithm performance results shown herein are obtained using a reference frame, however, this requirement is not mandatory. To prove this hypothesis that we really do not need any specific reference frame, we have done pre-processing on another frame as shown in Fig. 3(b). We show the resulting detection and tracking in Fig. 4.

The dark box corresponds to the box created using the tracking algorithm and bright box is the box created using the GT data. Figure 4 and suggests that the pre-processing is good enough to select 'any' reference from a sequence for successful detection and tracking.

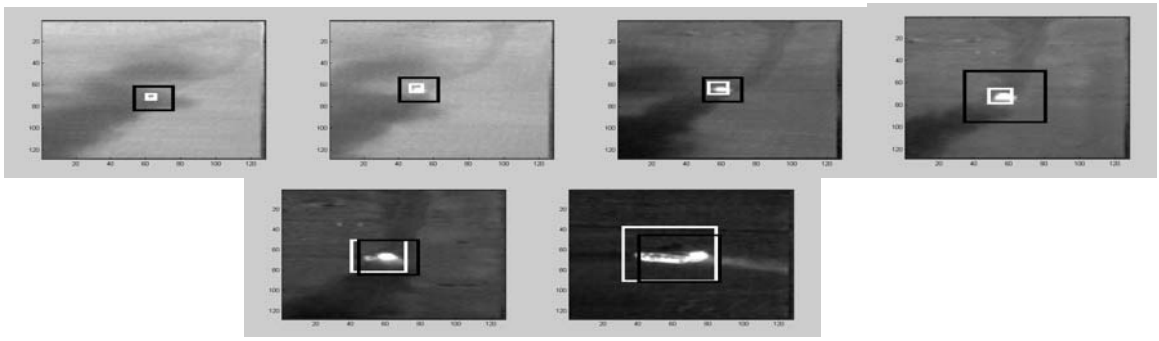

Fig. 4 Verification of detection and tracking based on intensity with ground truth data.

2.2 Bayesian Algorithm

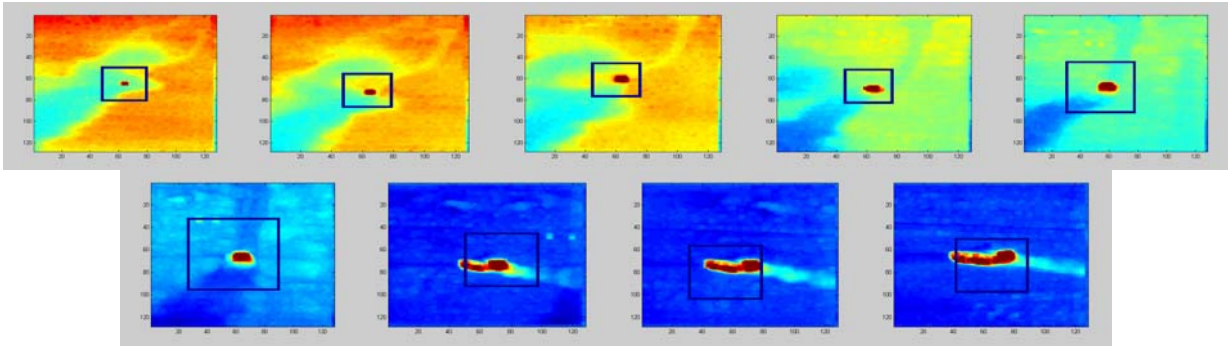

Fig 5 Single Target Detection and Tracking results using Bayesian algorithm (sequence L17_20)

Figure 5 shows the detection and tracking results obtained using Bayesian algorithm. From the Figure it is evident that the relative change in intensity is not much and hence we obtain better detection and tracking results. Figure 6 shows the error in detection and tracking of the object due to the drastic changes in the intensity using algorithm.

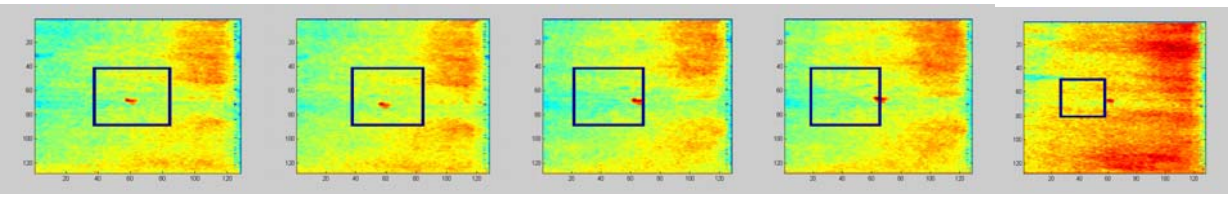

Fig.6 Drastic change in intensity in successive frames results in error in the successive frames (Sequence L22_08)

Figure 7 shows the multi-target detection and tracking results. From the Figure, it is evident that satisfactory detection and tracking results have been obtained.

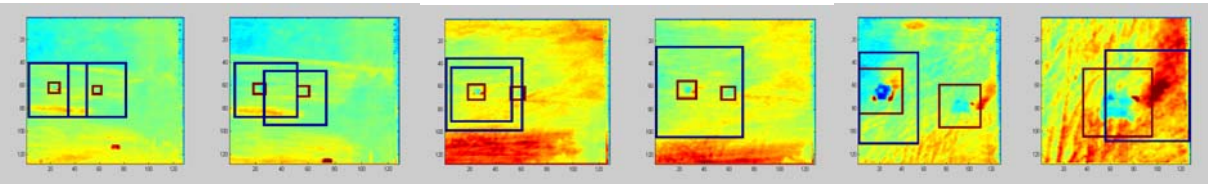

Fig.7 Multiple Target Detection and Tracking results using Bayesian algorithm (Sequence L18_16)

3.3 Hilbert-wavelet based Analysis

a) Out-of-plane rotation angle detection

We first select the 278 image frames that represent out-of-plane rotation from the L17_20 sequence of 778 frames at regular intervals. Frames in Fig. 8 clearly show an example of out-of-plane rotation and scaling since the image in the first frame is moving towards the northeast direction while the last frame is moving towards northwest.

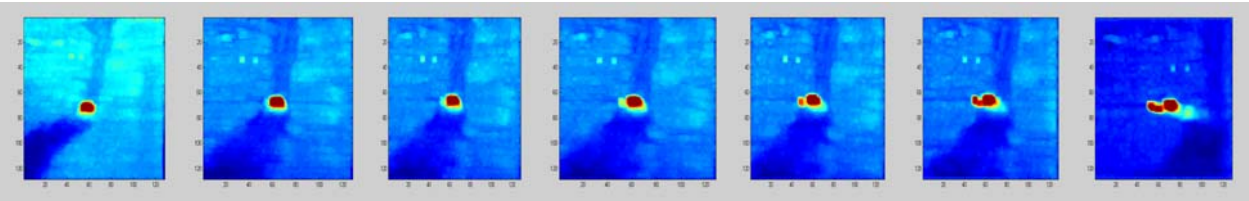

Image at 0^0 Image at 15^0 Image at 30^0 Image at 45^0 Image at 60^0 Image at 75^0 Image at 90^0

Fig. 8 Out of plane rotated and scaled image database

From the results obtained in Fig.9 (a), we find that there are only two cases, wherein the rotation angles have been improperly determined. A close observation of the test images in the database suggests that objects in the same two frames do not have enough information. Graphs with corresponding correlation values are shown in Fig. 9(b). The two dips at frame numbers 41 and 154 correspond to the two hikes corresponding to two confused cases in Fig. 9(a).

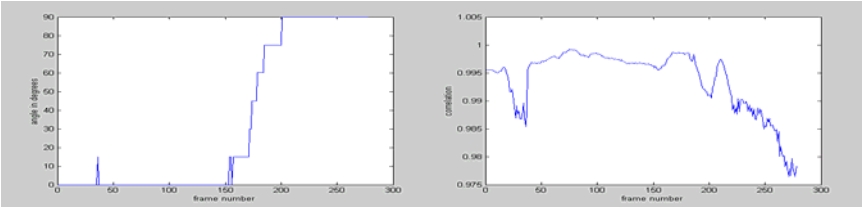

(a) (b)

Fig .9 Rotation angle determinations with Hilbert wavelet (a) Frame number vs. Rotation angle (b) Frame number vs. Correlation

b) Improved Detection and Tracking (Distorted case using Hilbert-wavelet)

The next task involves the detection and tracking of the object based on the correlation value. Note that this Hilbert-wavelet analysis is performed as part of our other ongoing research in the relevant areas. The tracking of the target improves further when we use the reference images exactly similar to the test image as shown in Fig. 8. The tracking results using the Hilbert wavelet correlation is shown in Fig. 10. Comparing Fig. 5 and Fig. 10 it is clear that objects may be tracked by using reference images similar to test cases but different in scale, angle (in plane and out of plane) or combination of both and more efficient tracking can be achieved by using the images exactly similar to the test cases.

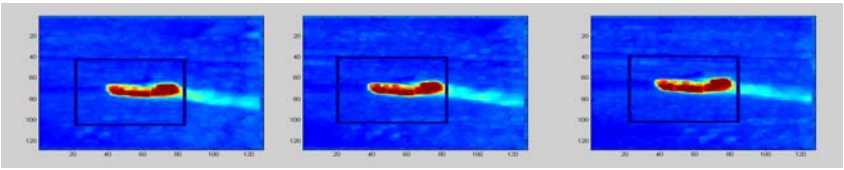

Fig. 10 Tracking of objects, improved cases**.**

In summary, four general purpose algorithms and one mathematical analysis for image preprocessing, detection and tracking the targets have been proposed. We discuss two of these techniques in detail since the other techniques involve similar steps. The results obtained for detection and tracking have been presented. We have experimented our detection and tracking algorithms on other sequences in our database and obtained the similar results. Detection and tracking of the multiple objects in the frame has also been successful. Most of the frames in the image sequence have been detected and tracked successfully.

3. Classification

a) SOM Classification with Intensities as feature vector

Consider the extracted intensity features obtained from the IR image database [25] as shown in the Fig 11.

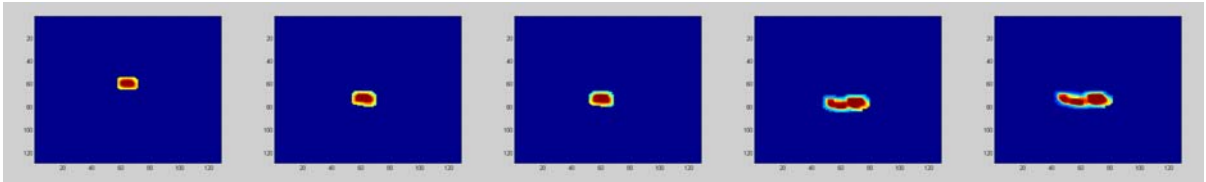

Fig. 11 Features of the object with background removed.

Fig. 11 shows the resulting intensity features. The dataset consists of images, which contains out-of-plane rotation and scale variations. From Fig. 11, it is obvious that the images in the first row show the scale change and the images in the bottom row show both angle and scale changes. We take the images at regular intervals of 30 frames in a sequence of 378 images for training such that the images are sufficiently different from each other. Euclidean distance is a good measure of similarity between the images. Thus, we calculate the Euclidean distance as shown in Table 1 to ascertain that the resulting eight training cases are sufficiently different from each other. From the Table 1 it is clear that only training cases 2 and 3 are similar, and the rest of the cases are sufficiently different from each other. Thus, ignore training case 3 and trained the network using the rest of the cases.

Table 1. Euclidean distance between the training cases.

Training Image	1	2	3	4	5	6	7	8
1	0	0.0290	0.0290	0.0309	0.0271	0.0297	0.0584	0.0666
2	0.0290	0	2.4734e-004	0.0027	0.0133	0.0206	0.0337	0.0486
3	0.0290	2.4734e-004	0	0.0026	0.0132	0.0206	0.0338	0.0486
4	0.0309	0.0027	0.0026	0	0.0125	0.0198	0.0314	0.0464
5	0.0271	0.0133	0.0132	0.0125	0	0.0086	0.0323	0.0417
6	0.0297	0.0206	0.0206	0.0198	0.0086	0	0.0321	0.0375
7	0.0584	0.0337	0.0338	0.0314	0.0323	0.0321	0	0.0214
8	0.0666	0.0486	0.0486	0.0464	0.0417	0.0375	0.0214	0

Examples of 3 different clusters out of 8 are shown in Fig. 12 with cluster centers along with corresponding few images in each cluster. From the classification plots in Fig. 12, it is obvious that the similar images have been clustered in one cluster. Images in cluster 1 are the ones after the image has undergone out-of-plane rotation of 90^0 while moving along y-axis. Images at smaller scales are grouped in cluster 2, while those at an intermediate scale are grouped in cluster 3. The images in cluster 7 are at a higher scale and those in cluster 8 are at smaller scales and are moving at 0 degrees with respect to y-axis respectively. The images in cluster 4 are the ones when the image was undergoing some angle change with respect to y-axis. Cluster 5 captured the occluded objects. They are classified as the images which have undergone out-of-plane rotation of 90^0 but smaller in scale. Finally, cluster 6 consists of predominantly the noise points.

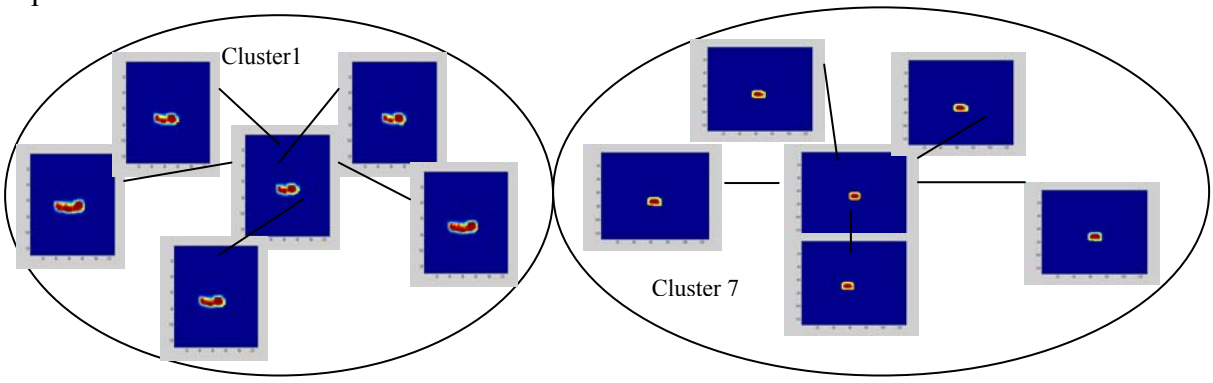

Fig. 12 Cluster plots for Image sequence database 1.

b) SOM Classification with Shape as feature vector

As discussed earlier we keep the first 30 DCT coefficients to retain most of the information. The training set is selected manually and care has been taken that they are taken at regular intervals of 30 so that they can be sufficiently different from one another. We determine the Euclidean distance among the images in order to find how similar or dissimilar the images are as shown in Table 2.

Table 2. Euclidean distance between training cases

Training image	1	2	3	4	5	6	7	8
1	0	5.1710	2.7832	6.0188	6.6933	7.5902	38.3086	69.9684
2	5.1710	0	3.6456	1.7805	1.9442	3.3205	33.5627	66.8063
3	2.7832	3.6456	0	4.7818	5.0050	5.9175	36.4828	69.5037
4	6.0188	1.7805	4.7818	0	2.0195	3.3377	32.9519	65.9773
5	6.6933	1.9442	5.0050	2.0195	0	2.1245	32.0379	66.3667
6	7.5902	3.3205	5.9175	3.3377	2.1245	0	31.1081	67.1602
7	38.3086	33.5627	36.4828	32.9519	32.0379	31.1081	0	58.3008
8	69.9684	66.8063	69.5037	65.9773	66.3667	67.1602	58.3008	0

From the Table 2, it is evident that the training images are dissimilar enough to be considered as different training cases. When we train the SOM using the different training cases, the similar shapes are grouped as centers of nearby clusters while the dissimilar shapes are grouped in different clusters. From Fig. 13 (2 out of six are shown), it is clear that the images belonging to the similar shape are classified as one cluster. The images in cluster 1 show the shape of the image after the image has undergone 90^0 rotation with respect to its original motion.

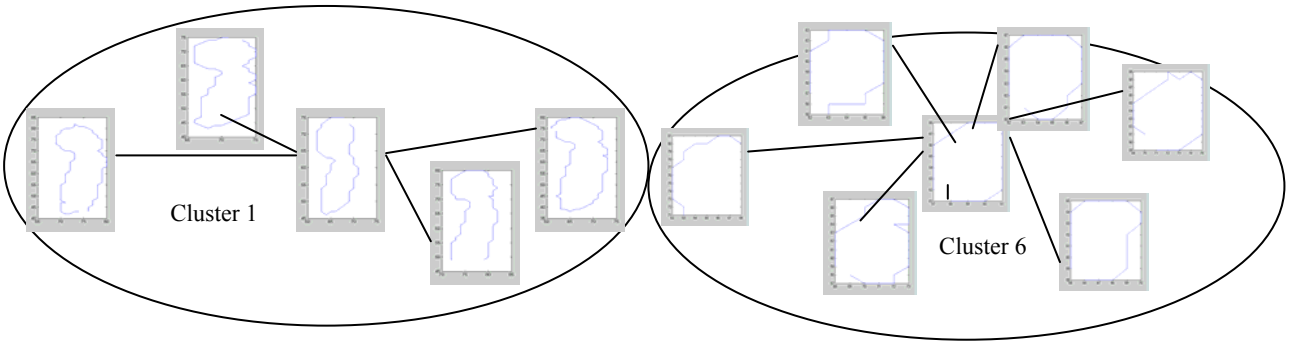

Fig. 13 Classification using the SOM with edges as feature vectors.

Cluster 2 consists of images that may not be traced properly. It also includes the images that are similar to mis-traced images. Cluster 4 consists of images that are partially occluded. Cluster 3, 5, 6 have images of similar shape but cluster 5 has mis-traced images. From our observation of the dataset we find that the object moves at an angle of 90^0 with respect to its original motion

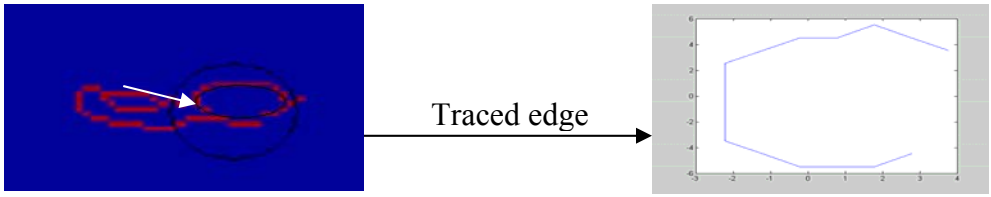

Fig. 14(a) Edge and (b) Mis-traced edge.

after frame number 300 (out of 375 frames) are the ones after the image has moved at an angle of 90^0 with respect to its original motion. When we plot the traced contour of these confused cases, we observe that image frames are not traced correctly as shown in Fig. 14. As a result, these partially edge-traced frames were grouped in the wrong clusters by SOM classifier.

c) k-NN Classification with Shape as feature vector

The results of the k-nearest neighbor classifier are obtained and results obtained by varying the usage of statistical features are observed.

i) Results using intensity features

We show an example classification result using the intensity features form L17_20 data sequence below.

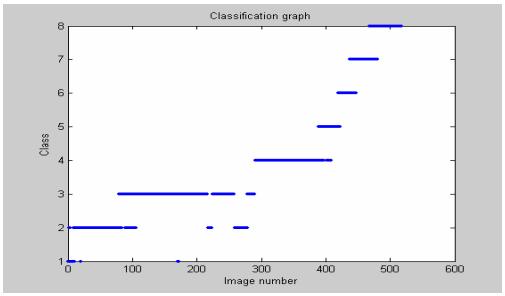

Fig.15 Class vs. image number using all intensity features

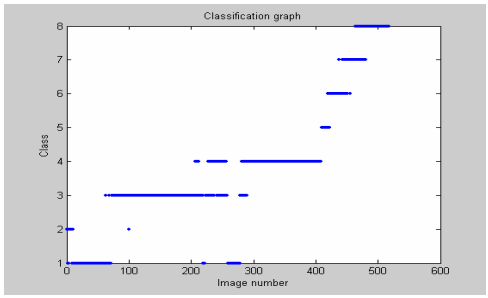

Fig.16 Classes vs. image number using statistical features

Figure 15 shows how many images are classified under in each of the 8 classes that we have pre-defined. The description of the individual classes is shown in Fig. 16.

Class1	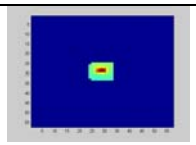	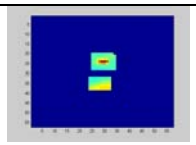	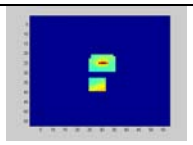	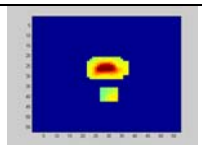
Class3	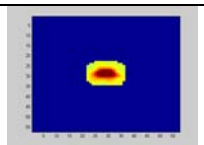	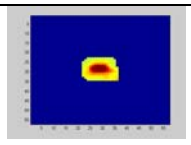	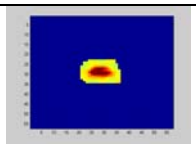	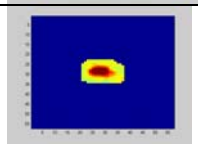
Class5	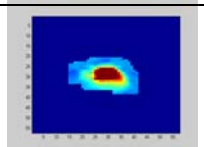	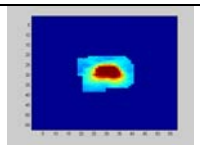	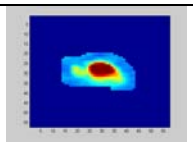	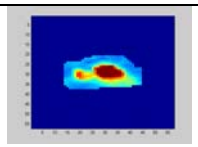

Class8	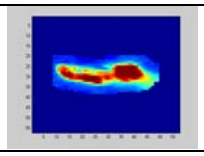	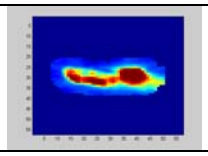	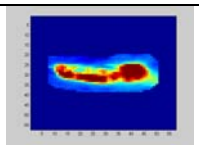	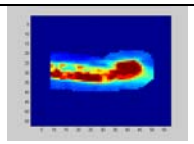

Fig.17 Example of different classes

Cluster 1 consists of images with improper segmentation. Cluster 2 consists of images when the object has not undergone rotation at higher scale. Cluster5 shows images when object is just making a turn. Cluster 8 shows objects at high scale when object has undergone 90 degrees rotation and it also shows occluded objects classified correctly as one of non occluded objects.

ii) Results using statistical features

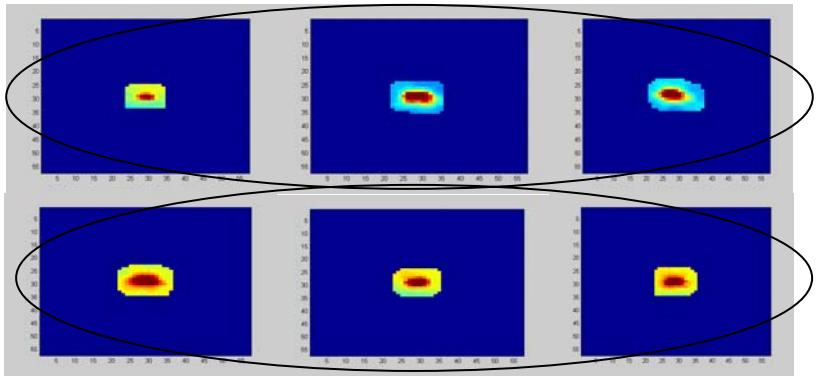

Fig.18 Similar images from cluster1 and cluster 3

We show an example classification result using the statistical features such as mean, variance, maximum, minimum form L17_20 data sequence in Fig. 17. All the intensity features are now replaced by statistical features. The image (region of interest (57 x 57)) is now taken and divided into blocks of 8 x 8 and each block is replaced by statistical features. Each of these statistical features are first normalized by dividing the whole matrix by maximum number in that matrix. This is done in order that one particular feature not have major impact on classification. The results obtained are similar to the ones shown above.

The improperly segmented images now fall into cluster2. Some of the images from cluster 1(previously using all intensity features) are now classified under cluster 3. Careful observation of data shows that there is not much change between images of cluster 1 and cluster 3 respectively as shown in Fig. 18.

4. Performance Metrics

We obtain the Receiver Operating Curves (ROC) metrics for our Intensity-based algorithm as shown below.

4.1 Results for the ROC curves

We plot detection and tracking performance vs. filter size and filter resolution in Figs. 20 and 21 respectively.

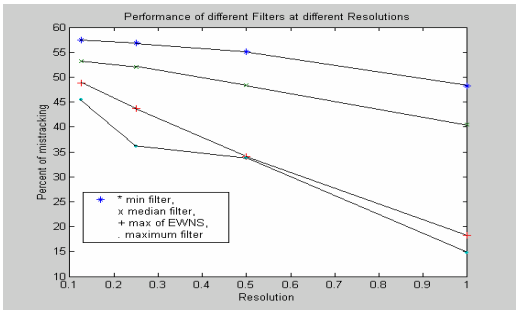

Fig 19 Performance of 1) Minimum filter, 2) Median filter, 3) Max of east west north south filter and 4) Maximum filter for varying window size.

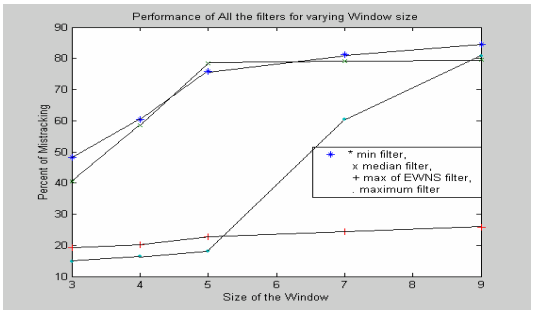

Fig 20 Performance of the filters at different resolutions

In Fig. 19 note that the x-axis variable represents the following format (3 represents 3 x 3, 4 represents 4 x 4 and so on) for the size of the window. From the plot is clear that the maximum filter for the window size of 3 x 3 offers the best tracking performance. We perform the detection and tracking algorithm for various resolutions of the images. The resolution increases as we move from left to right along the x-axis. From the Fig. 20, it is evident that increasing the resolution offers better tracking for all types of rank-order filters considered. From Fig. 21 it is clear that higher percent of compression yields increasing percent of mis-tracking.

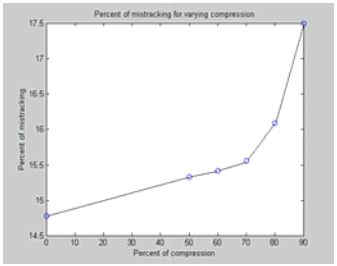

Fig 21 Change in % of tracking for varying compression

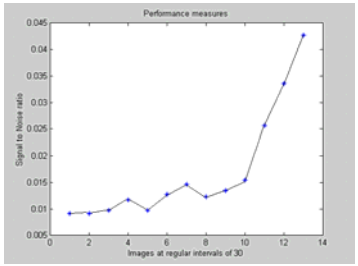

Fig. 22 Signal to noise ratio of the images taken at regular intervals of 30

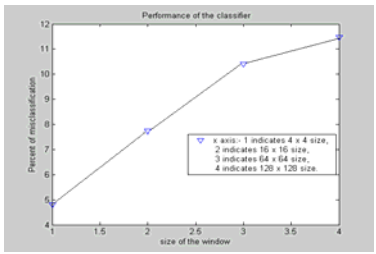

Fig. 23 Performance of the classifier for varying window size

The SNR is obtained and it is plotted in Fig. 22 for images at regular intervals of 30 for a sequence of 778 images. As the potential target size increases in the frame sequence (change of scale), the signal to clutter ratio also increases as shown in Fig. 23 as the target becomes larger. From Fig. 23 it is clear that smaller block size offers better classification.

4.4 Composite Metrics

We summarize our results and experiments of our proposed algorithm in Table 3. Table 3 shows the summary of most of the results obtained in this work. From the table it is obvious that discarding about 50 % of the coefficients offers a reasonable result. The classification using the SOM gave a reasonable classification of about 89 % using statistical features and about 82.16 % using the shape features. The rest of the results are obvious.

Table 3. Summary of results.

Image sequence		In-plane rotation identification results				Out-of plane rotation identification				Tracking	Classification	
SOC	MOC	Seg.	T* s/f	% M-det	Avg. corr	% of Comp.	T* s/f	% M-det	Avg. corr	% M-Tr.	Features	SOM (% of classification)
L1720	-	No	2.881	0	91.6	0	2.00	0.72	99.2	0.64	Intensity Shape	89.92 82.16
L1720	-	No	2.822	0	90.8	50	1.72	0.72	99	-	-	-
L1720	-	No	2.08	0	82.3	80	1.117	47.1	90	-	-	-
L1720	-	No	1.999	0	77.8	90	1.01	87.98	87.87	-	-	-
L1720	-	Yes	0.460	0	74.6	0	1.516	67.27	95.3	-	-	-
-	L1818	No	2.880	0	95.5	0	2.01	0.38	92.38	6	-	-
-	L1818	Yes	2.822	0	94.3	50	1.72	0.38	90.36	-	-	-
-	L1818	Yes	2.08	0	89.1	80	1.117	37.33	90.28	-	-	-
-	L1818	Yes	1.999	0	88.02	90	1.01	79.97	87.82	-	-	-

*933 MHz p-3 xeon processor with 256 MB of memory

SOC: Single object case.
MOC: Multiple object case.
Seg. : Segmentation.
T s/f: Time in seconds per frame
% M-Tr: Percentage of Mistracking (Ratio of number of images, which have not been tracked to the total number of images).

% M-det: Percentage of mis-detection (Ratio of number of images whose angle has been identified wrongly to the total number of images).
Avg. corr: Average correlation.
% of Comp: Percentage of compression (Ratio of number of discarded coefficients to the total number of coefficients).
SOM: Self organizing map.
T s/f: Time in seconds per frame

4.5 Comparison Metrics

In Table 4 below, we summarize the comparative performance metrics of our four general purpose detection and tracking algorithms described above for all 50 data sequences in the AMCOM database.

Results obtained at U of M

ID No.	Sequence name	No. of frames	No. of targets	description of targets in the sequence	SNR (# of target pixels divided by background)	% of Detection and Tracking (Intensity_algorithm)	% of Detection and Tracking (correlation_algorithm)	% of Detection and Tracking (bayesian_algorithm)	% of detection and tracking corr_frequency algorithm	%of Detection and tracking (manual_combined_summary)	%of Detection and tracking (automated_combined_summary)
1	L15_20	215	1	tank	0.0127	tank 85.58%	tank 83%	tank 100%	tank 18.13%	tank - 100%	tank - 74%
2	L15_NS	320	2	tank1, truck1	0.0097	tank1 76.42% & truck1- 9%	tank1- 75.4% truck1- 9.5%	tank1(75/320)23%, truck(8/20) 40%	tank1- 38.75%	tank1- 75%; truck 40%	tank1- 65%; truck 55%
3	L16_04	400	1	tank1	x	no binary files exists	66%	89%	30.57%	no GT to compare	no GT to compare
4	L16_07	410	3	tank1, mantruck, tank1	0.0093	tank1 86% mantruck 77.98% tank1 30%	tank1 90% mantruck 81.91% tank1 30%	tank1(244/410) 60% mantruck (386/386) 100%	tank1- 22.7%	tank1 - 90%; mantruck 100%; tank1 - 30%	tank1 - 86%; mantruck 78%; tank1 - 30%

5	L16_08	290	3	m60, apc1, mantruck	0.0175	mantruck 67.8% m60 100% apc1 32%	mantruck 69.38% m60 100% apc1 31.33%	mantruck (37/98)38 % m60(290/ 290)100 %;apc1(5 2/83)63%	m60%- 50%	m60- 100%; apc1 - 84%; mantruck - 69%	m60-100%; apc1 - 100%
6	L16_18	300	3	apc1, m60, truck	0.0184	apc1 for 83.85%, m60 for 12.12%	apc1 83% m60 13.33% truck 0%	apc1(291 /291)100 %;m60(3 4/102)33 %truck(7/ 7)100%	apc1- 40.54%	apc1- 100%; m60-33%; truck- 100%	apc1-100%; m60-95%; truck-100%
7	L17_01	388	2	bradely,pic kup	0.0125	bradely 84.7% pickup 0%	bradely 95.14% pickup 0%	bradely(1 00/371)2 7% pickup(16 /46)35%	bradely- 41.5%	bradely- 95%; pickup- 42%	bradely- 75%; pickup-0%
8	L17_02	698	5	Man pickup bradely	0.0047	mantruck 53.9% and bradely 27%	mantruck 1 40% pickup 0% bradely 30%	mantruck (273/459) 60%,pick up(46/69) 67%,brad ely(214/3 43)62%,t ank(50/5 0)100%	mantruck - 33.2% tank1- 8.1% bradely- 40.24%	mantruck- 60%; bradely- 62%; tank- 100%; pickup- 67%	mantruck- 59%; bradely- 49%; tank- 100%; pickup-0%
9	L17_20	778	2	target, m60	0.011	m60 70.5% target 0%	target 5.7% m60 71.16%	target(0/3 5)0% m60(743/ 743)100 %	target- 73.6% m60- 69.45%	target- 73.6%; m60-100%	target-14%; m60-78%
10	L18_03	450	1	bradely	0.0046	bradely 58%	bradely 69.12%	27%	bradely- 54.8%	bradely- 69%	bradely- 64%
11	L18_05	779	4	tank1, apc1, m60, tank	0.0053	no GT data	no GT data	no GT data	no GT data	no GT to compare	no GT to compare)
12	L18-07	260	1	bradely	0.00952	bradely 94%	bradely 97%	bradely 78%	bradely- 36.5%	bradely- 97%	bradely- 96%
	L18_12	300	3	bradely, tank1, m60	0.0108	bradely 96%	bradely 86.66% tank1 15.08%; m60 8.6%	bradely(3 00/300)1 00%;tank 1(202/20 2)100%; m60(94/9 4) 100%	bradely- 37.66%	bradely- 100%; tank1- 100%; m60-100%	bradely- 97%; tank1- 92%; m60- 100%
14	L18_13	326	3	tank1, m60, apc1	0.0204	tank1 82.52% m60 48% apc1 22%	apc1- 26.58% tank1- 84.59% m60- 53.04%	apc1- (78/170) 46%	tank1- 40.97%	tank1- 85%; m60- 53%; apc1-46%	tank1-85%; m60-95%; apc1-83%
15	L18_15 seq-1	339	4	m60, truck, tank1, bradely	0.0098	tank1- 68.9% bradely 75%	m60- 45.62% truck-9% tank1- 81.75% bradely- 74.886%	m60- (238/238) 100% tank1- (103/285) 36%	m60- 43.67% tank1- 20.33% bradely- 18.7%	m60- 100%; truck- 100%; tank1- 82%; bradely- 100%	m60-99%; truck-92%; tank1-97%; bradely- 85%
								truck(12/ 12) 100% bradely(1 87/187) 100%			

16	L18_15 seq-2	342	3	m60, tank1, bradely	0.0121	tank1 87%	m60-46.63% tank1-84.27% bradely-77.77%	m60 (243/243) 100% tank1 (208/314) 66% bradely (181/191) 95%	m60-2.9% tank1-27.24% bradely-29.25%	m60-100%; tank1-87%; bradely-95%	m60-100%; tank1-90%; bradely-90%
17	L18-17 seq-1	240	2	tank1, m60	0.0145	different objects for 66%	tank1-57.9% m60-96%	tank1(120/240) 50% m60(198/198) 100%	tank-2.5%	tank1-58%; m60-100%	tank1-88%; m60-100%
18	L18_17 seq-2	266	2	tank1, m60	0.00153	no gt.lis file various objects 70%	no gt.lis file	no gt.lis file	no GT.lis file	no GT file to compare	no GT file to compare
19	L18_16	328	2	tank1, m60	0.0205	tank1-44.9% and m60 20.43%	tank1-61.58% m60-51.54%	tank1 (145/329) 44% m60 (290/290) 100%	tank1-22.86%	tank1-62%; m60-100%	tank1-53%; m60-99%
20	L18_18	365	6	mantruck, target, apc1, m60, tank1, testvan	0.0224	tracking algorithm confuses for first 140 frames tank1 for 78.1%	mantruck -4.2% apc1-24% m60-21.77% tank1-81.86% testvan-0% target-25%	mantruck - (33/44) 75%, target - (3/4) 75%, apc1 - (56/95) 59%, m60 - (44/121) 37%, tank1 - (205/213) 96%, testvan - (4/4) 100%	mantruck - 7.4% target-9.6% apc1-5.31% m60-11.4% tank1-13.6%	mantruck-75%; target-75%; apc1-59%; m60-37%; tank1-96%; testvan-100%	mantruck-60%; target-75%; apc1-66%; m60-53%; tank1-99%; testvan-100%
21	L19_01	240	1	tank1	0.0145	Tank1 74.3%	tank1-68.3%	Tank1 0%	tank1-53.33%	tank1-74%	tank1-79%
22	L19_02	270	1	tank1	0.0359	tank1 10%	tank1-84.7%	Tank1 0%	tank1-31.88%	tank1-85%	tank1-91%
23	L19_04	270	1	tank1	0.0454	tank1 80.74%	tank1-73.34%	Tank1 37%	tank1-44.44%	tank1-81%	tank1-78%
24	L19_06	265	4	tank1, apc1, mantruck, van	0.041	tank1 for 27.42%	tank1-84.9% apc1-92.4% mantruck-65% van-0%	tank1 (265/265) 100% apc1 (238/265) 90% mantruck (69/197) 35% van (20/20) 100%	tank1-34.45%	tank1-100%; apc1-90%; mantruck-65%; van-100%	tank1-69%; apc1-83%; mantruck-61%; van-100%
25	L19_07	195	1	mantruck	0.0441	mantruck 14.53%	mantruck -7%	mantruck 94%	mantruck - 58.8%	mantruck-94%	mantruck-83%

26	L19_10	130	2	tank1, apc1	0.0413	tank1 87%	apc1-51.35% tank1-83.33%	tank1 (130/130) 100% apc1 (90/90) 100%	tank1-41.22%	tank1-100%; apc1-100%	tank1-100%; apc1-100%
27	L19_11	165	2	tank1, apc1	0.0874	tank1 for 93.94%	tank1-95.15% apc1-98.78%	tank1 (165/165) 100% apc1 (165/165) 100%	tank1-23.6%	tank1-100%; apc1-100%	tank1-100%; apc1-100%
28	L19_13	265	4	tank1, apc1, m60, mantruck	0.0474	tank1 for 77.78% t	tank1-83.9% apc1-86.79% m60-80% mantruck -40%	tank1 (106/264) 40% apc1 (208/264) 79%; m60 (35/66) 53% mantruck (12/12) 100%	tank1-32.07%	tank1-84%; apc1-87%; m60-80%; mantruck-100%	tank1-93%; apc1-84%; m60-82%; mantruck-100%
29	L19_15	350	5	tank1, apc1, m60, van, apc1	0.0454	tank1 for 70.86%	m60-63.41% tank1-63.6% van-59.44% apc1-54.16%	m60 (184/347) 53% tank1 (129/332) 39% apc1 (76/189) 40% van (65/216) 30%	m60-26.7% apc1-25.2% tank1-20.4% van- 18%	tank1-71%; apc1-54%; m60-63%; van-59%; apc1-54%	tank1-86%; apc1-84%; m60-86%; van-74%; apc-72%
30	L19_18	260	2	tank1, m60	0.0078	tank1 60% m60 98%	tank1 52.99% m60 90%	tank1 (54/260) 21% m60 (12/12) 100%	tank1-18.37%	tank1 - 60%; m60-100%	tank1 - 48%; m60-100%
31	L19_NS	275	3	m60, mantruck, tank1	0.0509	different objects 78.6%	m60-63.79% mantruck -62.6% tank1-77.51%	m60 (40/50) 80% mantruck (117/137) 85% tank1 (41/99)41 %	m60-50.24% mantruck - 37.13% tank1-32.8%	m60-80%; mantruck-85%; tank1-78%	m60-91%; mantruck-62%; tank1-68%
32	L20_04	368	1	apc1	0.0039	apc1-87%	apc1-83%	apc1-100%	apc1-26.35%	apc1-100%	apc1-66%
33	L20_08	348	1	apc1	0.0121	apc1 60.81%	apc1-44.8%	no object	apc1-11.49%	apc1-61%	apc1-32%
34	L20_17	308	1	tank1	0.0108	tank1-100%	tank1-96.3%	no object	tank1-23.43%	tank1-100%	tank1-66%
35	L20_18	448	1	tank1	0.0034	tank1-100%	tank1-85%	72%	tank1-25.66%	tank1-100%	tank1-59%
36	L20_20	420	2	tank1, target	0.0037	target-72%	no gt data	no gt data	no GT data	no GT to compare	no GT to compare

37	L21_04	760	2	bradely, tank1	0.0087	follows the gt data 100%	bradely-17.55% tank1-88.5%	bradely (44/321) 14% tank1 (481/746) 65%	bradely-1.4% tank1-0%	bradely-18%; tank1-89%	bradely-35%; tank1-89%
38	L21_15	738	1	bradely	0.0105	bradely-98.8%	bradely-93.76%	hard to see object	bradely-21%	bradely-98%	bradely-89%
39	L21_17	360	1	apc1	0.0087	apc1-96.11%	apc1-94.44%	apc1-100%	apc1-47.77%	apc1-100%	apc1-74%
40	L22_06	348	1	tank1	0.0237	tank1-47.42%	tank1-17%	tank1-77%	tank1-45.4%	tank1-77%	tank1-36%
41	L22_08	380	1	apc1	0.0219	apc1-98.1%	apc1-93%	apc1 -100%	apc1-67.1%	apc1-100%	apc1-100%
42	L22_10	398			x	no Gt data	no Gt data	no Gt data	no GT data	no GT data	no GT data
43	L22_14	350	2	m60, target	0.0221	m60-54.18% target-43%	target - 26.31% m60-48.175%	m60 (112/273) 41% target (75/75) 100%	m60-12.68% target-14.86%	m60-54%; target-100%	m60-42%; target-100%
44	L23_12	368	1	apc1	0.0071	apc1-82.1%	apc1-89.4%	apc1-100%	apc1-82.88%	apc1-100%	apc1-87%
45	M14_06	380	1	bradely	0.0121	bradely-53.23%	bradely-61.49%	bradley-100%	bradely-36%	bradely-100%	bradely-100%
46	M14_07	400	1	bradely	0.0125	bradely-66.84%	bradely-57.43%	breadely 100%	bradely-21.42%	breadely-100%	breadely-100%
47	M14_10	498	2	tank1, mantruck	0.0236	tank1-68.1%	tank1-73.8% mantruck -57.14%	tank1-40% mantruck -50%	tank1-66.93%	tank1-74%; mantruck-57%	tank1-100%; mantruck-99%
48	M14_13	380	1	mantruck	0.0147	mantruck -51.89%	mantruck -76.34%	mantruck -30%	mantruck - 27.36%	mantruck-76%	mantruck-76%
49	L14_15	281	1	mantruck	0.0127	mantruck -76.16%	mantruck -83.6%	mantruck -100%	mantruck - 52.44%	mantruck-76%	mantruck-76%
50	M14_15	528	2	mantruck, target	0.0132	target-38%	mantruck -56.37% target-0%	mantruck (35/380) 9% target (20/20) 100%	mantruck - 45.24%	mantruck-56%; target-100%	mantruck-53%; target-84%

5. Conclusion

In this work, we first propose an image pre-processing and segmentation algorithm to remove most of the background noise and clutter from IR image dataset. We then introduce four novel algorithms and an elegant mathematical technique to detect and track the objects of interest. We also introduce techniques for building the tracking box to capture the image of interest and extraction of the features for classification once the target is detected. The proposed algorithms have been used on different image sequences in the IR database, and the resulting image detection and tracking performance has been summarized extensively. Our single object-based algorithm exploits the image correlation statistics for tracking the most dominant object in the frame. Based on the knowledge of the histogram, we have extended our algorithm to track multiple objects in a frame. In the unlikely but possible event when two objects contain same intensity, our tracking algorithm may track one object or the other object at a time. Further, if the

similar intensities are present in the background as well as in dominant object, intensities of object may be lost due to the pre-processing, and, hence it is never tracked. For an example, for L18_16, even though we observe only one window for tracking, it corresponds to more than one object, and the random placement of the window is due to the existence of highest frequency component randomly occurring in the frame. Thus, it appears that the same window is tracking different objects.

As mentioned above, we do not assume any prior knowledge of the target in our Intesity, Correlation_time and Correlation_frequency algorithms while we assume full knowledge of target location in our Bayesian algorithms using the GT data. Off course, we pay a price for this uncertainty of knowledge of the target in our first three algorithms- i.e., we obtain relatively poor performance as evidenced in the performance metrics summary results. Thus, we detect and track background sometimes in the first three algorithms. Note that in Intensity algorithm we detect and track one target at a time while in Correlation_time algorithm, we detect and track two dominant intensity targets at a time. At this time, this appears to be a reasonable limit of our image preprocessing and segmentation function that retains only enough intensity information of two targets at a time. However, in all cases, when we detect and track any target, we verify its accuracy using GT data automatically.

For the mathematical technique development, we explore the wavelets in the determination of the exact angle of rotation between the images. We compare the performance of the Hilbert transform only and Hilbert wavelet transform in the determination of the exact angle of rotation between the images. Note that this Hilbert-wavelet analysis is performed as part of our other ongoing research in the relevant areas. Further, to enhance the speed of operation as well as data reduction, we have developed a zonal mask that discards up to 50% of the insignificant transformed coefficients while retaining most of the information. In the determination of in-plane rotation, the performance of the Hilbert wavelet and the Hilbert transform is comparable. However, for the out-of-plane rotation case, Hilbert wavelet offers improved performance with a less number of false alarms. Detection and tracking performance with Hilbert transform and Hilbert wavelet are the same except the fact that Hilbert wavelet offers greater correlation value and thereby improve tracking. Further, we have developed very flexible GUI that allows for integration for not our algorithms, by also additional relevant algorithms quite easily. This GUI may be instrumental in automated comparison and decision fusion of algorithms for better target detection and tracking.

We take advantage of our novel pre-processing, detection and tracking algorithms in discarding unwanted frames in a sequence of images. This improves the subsequent classification performance of our classifier. We perform block processing on the remaining pre-processed and noiseless frames and extract various statistical intensity features such as the mean, variance, minimum and maximum intensity values of the image from every block and use them as feature vectors for classification. We propose an algorithm to extract shape features of the object based on the clean edges of an image. We have proposed an edge-tracing algorithm to trace the coordinates of the edge points of the image. We render the edges invariant by shifting them to the centroid of the image. We sample it to have edges of the order of powers of 2. We take the first few DCT coefficients to represent the shape and make them invariant to scale. Finally, we use the reduced number of shape-related DCT coefficients as the input for classification.

We use self-organizing maps (SOM) as the classification algorithm as we consider the data to be unlabeled. The usage of SOM classification offers a reasonable number of clusters

(average of 7 or 8) for 400 frames for an example sequence from image database. In addition, detection and classification of infrared images is performed using the Bayesian conditional probability algorithm and K- nearest neighbor (NN) classifier. We also investigate the sensitivity of the algorithm to different parametric variations. Various examples illustrating the limitation have been shown. From the results, it is clear that the statistical features offer better classification results. However, we must emphasize that in order to obtain a reasonably accurate classification of data, we require robust reference (example) images for training and target class identification. The current dataset provided by AMCOM do not contain such 'pristine' reference targets. Thus, all these classification results in this report are intended to demonstrate the possible directions in the event if such reference images are available.

6. References

1. K. M. Iftekharuddin, C. Rentala and A. Dani, "Determination of exact rotation angle and classification for rotated images", vol. 34, pp. 313-327, Optics and Laser Technology, 2002.
2. E. W. Selesnick, "Hilbert Transform Pairs of Wavelet bases", Invited paper for information systems, The Johns Hopkins University March 21-23, 2001.
3. S. L .Diab and M. A. Karim and K. M. Iftekharuddin, "Multiobject detection of targets with fine details, scale and translation variations", Optical Engineering, vol.37, 876-883, 1998.
4. J. P. Thiran, "Recursive digital filters with maximally flat group delay", IEEE Transactions on Ckt. Theory vol. 18, pp 659-664 Nov 1971.
5. R. Nagendra and M. Laxminarayana." The principle of complex frequency scaling applicability in inclined continuation of potential fields", Geophysics, vol. 49, pp 2019-2023.
6. S. Richard F. Sims "Putting ATR Performance on an equal basis- The measurement of knowledge base distortion and relevant clutter" U.S. Army Aviation & Missile command.
7. S. Richard F. Sims "Data compression issues in automatic target recognition and measuring of distortion" U.S. Army Aviation & Missile command.
8. K. M. Iftekharuddin and J. Shaik, A. A. S. Awwal and M. S. Alam, "Hilbert-wavelet transform for recognition of image rotation", Proc. of SPIE, vol. 4788, pp. 147-158, Seattle, WA, July 2002.
9. K .M. Iftekharuddin and J. S. Shaik, "Hilbert-Wavelet transform for recognition of image rotation", SPIE Proc.,vol. 4788, pp. 147-158, 2002.
10. J. S. Shaik and K. M. Iftekharuddin, "Detection and tracking of rotated and scaled targets by use of Hilbert-wavelet transform", Applied Optics, vol. 42, pp. 4718-4735, 2003.
11. J. S. Shaik and K. M. Iftekharuddin, "Automated Tracking and Classification of Infrared Images", pp. 147-158, Vol. 4788, International Joint Conference on Neural Networks (IJCNN'03), Portland, OR, July 2003.
12. K. M. Iftekharuddin and J. Shaik, "Distorted IR target detection and tracking using composite filters", SPIE Proc., vol. 5201, pp. 73-84, San Diego, CA, August 2003.
13. K. M. Iftekharuddin and J. Shaik, "Probabilistic detection and tracking of IR targets", To appear, SPIE annual meeting in Photonic Devices and Algorithms San Diego, CA, August 2004.
14. J. S. Shaik and K. M. Iftekharuddin, "Automated Target Detection, Tracking and Classification of IR images", Under Preparation.

Theses Generated From This Project at University of Memphis

1. J. S. Shaik, Masters Thesis Title: Hilbert-wavelet transform-based rotated target detection and tracking, May 2003.

Evaluating Phase-Only Filter Algorithm Performance on ARO IR Image Sequences Using the Quality Metric Scene Evaluator
(Final report on the work performed at Wright State University)

Dr. A. A. S. Awwal (Co-PI)* and K. S. Gudmundsson (Graduate Student)
Department of Electrical Engineering, Wright State University, Dayton, Ohio 45435
*Lawrence Livermore National Laboratory, Livermore, CA 94551

Executive summary

This report summarizes the work performed at Wright State University. The Quality Metric Scene Evaluator (QMSE), a front end GUI and the search engine that was implemented earlier during this project was used to process the data. Trying to visually determining data quality is misleading[1], therefore, the ATR performance comparison is measured with the quantitative knowledge provided by the ground truth data provided. Visual inspection on the other hand can provide insight while debugging and improving algorithms.

The search engine design allows for easy plug in of multiple search methods. Therefore, scenes can be evaluated based upon the performance of different matching algorithms. The key idea of this search method is to take advantage of the "divide and conquer" concept. Instead of searching for a pattern in a large image, a smart approach is taken to divide the image space into overlapping pattern of sub-images. Search is then based on upon best match with sub-image. The QMSE uses the Ground Truth Data (GTD), supplied by ARO, to compare actual target location to the location determined by the tracker.

Introduction

This report is the final report from Wright State University on the ARO project. Progress made during the last trimester of 2003 is discussed. The direction of the project at Wright State University shifted by the year-end 2002, from one exploring and designing platform to evaluate different search algorithms, to the one of actually developing framework for performing experiments. ARO provided files containing Ground Truth data information to aid in this effort.

Quality Metric Scene Evaluator (QMSE)

During second quarter a Graphical User Interface (GUI) was developed to ease the task of evaluating different scenes, using different algorithms. This is the front end of the search engine designed and developed at WSU earlier to evaluate images. Still only a phase only filter is available to track objects in the scenes, but with two different algorithms to define area of interest. However, the search engine design allows for easy plug in of other search methods. Therefore, scenes can be evaluated based upon the performance of different search algorithms.

The key idea of this framework is to take advantage of the "divide and concur" concept. Instead of searching for a pattern in a large image, a smart approach is taken to divide the image space into overlapping pattern of sub-images. Search is then based upon best match of input target with sub-image. Adaptive algorithm using POF was designed for this purpose during the first phase. The algorithm takes target sub-image of previous scene as the search pattern for the next scene.

The search engine framework is capable of dividing image space into sub-images of 64x64, 32x32, 16x16, and 8x8 pixels. This feature allows experimenter to evaluate susceptibility of different search algorithm to the speed of target, background noise, frame losses and other performance issues of image quality.

Data Analysis

To facilitate automatic processing of the scenes, an extensive analysis of the ground truth data was needed. During the first attempt processing the data (spring and summer quarter) only the first target in each scene was tracked. During that phase it came apparent that the complexity of the different scenes and the variety of data format in the ground truth files opposed a problem during processing. The vast number of ground truth data files (approximately 20k files) and the variety of situations in the scenes made this a challenging task. In order to understand the underlying requirements for the search engine program, a Matlab program was written to generate data file which then was imported into spreadsheet program for analysis. From the fifty sequences less than half had only one target present. One sequence had five targets present in the scene at one time although all in all there were more than five targets in the scene at different times Figure 1.

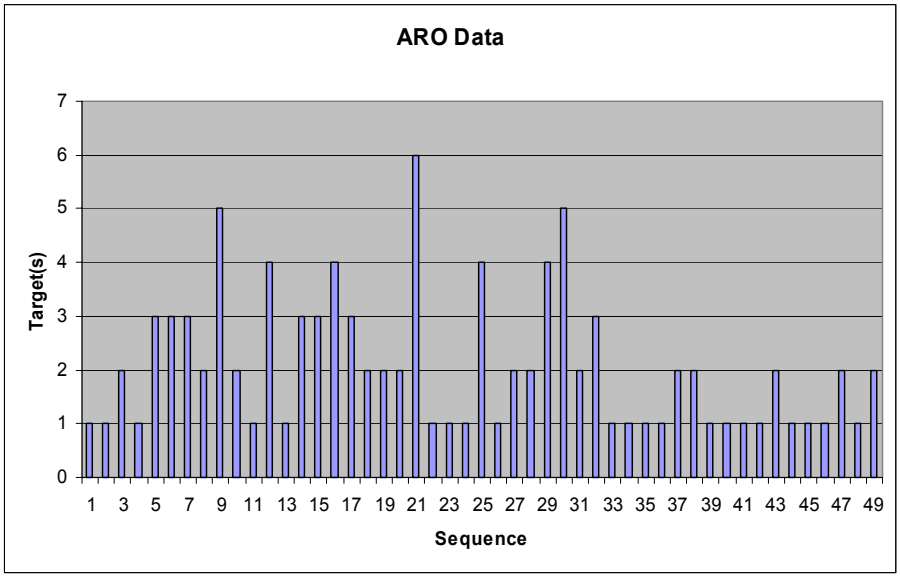

Figure 1 Number of targets at one time in a sequence

The following charts, figures 2 through 8, illustrate the wide variety of scenes encountered in the sequences. Sequence L1415 belongs to the simplest of data. Only one target present from the beginning to the end, starting in frame one.

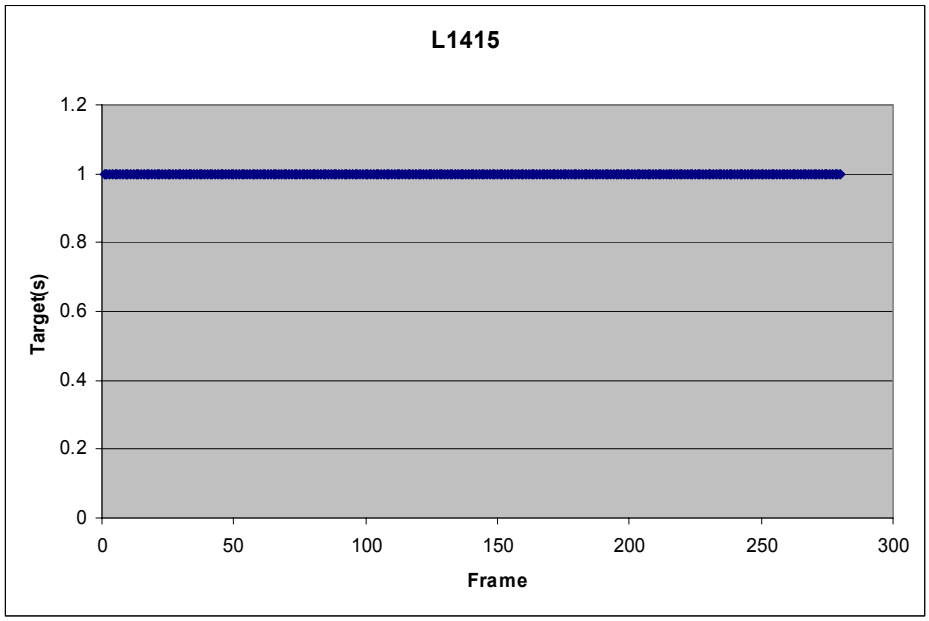

Figure 2 Simple sequence

Figure 2, represents one of the simplest sequences. Another simple sequence follows in figure 3. Sequence L1520 is still a sequence of only one target, but the ground truth data not available for the first 44 files.

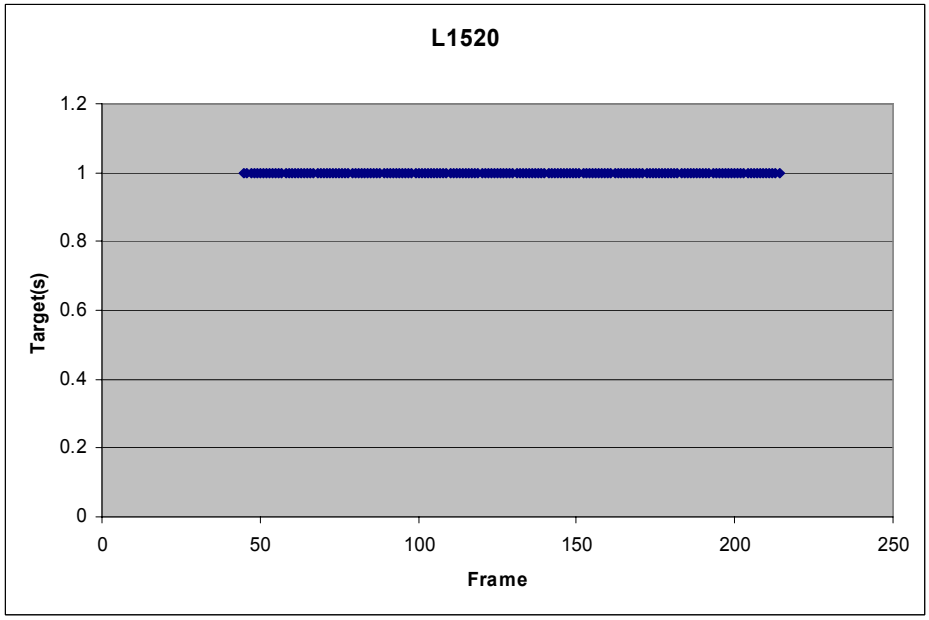

Figure 3 Little more complex data

Still the complexity increases, or the variety of processing requirements. In figure 4 sequence L15NS we have a sequence that starts out with a one target and then reduces to only one target and stays there for the reminder of the sequence.

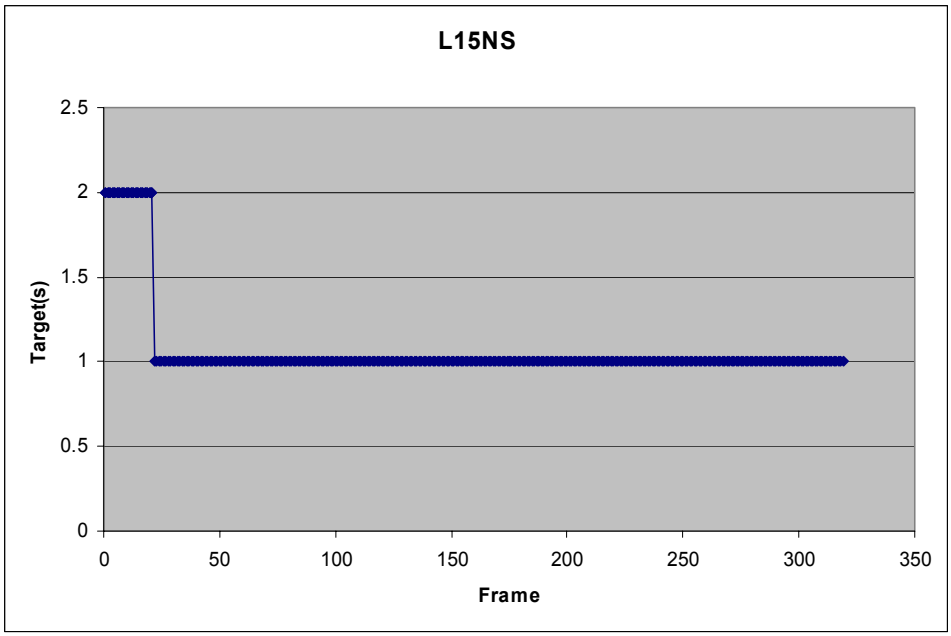

Figure 4 Still increasing complexity

Some sequences have variable number of target present over the course of the scene but are still relatively easy to process automatically, see figure 5.

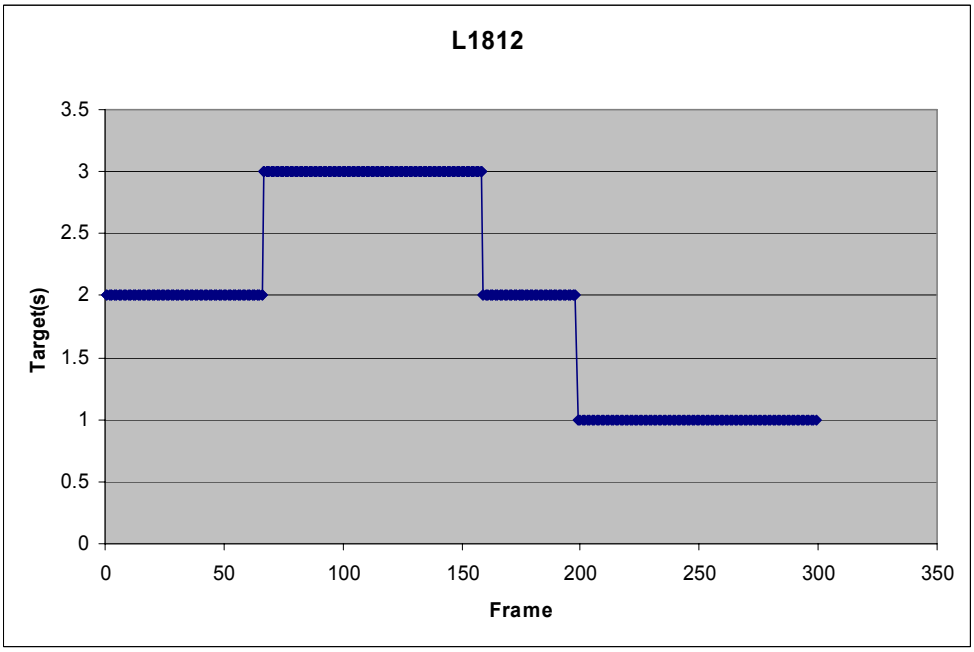

Figure 5 Still relatively simple to process

But the complexity in automatic processing increases as the variety of the format increases. Few of the more difficult sequences follow.

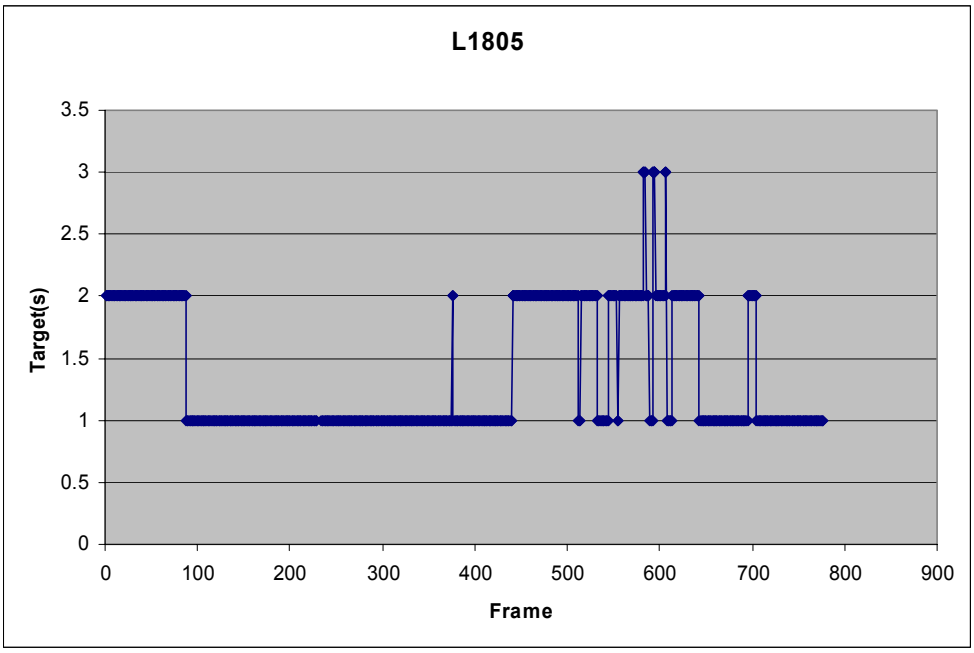

Figure 6 Number of targets in the scene changes multiple times

Sequence L1702 is one of the more challenging sequences counting seven different targets although there are maximum three visible at any given time.

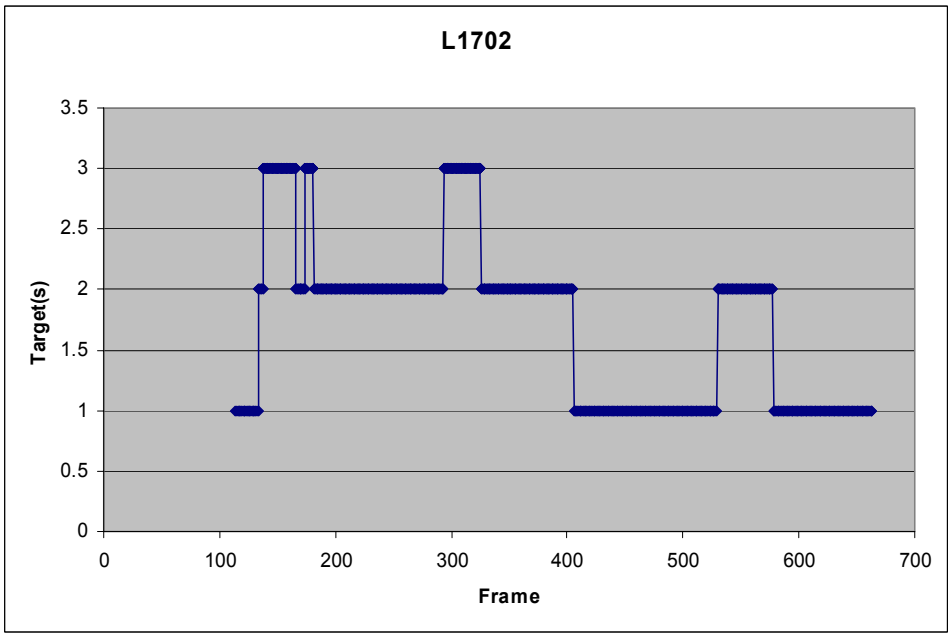

Figure 7 Missing initial ground truth data and varying number of targets

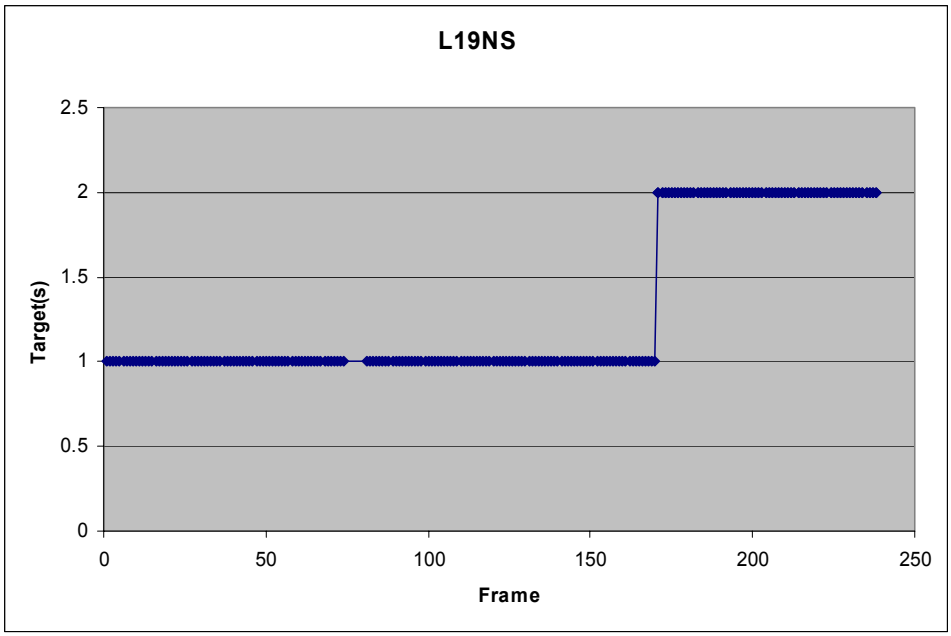

Figure 8 Missing ground truth data (target) in the middle of a sequence

A complete set of ground truth data tables and graphs is provided in the appendix. Due to the variety of the data a database was constructed including all the given ground truth data. Using this database, a lookup table is created for bookkeeping of the targets in each scene. Moreover, the multiple mat-files for each sequence were combined into one file per sequence.

Scene Evaluation

Using the Phase Only Filter (POF) two experiments were run on all the image sequences. One experiment uses Gaussian weighting function and the other experiment uses a distance function to define the region of interest. The functionality and operator instructions for the QMSE can be found in the June 2003 report as well as in the appendix of this report. Trying to visually determining data quality is misleading[1], therefore, the ATR performance is measured only with the quantitative knowledge gained from the ground truth data provided. Visual inspection on the other hand can provide insight while debugging and improving the algorithms.

The QMSE reads data from the Ground Truth Data-base and uses this data to compare actual target location to the location determined by the tracker. The QMSE pumps out information to the user interface and to a text file regarding the tracking progress. If the target moves out of the tracking gate an error message is displayed and this data is used to calculate the success rate. The success rate is determined by:

$$SuccessRate = 100 - \frac{miss}{number\_of\_frames}$$

It should be noted that the variable *number_of_frames* is not equal to the number of frames in the sequence. The variable refers to the number of frames were the target is present according to the ground truth data files.

The first time a target appears the ground truth data is used to obtain the reference target. This is the only time ground truth data is used to provide tracking data for the algorithm. Following this initial extraction of the target the ground truth data provides quantitative data to measure the performance of the algorithm.

It is relatively easy to add different search algorithms, weighting functions and preprocessing functionality to the QMSE. The user interface provides the entry hook and the function (search algorithm) can be added as a new separate "m" file to the project. A switch statement would be needed in the main loop to accommodate multiple search algorithms. Pre processing would be added in the outer loop right after the "mat" file containing the sequence is opened.

Some experimentation with the weighting function might provide improved performance. However, tweaking of the weighting function requires the entire data set to be evaluated each time to avoid tailoring the function to certain scenes or targets.

When working with multiple targets the QMSE displays a number next to the gate (sub-image). This number refers to the target that is being tracked. The name of the target is presented in the Ground truth data area. For example: if there are three active targets, tank, truck, and Bradley appearing in this order in the ground truth data file. While tracking the tank a number "1" will be displayed next to the gate. While tracking the truck a "2" will be displayed and so on. Rather than running the same sequence multiple times when tracking multiple targets, the tracker multiplexes the targets. This method makes it easy to analyze and understand why the algorithm fails. In some cases where the targets are initially very close to each other the algorithm can fail to track the correct target when the targets separate.

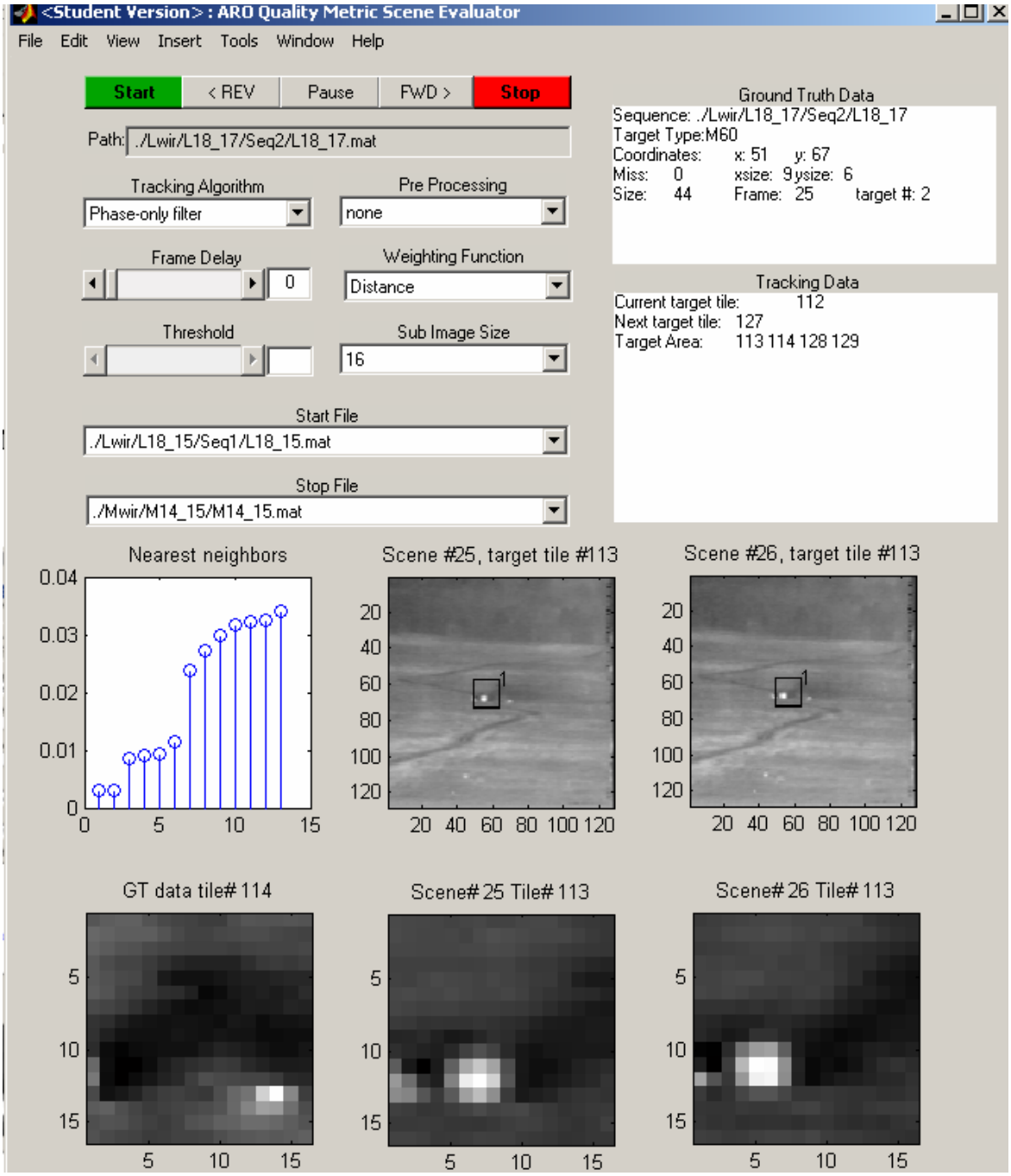

Figure 9 QMSE Gate Labeling

In the case of two targets close together, we can have four general situations:

1. The algorithm correctly tracks both targets
2. The algorithm tracks the same target twice
3. The tracker assigned initially to target one actually tracks target number two and the tracker assigned to target two tracks target number one.
4. Not tracking at all, lost.

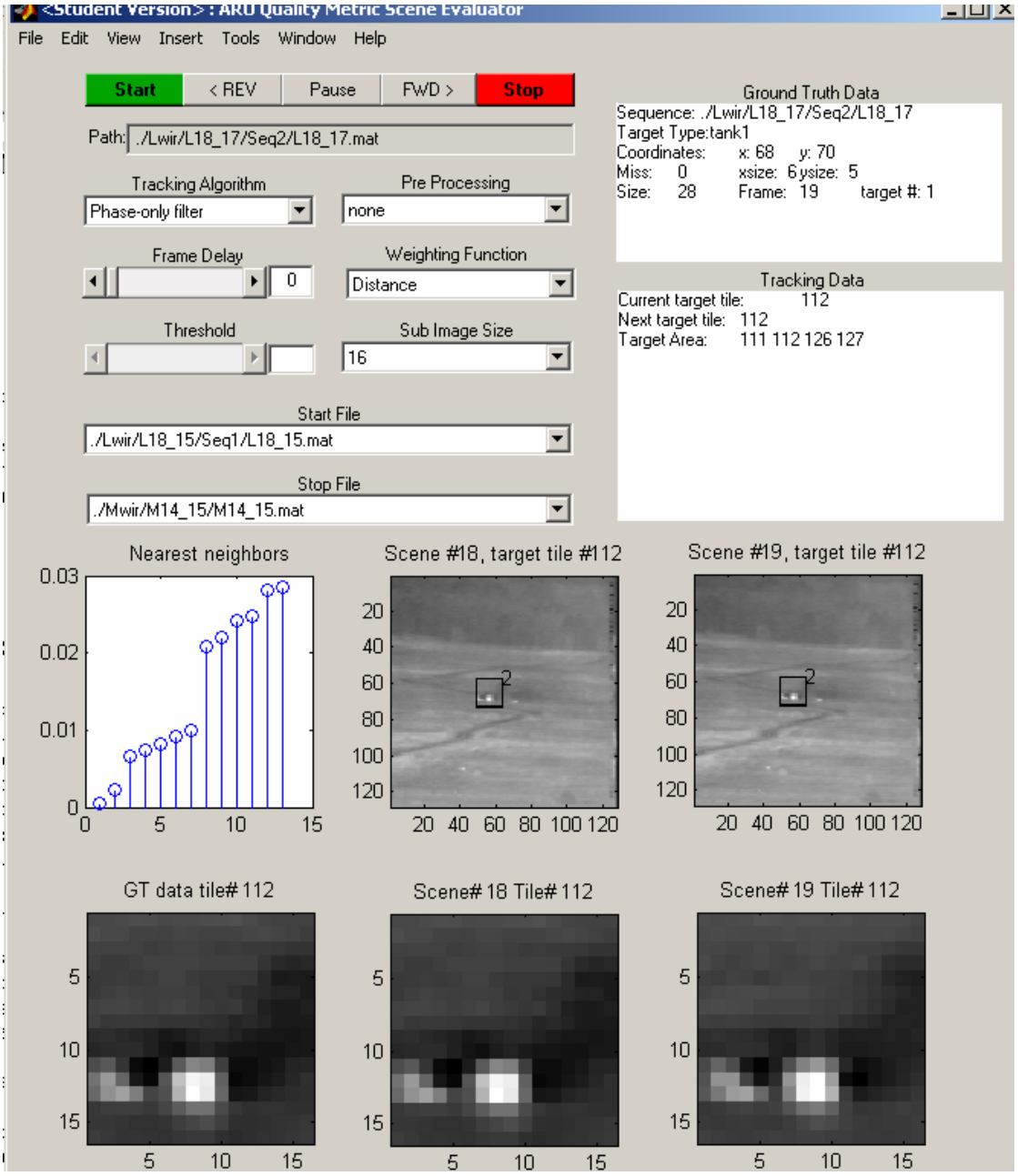

Figure 10 QMSE Gate label

Of course this problem compounds when the number of targets increases.

Processing the scene

Sub-Imaging

An image can be represented by the following set:

$$\mathrm{Im} = \{p_{1,1}, p_{1,2}, ...p_{128,128}\} \tag{1}$$

Similarly the target can be represented by the set:

$$T = \{t_{1,1}, t_{1,2}, ...t_{\max,\max}\} \tag{2}$$

We know that target ***T*** is embedded in the scene **Im** since ***T*** is a proper subset of **Im**:

$$T \in \mathrm{Im} \tag{3}$$

This leads to one task only; the task of finding the subset of **Im** (sub-image) containing the target ***T***. Such that:

$$T \in S\,\mathrm{Im} \subseteq \mathrm{Im} \tag{4}$$

To focus on features rather than the energy of the image we must establish a reference value.

Sub-imaging and comparing can select the best match as being:

$$T \approx S\,\mathrm{Im} \subseteq \mathrm{Im} \tag{5}$$

Therefore, the search algorithm is precisely as follows:

$$\forall S\,\mathrm{Im} \otimes T, \exists S\,\mathrm{Im} \otimes T \,|\, S\,\mathrm{Im} \otimes T \approx T \otimes T \tag{6}$$

This search algorithm truly eliminates the effect of high-energy pixels, and the POF searches for the best matching features. This algorithm can be stated as: For all sub-images convolved with target image, there must exist sub-image convolved with target image such that sub-image convolved with target image is approximately same as target image convolved with target image. So the task on hand is to find the cross correlation of sub-image with target image that is closest in magnitude to the autocorrelation of the target image.

A simple checkerboard sub-imaging is not sufficient to produce reliable results. A more sophisticated approach must be taken in order to preserve information between scenes. Figure 11 shows one such approach. Sub-images are created in overlapping fashion.

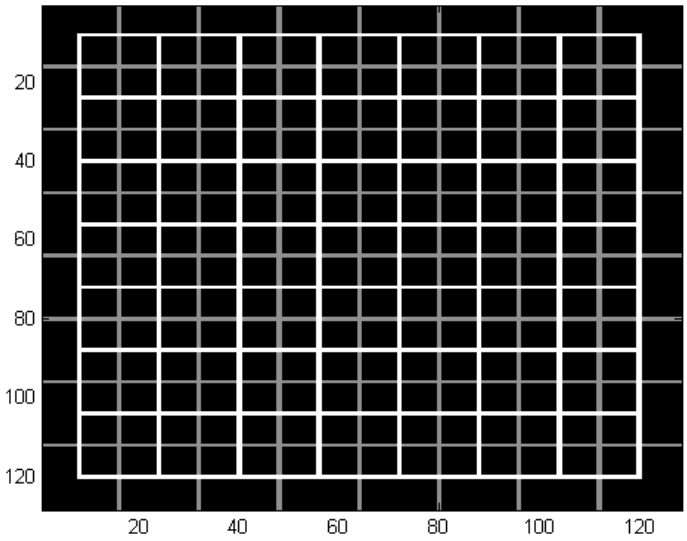

Figure 11 Sub-image grid

One of the most important parameters, to be considered when selecting granularity of the sub-imaging, is the size of the target. The smaller the target the smaller the sub-image must be. However, to ensure maximum detection capability the target size needs to be ¼ of the sub-image size. If the sub-image is smaller than the target a maximum pattern matching will not be achieved due to clipping. If the sub-image on the other hand is bigger than the target some of the background will be included, and the edge detection weight of the POF might be overcome by the weight of the energy summed up by the integration[2].

Algorithm

Figure 11 describes the adaptive POF ATR system. A target is extracted at its first appearance in the input image. The target along with the image frame is passed on to the POF ATR system. The POF ATR System consists of four main modules: The module extracting sub-images from the input image, auto-correlator module to establish the reference value for match, correlator module which correlates each sub-image to the input target, and finally a selector module to select the target sub-image. In this research we have provided results from selector module using two different weighting functions. One is based on the Gaussian weight, and the other method is based on actual distance from the center of target area. The selector feeds back the new target to the auto-correlator module to update the input target, and to the output for displaying. Next it updates the target and feeds it back to the auto-correlator to be used as an input filter for the next image frame. Finally it passes information on to the output module to display the tracking results.

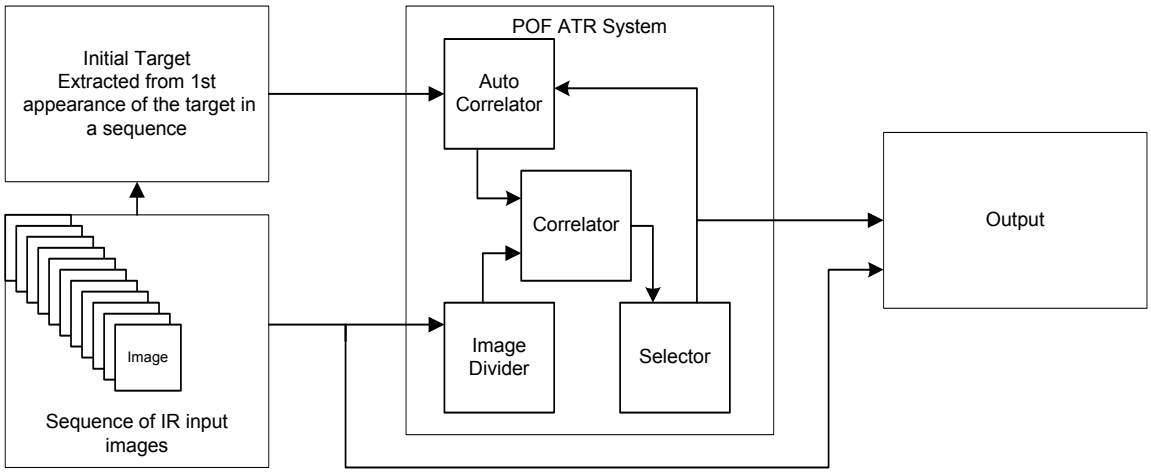

Figure 12 POF Tracking System

The ATR algorithm performance is clearly directly related to the target signature and the clutter of the scene[3]. Providing the two different weighting methods for the selector module clearly shows this.

Results

All 102 targets were tracked automatically and evaluated based on the ground truth data provided by ARO for two different weighting functions. The results are provided in tables 1 and 2. Figure 13 compares the two weighting functions.

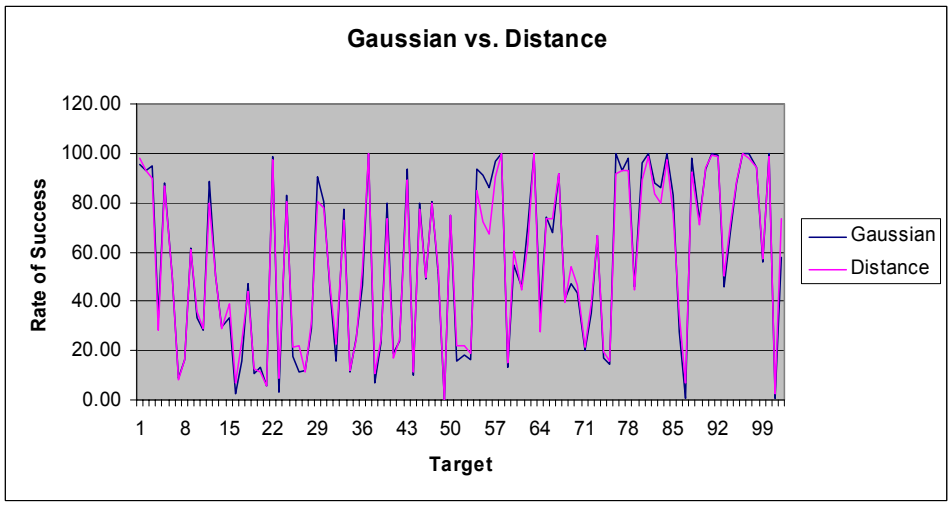

Figure 13 Performance comparison of Gaussian vs. Distance weight function

Following table shows the results from tracking the targets using weighting function based on the Gaussian distribution. In the tables 1 and 2, the values of min, mean, max, and std represent the average values over the sequence. The miss value reflects the total number of frames missed while tracking, irrespective of the location of the frame in the sequence.

Table 1 Results with Gaussian weighting function.

Sequence#	min	mean	max	std	target	misses	# of scenes	rate
./Lwir/L14_15/L14_15	91	133.92	244	3.34	Mantruck	0	280	100.00
./Lwir/L15_20/L15_20	85	132.25	231	2.95	tank1	95	170	44.12
./Lwir/L15_NS/L15_NS	84	142.20	225	2.37	tank1	302	319	5.33
./Lwir/L15_NS/L15_NS	84	142.20	225	2.37	truck	2	21	90.48
./Lwir/L16_04/L16_04	83	154.87	249	2.85	tank1	396	399	0.75
./Lwir/L16_07/L16_07	81	140.98	251	2.86	tank1	185	210	11.90
./Lwir/L16_07/L16_07	81	140.98	251	2.86	tank1	0	188	100.00
./Lwir/L16_07/L16_07	81	140.98	251	2.86	tank1	0	10	100.00
./Lwir/L16_08/L16_08	47	111.72	255	4.24	M60	42	289	85.47
./Lwir/L16_08/L16_08	47	111.72	255	4.24	apc1	0	81	100.00
./Lwir/L16_08/L16_08	47	111.72	255	4.24	mantrk?	44	100	56.00
./Lwir/L16_18/L16_18	37	124.18	251	4.57	apc1	264	290	8.97
./Lwir/L16_18/L16_18	37	124.18	251	4.57	M60	0	101	100.00
./Lwir/L16_18/L16_18	37	124.18	251	4.57	truck	0	6	100.00
./Lwir/L17_01/L17_01	50	127.49	220	2.26	Bradley?	0	370	100.00
./Lwir/L17_01/L17_01	50	127.49	220	2.26	pickup(trk)?	12	43	72.09
./Lwir/L17_02/L17_02	55	147.29	229	2.09	Mantruck?	32	100	68.00
./Lwir/L17_02/L17_02	55	147.29	229	2.09	pickup(trk)?	0	32	100.00
./Lwir/L17_02/L17_02	55	147.29	229	2.09	Bradley?	325	340	4.41
./Lwir/L17_02/L17_02	55	147.29	229	2.09	Mantruck?	158	418	62.20
./Lwir/L17_02/L17_02	55	147.29	229	2.09	tank	16	48	66.67
./Lwir/L17_20/L17_20	44	126.33	240	7.87	target	34	35	2.86
./Lwir/L17_20/L17_20	44	126.33	240	7.87	M60	591	734	19.48
./Lwir/L18_03/L18_03	38	117.98	226	4.87	Bradley	389	446	12.78
./Lwir/L18_05/L18_05	67	163.61	248	6.32	tank1	605	747	19.01
./Lwir/L18_05/L18_05	67	163.61	248	6.32	apc1	44	135	67.41
./Lwir/L18_05/L18_05	67	163.61	248	6.32	M60	104	159	34.59
./Lwir/L18_05/L18_05	67	163.61	248	6.32	tank	8	9	11.11
./Lwir/L18_07/L18_07	66	156.13	241	6.20	Bradley	241	259	6.95
./Lwir/L18_12/L18_12	51	142.46	231	5.64	Bradley	94	299	68.56
./Lwir/L18_12/L18_12	51	142.46	231	5.64	tank1	167	198	15.66
./Lwir/L18_12/L18_12	51	142.46	231	5.64	M60	0	92	100.00
./Lwir/L18_13/L18_13	55	143.89	235	5.52	tank1	292	325	10.15
./Lwir/L18_13/L18_13	55	143.89	235	5.52	M60	0	228	100.00
./Lwir/L18_13/L18_13	55	143.89	235	5.52	apc1	0	168	100.00
./Lwir/L18_15/Seq1/L18_15	54	142.57	250	5.59	M60	0	242	100.00
./Lwir/L18_15/Seq1/L18_15	54	142.57	250	5.59	truck?	0	12	100.00
./Lwir/L18_15/Seq1/L18_15	54	142.57	250	5.59	tank1	262	288	9.03
./Lwir/L18_15/Seq1/L18_15	54	142.57	250	5.59	bradley	22	192	88.54
./Lwir/L18_15/Seq2/L18_15	49	139.27	227	5.43	M60	206	237	13.08
./Lwir/L18_15/Seq2/L18_15	49	139.27	227	5.43	tank1	265	306	13.40
./Lwir/L18_15/Seq2/L18_15	49	139.27	227	5.43	bradley	88	186	52.69
./Lwir/L18_16/L18_16	48	142.48	243	5.93	tank1	300	327	8.26
./Lwir/L18_16/L18_16	48	142.48	243	5.93	M60	0	289	100.00
./Lwir/L18_17/Seq1/L18_17	51	150.07	252	5.88	tank1	172	239	28.03
./Lwir/L18_17/Seq1/L18_17	51	150.07	252	5.88	M60	0	194	100.00

./Lwir/L18_17/Seq2/L18_17	47	148.04	252	6.04	tank1	200	265	24.53
./Lwir/L18_17/Seq2/L18_17	47	148.04	252	6.04	M60	0	190	100.00
./Lwir/L18_18/L18_18	52	146.41	252	5.70	mantruck	43	45	4.44
./Lwir/L18_18/L18_18	52	146.41	252	5.70	target	1	4	75.00
./Lwir/L18_18/L18_18	52	146.41	252	5.70	apc1	52	92	43.48
./Lwir/L18_18/L18_18	52	146.41	252	5.70	M60?	114	122	6.56
./Lwir/L18_18/L18_18	52	146.41	252	5.70	tank1	203	213	4.69
./Lwir/L18_18/L18_18	52	146.41	252	5.70	testvan	0	3	100.00
./Lwir/L19_01/L19_01	54	143.46	252	5.90	tank1	210	239	12.13
./Lwir/L19_02/L19_02	53	143.93	252	5.88	tank1	201	269	25.28
./Lwir/L19_04/L19_04	43	140.32	252	6.74	tank1	186	269	30.86
./Lwir/L19_06/L19_06	55	149.00	252	5.35	tank1	234	264	11.36
./Lwir/L19_06/L19_06	55	149.00	252	5.35	apc1	202	264	23.48
./Lwir/L19_06/L19_06	55	149.00	252	5.35	Mantruck	0	205	100.00
./Lwir/L19_06/L19_06	55	149.00	252	5.35	Van	0	22	100.00
./Lwir/L19_07/L19_07	56	151.43	253	5.53	Mantruck	57	75	24.00
./Lwir/L19_10/L19_10	54	148.14	248	5.40	tank1	0	113	100.00
./Lwir/L19_10/L19_10	54	148.14	248	5.40	apc1	68	73	6.85
./Lwir/L19_11/L19_11	51	142.89	253	5.41	tank1	5	164	96.95
./Lwir/L19_11/L19_11	51	142.89	253	5.41	apc1	0	164	100.00
./Lwir/L19_13/L19_13	54	152.68	253	5.20	tank1	121	264	54.17
./Lwir/L19_13/L19_13	54	152.68	253	5.20	apc1	238	264	9.85
./Lwir/L19_13/L19_13	54	152.68	253	5.20	M60	0	66	100.00
./Lwir/L19_13/L19_13	54	152.68	253	5.20	Mantruck	1	12	91.67
./Lwir/L19_15/L19_15	39	140.70	255	5.10	tank1	306	321	4.67
./Lwir/L19_15/L19_15	39	140.70	255	5.10	apc1	3	190	98.42
./Lwir/L19_15/L19_15	39	140.70	255	5.10	M60	319	326	2.15
./Lwir/L19_15/L19_15	39	140.70	255	5.10	Van	19	210	90.95
./Lwir/L19_15/L19_15	39	140.70	255	5.10	apc1	9	12	25.00
./Lwir/L19_18/L19_18	41	144.89	252	4.74	tank1	141	233	39.48
./Lwir/L19_18/L19_18	41	144.89	252	4.74	M60?	0	12	100.00
./Lwir/L19_NS/L19_NS	38	140.73	252	4.78	M60?	5	58	91.38
./Lwir/L19_NS/L19_NS	38	140.73	252	4.78	mantruck	77	114	32.46
./Lwir/L19_NS/L19_NS	38	140.73	252	4.78	tank1	87	128	32.03
./Lwir/L20_04/L20_04	44	139.58	230	3.36	apc1	0	367	100.00
./Lwir/L20_08/L20_08	44	143.50	236	3.93	apc1	164	347	52.74
./Lwir/L20_17/L20_17	42	141.03	233	3.77	tank1	123	191	35.60
./Lwir/L20_18/L20_18	43	138.61	224	3.30	tank1	0	447	100.00
./Lwir/L20_20/L20_20	50	140.40	216	3.14	tank1	192	419	54.18
./Lwir/L20_20/L20_20	50	140.40	216	3.14	target	111	172	35.47
./Lwir/L21_04/L21_04	55	144.01	183	1.37	bradley	319	321	0.62
./Lwir/L21_04/L21_04	55	144.01	183	1.37	tank1	386	690	44.06
./Lwir/L21_15/L21_15	54	140.29	194	2.08	Bradley	731	737	0.81
./Lwir/L21_17/L21_17	54	136.28	196	2.04	apc1	0	359	100.00
./Lwir/L22_06/L22_06	51	139.39	211	2.52	tank1	0	347	100.00
./Lwir/L22_08/L22_08	45	130.85	212	2.98	apc1	0	379	100.00
./Lwir/L22_14/L22_14	47	134.95	209	2.71	M60	270	273	1.10
./Lwir/L22_14/L22_14	47	134.95	209	2.71	target	72	74	2.70

./Lwir/L23_12/L23_12	49	134.09	216	2.46	apc1	0	367	100.00
./Mwir/M14_06/M14_06	35	141.62	216	2.44	Bradley	0	378	100.00
./Mwir/M14_07/M14_07	34	143.36	218	2.39	Bradley	0	399	100.00
./Mwir/M14_10/M14_10	25	125.03	228	3.71	tank1	0	497	100.00
./Mwir/M14_10/M14_10	25	125.03	228	3.71	Mantruck	14	77	81.82
./Mwir/M14_13/M14_13	25	126.70	228	4.04	Mantruck	0	379	100.00
./Mwir/M14_15/M14_15	25	138.22	228	3.00	Mantruck	513	523	1.91
./Mwir/M14_15/M14_15	25	138.22	228	3.00	target	11	19	42.11

The following bar graph summarizes the results using the Gaussian weighting function.

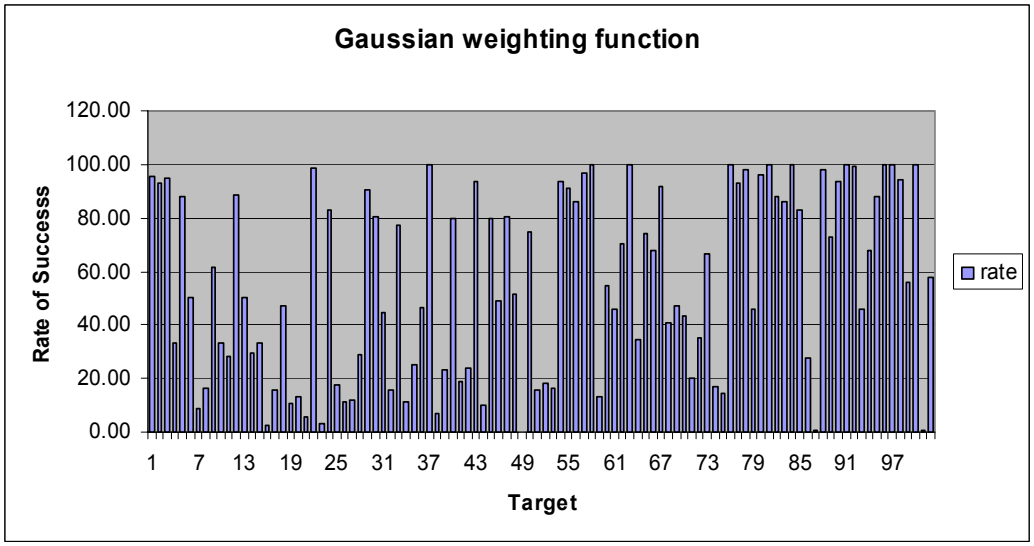

Figure 14 Results using Gaussian weighting function

The results using the Distance weighting function follows in table 2.

Table 2 Results using Distance weighting function.

Sequence#	min	mean	max	std	target	misses	# of scenes	rate
./Lwir/L14_15/L14_15	91	133.92	244	3.34	Mantruck	0	280	100.00
./Lwir/L15_20/L15_20	85	132.25	231	2.95	tank1	97	170	42.94
./Lwir/L15_NS/L15_NS	84	142.20	225	2.37	tank1	299	319	6.27
./Lwir/L15_NS/L15_NS	84	142.20	225	2.37	truck	1	21	95.24
./Lwir/L16_04/L16_04	83	154.87	249	2.85	tank1	396	399	0.75
./Lwir/L16_07/L16_07	81	140.98	251	2.86	tank1	192	210	8.57
./Lwir/L16_07/L16_07	81	140.98	251	2.86	tank1	0	188	100.00
./Lwir/L16_07/L16_07	81	140.98	251	2.86	tank1	0	10	100.00
./Lwir/L16_08/L16_08	47	111.72	255	4.24	M60	46	289	84.08
./Lwir/L16_08/L16_08	47	111.72	255	4.24	apc1	0	81	100.00
./Lwir/L16_08/L16_08	47	111.72	255	4.24	mantrk?	45	100	55.00
./Lwir/L16_18/L16_18	37	124.18	251	4.57	apc1	265	290	8.62
./Lwir/L16_18/L16_18	37	124.18	251	4.57	M60	0	101	100.00
./Lwir/L16_18/L16_18	37	124.18	251	4.57	truck	0	6	100.00

./Lwir/L17_01/L17_01	50	127.49	220	2.26	Bradley?	0	370	100.00
./Lwir/L17_01/L17_01	50	127.49	220	2.26	pickup(trk)?	12	43	72.09
./Lwir/L17_02/L17_02	55	147.29	229	2.09	Mantruck?	32	100	68.00
./Lwir/L17_02/L17_02	55	147.29	229	2.09	pickup(trk)?	0	32	100.00
./Lwir/L17_02/L17_02	55	147.29	229	2.09	Bradley?	327	340	3.82
./Lwir/L17_02/L17_02	55	147.29	229	2.09	Mantruck?	416	418	0.48
./Lwir/L17_02/L17_02	55	147.29	229	2.09	tank	34	48	29.17
./Lwir/L17_20/L17_20	44	126.33	240	7.87	target	34	35	2.86
./Lwir/L17_20/L17_20	44	126.33	240	7.87	M60	719	734	2.04
./Lwir/L18_03/L18_03	38	117.98	226	4.87	Bradley	395	446	11.43
./Lwir/L18_05/L18_05	67	163.61	248	6.32	tank1	680	747	8.97
./Lwir/L18_05/L18_05	67	163.61	248	6.32	apc1	44	135	67.41
./Lwir/L18_05/L18_05	67	163.61	248	6.32	M60	128	159	19.50
./Lwir/L18_05/L18_05	67	163.61	248	6.32	tank	8	9	11.11
./Lwir/L18_07/L18_07	66	156.13	241	6.20	Bradley	241	259	6.95
./Lwir/L18_12/L18_12	51	142.46	231	5.64	Bradley	2	299	99.33
./Lwir/L18_12/L18_12	51	142.46	231	5.64	tank1	169	198	14.65
./Lwir/L18_12/L18_12	51	142.46	231	5.64	M60	0	92	100.00
./Lwir/L18_13/L18_13	55	143.89	235	5.52	tank1	292	325	10.15
./Lwir/L18_13/L18_13	55	143.89	235	5.52	M60	0	228	100.00
./Lwir/L18_13/L18_13	55	143.89	235	5.52	apc1	0	168	100.00
./Lwir/L18_15/Seq1/L18_15	54	142.57	250	5.59	M60	187	242	22.73
./Lwir/L18_15/Seq1/L18_15	54	142.57	250	5.59	truck?	0	12	100.00
./Lwir/L18_15/Seq1/L18_15	54	142.57	250	5.59	tank1	261	288	9.38
./Lwir/L18_15/Seq1/L18_15	54	142.57	250	5.59	bradley	79	192	58.85
./Lwir/L18_15/Seq2/L18_15	49	139.27	227	5.43	M60	199	237	16.03
./Lwir/L18_15/Seq2/L18_15	49	139.27	227	5.43	tank1	263	306	14.05
./Lwir/L18_15/Seq2/L18_15	49	139.27	227	5.43	bradley	91	186	51.08
./Lwir/L18_16/L18_16	48	142.48	243	5.93	tank1	314	327	3.98
./Lwir/L18_16/L18_16	48	142.48	243	5.93	M60	0	289	100.00
./Lwir/L18_17/Seq1/L18_17	51	150.07	252	5.88	tank1	168	239	29.71
./Lwir/L18_17/Seq1/L18_17	51	150.07	252	5.88	M60	0	194	100.00
./Lwir/L18_17/Seq2/L18_17	47	148.04	252	6.04	tank1	204	265	23.02
./Lwir/L18_17/Seq2/L18_17	47	148.04	252	6.04	M60	0	190	100.00
./Lwir/L18_18/L18_18	52	146.41	252	5.70	mantruck	41	45	8.89
./Lwir/L18_18/L18_18	52	146.41	252	5.70	target	2	4	50.00
./Lwir/L18_18/L18_18	52	146.41	252	5.70	apc1	71	92	22.83
./Lwir/L18_18/L18_18	52	146.41	252	5.70	M60?	114	122	6.56
./Lwir/L18_18/L18_18	52	146.41	252	5.70	tank1	199	213	6.57
./Lwir/L18_18/L18_18	52	146.41	252	5.70	testvan	0	3	100.00
./Lwir/L19_01/L19_01	54	143.46	252	5.90	tank1	195	239	18.41
./Lwir/L19_02/L19_02	53	143.93	252	5.88	tank1	230	269	14.50
./Lwir/L19_04/L19_04	43	140.32	252	6.74	tank1	182	269	32.34
./Lwir/L19_06/L19_06	55	149.00	252	5.35	tank1	233	264	11.74
./Lwir/L19_06/L19_06	55	149.00	252	5.35	apc1	202	264	23.48
./Lwir/L19_06/L19_06	55	149.00	252	5.35	Mantruck	0	205	100.00
./Lwir/L19_06/L19_06	55	149.00	252	5.35	Van	0	22	100.00
./Lwir/L19_07/L19_07	56	151.43	253	5.53	Mantruck	50	75	33.33

./Lwir/L19_10/L19_10	54	148.14	248	5.40	tank1	0	113	100.00
./Lwir/L19_10/L19_10	54	148.14	248	5.40	apc1	0	73	100.00
./Lwir/L19_11/L19_11	51	142.89	253	5.41	tank1	0	164	100.00
./Lwir/L19_11/L19_11	51	142.89	253	5.41	apc1	0	164	100.00
./Lwir/L19_13/L19_13	54	152.68	253	5.20	tank1	118	264	55.30
./Lwir/L19_13/L19_13	54	152.68	253	5.20	apc1	261	264	1.14
./Lwir/L19_13/L19_13	54	152.68	253	5.20	M60	1	66	98.48
./Lwir/L19_13/L19_13	54	152.68	253	5.20	Mantruck	1	12	91.67
./Lwir/L19_15/L19_15	39	140.70	255	5.10	tank1	303	321	5.61
./Lwir/L19_15/L19_15	39	140.70	255	5.10	apc1	3	190	98.42
./Lwir/L19_15/L19_15	39	140.70	255	5.10	M60	319	326	2.15
./Lwir/L19_15/L19_15	39	140.70	255	5.10	Van	23	210	89.05
./Lwir/L19_15/L19_15	39	140.70	255	5.10	apc1	9	12	25.00
./Lwir/L19_18/L19_18	41	144.89	252	4.74	tank1	26	233	88.84
./Lwir/L19_18/L19_18	41	144.89	252	4.74	M60?	0	12	100.00
./Lwir/L19_NS/L19_NS	38	140.73	252	4.78	M60?	3	58	94.83
./Lwir/L19_NS/L19_NS	38	140.73	252	4.78	mantruck	100	114	12.28
./Lwir/L19_NS/L19_NS	38	140.73	252	4.78	tank1	87	128	32.03
./Lwir/L20_04/L20_04	44	139.58	230	3.36	apc1	0	367	100.00
./Lwir/L20_08/L20_08	44	143.50	236	3.93	apc1	150	347	56.77
./Lwir/L20_17/L20_17	42	141.03	233	3.77	tank1	118	191	38.22
./Lwir/L20_18/L20_18	43	138.61	224	3.30	tank1	0	447	100.00
./Lwir/L20_20/L20_20	50	140.40	216	3.14	tank1	225	419	46.30
./Lwir/L20_20/L20_20	50	140.40	216	3.14	target	138	172	19.77
./Lwir/L21_04/L21_04	55	144.01	183	1.37	bradley	319	321	0.62
./Lwir/L21_04/L21_04	55	144.01	183	1.37	tank1	385	690	44.20
./Lwir/L21_15/L21_15	54	140.29	194	2.08	Bradley	694	737	5.83
./Lwir/L21_17/L21_17	54	136.28	196	2.04	apc1	0	359	100.00
./Lwir/L22_06/L22_06	51	139.39	211	2.52	tank1	0	347	100.00
./Lwir/L22_08/L22_08	45	130.85	212	2.98	apc1	0	379	100.00
./Lwir/L22_14/L22_14	47	134.95	209	2.71	M60	270	273	1.10
./Lwir/L22_14/L22_14	47	134.95	209	2.71	target	72	74	2.70
./Lwir/L23_12/L23_12	49	134.09	216	2.46	apc1	0	367	100.00
./Mwir/M14_06/M14_06	35	141.62	216	2.44	Bradley	0	378	100.00
./Mwir/M14_07/M14_07	34	143.36	218	2.39	Bradley	0	399	100.00
./Mwir/M14_10/M14_10	25	125.03	228	3.71	tank1	1	497	99.80
./Mwir/M14_10/M14_10	25	125.03	228	3.71	Mantruck	14	77	81.82
./Mwir/M14_13/M14_13	25	126.70	228	4.04	Mantruck	0	379	100.00
./Mwir/M14_15/M14_15	25	138.22	228	3.00	Mantruck	513	523	1.91
./Mwir/M14_15/M14_15	25	138.22	228	3.00	target	11	19	42.11

The following bar graph summarizes the results using the Distance weighting function.

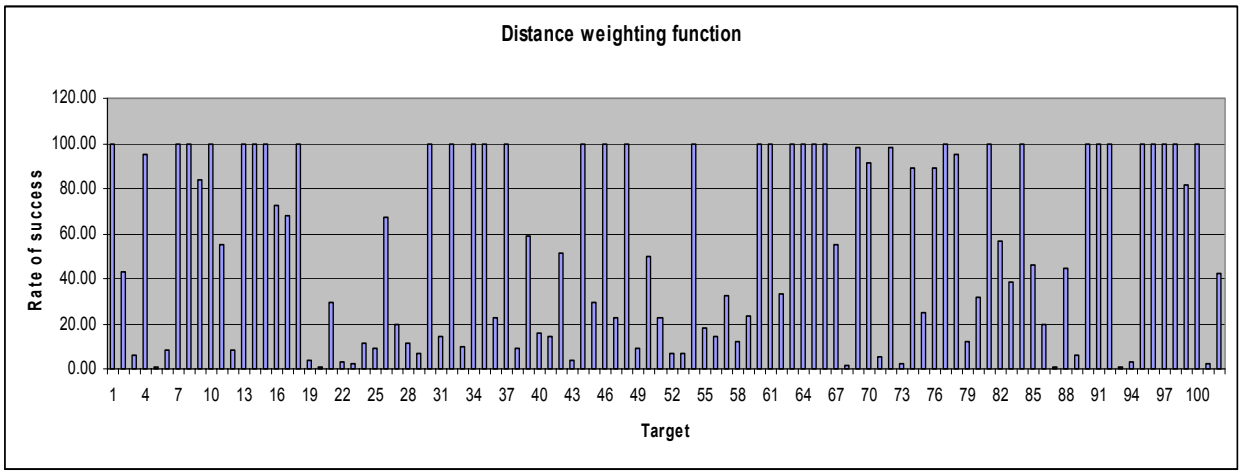

Figure 15 Results using Distance weighting function

Conclusions

In this report we have discussed the status of the ARO project at WSU. A multi-target tracking version of the "Quality Metric Scene Evaluator" (QMSE) has been developed using the Matlab programming tools. Using the QMSE we have evaluated the entire data set supplied by the Army Research Office twice using the Phase Only Filter in combination with two different weighting functions, Gaussian function and distance function. The QMSE uses sub-imaging technique. The sub-imaging technique shows very promising results when used in conjunction with the POF and a simple hot-spot filter. Using overlapping sub-images of relevant size transforms the task of tracking a target in a scene to the task of finding the best matching sub-image, which in turn has a fixed place in the scene. The critical parameter here is to select the sub-image size such as to maximize the target occupation in the sub-image. Future work in this area should include applying this technique to other ATR methods. Exploring methods of expanding and shrinking the grid size automatically based on target size also needs to be explored.

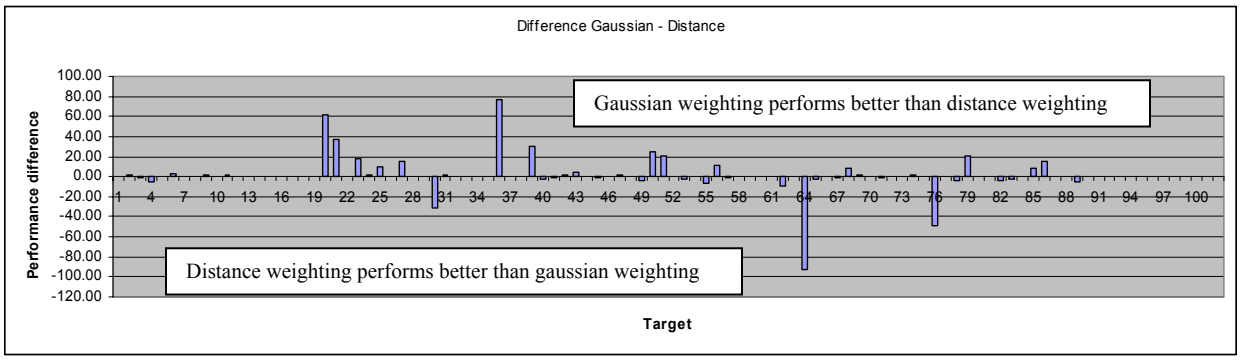

Figure 16 Comparison of Gaussian and Distance weighting function

The QMSE reads data from the Ground Truth Data (GTD) files and uses this data to compare actual target location to the location determined by the tracker.

Appendix A

Quality Metric Scene Evaluator

The following figure shows the QMSE GUI. Various information about the images are displayed. The following list describes each item of the GUI.

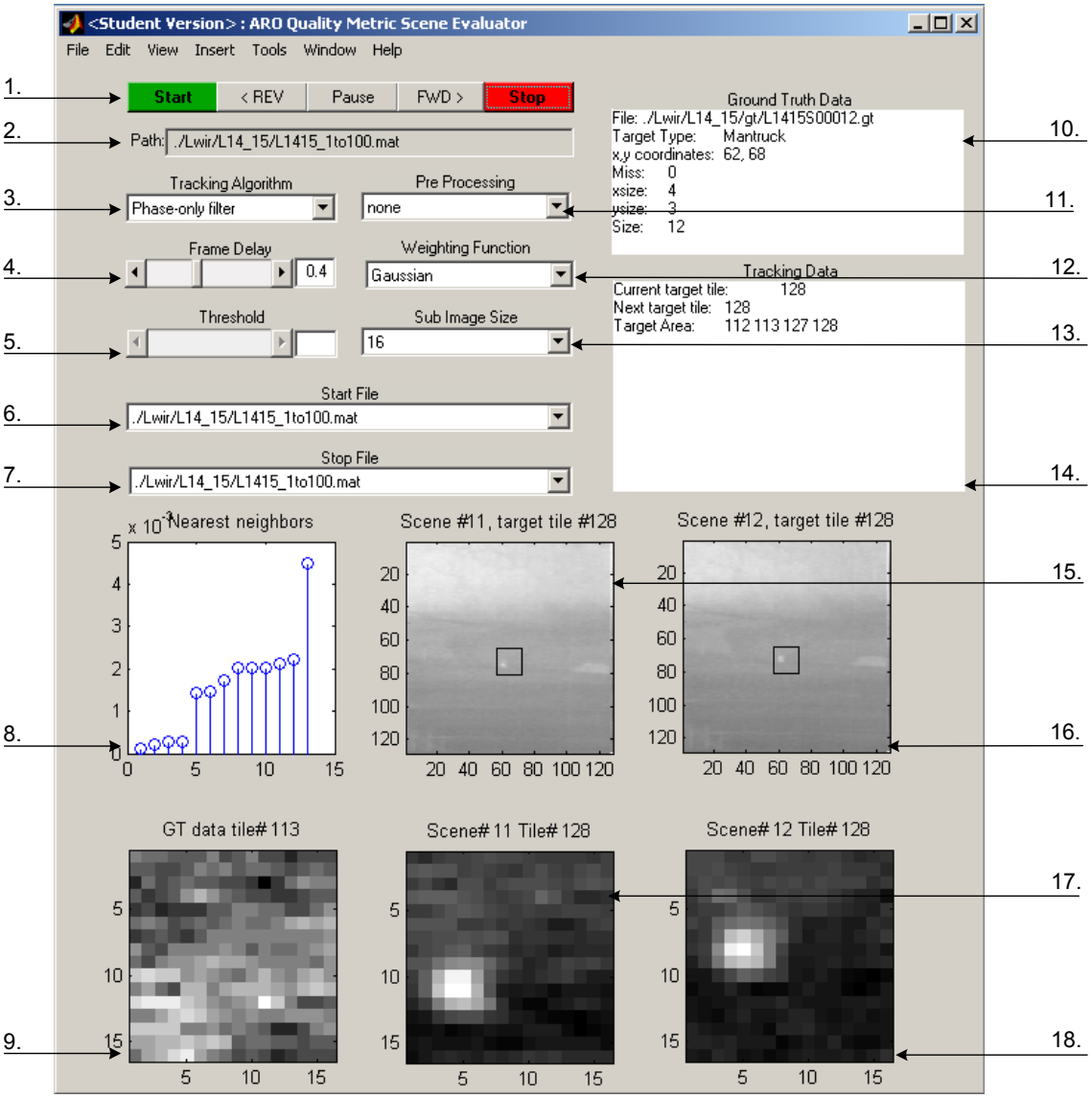

1. Button bar
   The button bar has five buttons. Only two have been implemented so far. Those are the **Start** button and the **Stop** button. The other three buttons are Pause, and buttons for Forward and Backwards stepping one frame at a time.
2. Path
   The field below the button bar displays the relative path of the file currently being processed.

3. Tracking algorithm
   Pull down list to select different search algorithms to evaluate.
4. Frame Delay
   The frame delay is to slow down or speed up the image processing. This can be handy when transitions between frames need to be examined without pausing the program.
5. Threshold
   The threshold slider is not implemented for the POF. However, it is provide for algorithms that will need to have some variable parameter such as threshold/
6. Start File
   Next we have the start file pull down list. Any of the files provided can be selected to be the first file processed.
   NOTE:
   In later version a capability to process the files in backwards order will be provided.
7. Stop File.
   The stop file pull down list serves is used to select the last file to process.
8. Nearest neighbours
   The stem diagram shows the relationship between the absolute differences of the correlation between the sub-images in the region of interest.
9. Ground Truth data display
   This image shows the sub-image that is according to the Ground Truth Data files supposed to contain the target.
10. Ground Truth Data
    In this area alphanumerical information from the Ground Truth files are displayed.
11. Preprocessing.
    This pull down list provides hook to plug in various preprocessing methods. At this time no preprocessing is provided.
12. Weighting function
    The current POF algorithm can use either a Gaussian function to determine region of interest for the search algorithm or a plain distance function.
13. Sub-image size.
    This pull down list allows the user to select which of 8x8, 16x16, 32x32, 64x64 sub-image size to use for processing.
14. Tracking Data.
    This area displays alphanumerical information from the tracking process.
15. Scene Display.
    In this scene display the new target area is displayed in the current frame.
16. Scene Display.
    Here the new target is displayed in the new frame.
17. Target Display.
    In this target display the new target is displayed in the current frame.
18. Target Display.
    Here the new target is displayed in the new frame.

References

1. Richard S. Sims, "Putting ATR performance on an equal basis: the measurement of knowledge base distortion and relevant clutter", Automatic Target Recognition X, Firooz A. Sadjad, editor. Proceedings of SPIE Vol.4050, p55-60.
2. Karl S. Gudmundsson, and A. A. S. Awwal , "Sub-imaging technique to improve POF search capability," Applied Optics, Vol. 42, No. 23, 10th August 2003.
3. Margaret A. Philips, S. Richard F. Sims, "Signal-to-clutter measure for ATR performance comparison". Automatic Target Recognition VII; Firooz A. Sajadi, editor. Proceedings of SPIE Vol. 3069, p 74-81.

Publications Generated from This Project at WSU

1. A. A. S. Awwal, K. S. Gudmundsson, M. Tabrez, M. Rahman, M. S. Alam and K. M. Iftekharuddin, "A new metric for 3D optical pattern recognition," Proceedings of the SPIE Conference on Photonic Devices and Algorithms for Computing IV, p. 183-190, Vol. 4788, Seattle, Washington, 7 – 11 July, 2002.
2. K. S. Gudmundsson, and A. A. S. Awwal, "Sub-imaging technique to improve POF search capability," Applied Optics, Vol. 42, No. 23, 10th August 2003.

Dissertation/Theses Generated from This Project at WSU

1. K. S. Gudmundsson, Ph.D. Dissertation Title: Sub-imaging technique to improve POF search capability, Wright State University, Graduation date: May 2004.
2. M. Tabrez, Master Thesis Title: Optical pattern recognition of three dimensional images using composite binary phase only filters.
3. M. Rahman, Master Thesis Title: Three dimensional pattern recognition using phase only filter.